SPATIAL VARIANCE OF MOBILE AQUATIC ORGANISMS: CAPELIN AND COD IN COASTAL NEWFOUNDLAND WATERS

JOHN K. HORNE

Spatial Variance of Mobile Aquatic Organisms: Capelin and Cod in Coastal Newfoundland Waters

By

© John K. Horne

A thesis submitted to the School of Graduate Studies
in partial fulfillment of the requirements for
the degree of Doctor of Philosophy

Ocean Sciences Centre and Department of Biology
Memorial University of Newfoundland
St. John's, Newfoundland

1995

To my parents,

who always thought I could do it,

they just didn't think it would take this long.

Abstract

Patchy distributions of organisms are a long recognized attribute of terrestrial and aquatic ecosystems. Quantitative descriptions of spatial variance provide clues to processes that generate patchiness. In aquatic environments, greater effort has focussed on quantifying spatial variance in distributions of plankton than on quantifying spatial variance in distributions of mobile organisms. To evaluate the relative importance of biological and physical processes that generate variance, a theoretical framework was developed that combines demographic, growth, and kinematic rates in dimensionless ratios. Ratio values are then plotted as a function of temporal and spatial scale. Application of this technique identified kinematics as the dominant process influencing capelin (*Mallotus villosus*) distribution along the coast during the spawning season.

Hydroacoustic distribution data of capelin and Atlantic cod (*Gadus morhua*) were analyzed to examine how shoaling, schooling, and the aggregative response of predators contribute to the spatial variance of mobile, aquatic organisms. A characteristic scale of patchiness was not observed at the temporal scale of a single transect (ca. 1 hour) or at the scale of a survey (ca 2 weeks). On average, spatial variance decreased slightly over intermediate scales (10 km - 0.5 km) and then dropped rapidly at smaller scales. Data manipulations and computer simulations demonstrated that shoaling potentially increases spatial variance at intermediate scales, and that schooling potentially reduces spatial variance at scales smaller than aggregation sizes. There was no evidence of an aggregative response by cod to concentrations of capelin throughout the analyzed scale range (20 m - 10 km). This unexpected lack of spatial association between predator and prey was explained using estimates of foraging

energetics to show that cod were not constrained by physiology to track prey during the capelin spawning season.

Theoretical and empirical results of this study have increased knowledge of scale-dependent spatial variance in mobile, aquatic organisms and provided insight to the biological processes that potentially generate these patterns. Scale-dependent plots of spatial variance combined with rate diagrams can be used to evaluate the relative importance of biological and physical processes that influence organism dispersion as a function of spatial and temporal scale.

Acknowledgments

I thank my supervisor Dr. David Schneider for always leading by example, for exposing me to his quantitative acumen, and for continuously challenging me just the right amount. These are the qualities I hope to emulate as a scientist. I also thank my committee members Drs. George Rose and Joe Brown for hydroacoustic training, for criticism at committee meetings, and for comments on an earlier draft of this manuscript.

There is one author on the title page of this thesis but several people made the job easier. Dr. Ram Myers originally invited me to give a seminar in Newfoundland. Brian Beck warned me about always being a bridesmaid. Jim Hiscock (captain of the Naughty Gal III), Ches Jackson, Gord Jackson, and Tommy (captains of the Marie Louise) cheerfully took their boats more or less where I wanted to go. Paul Normore, Craig Tuck, and Dale Fraser helped out in the field. I thank friends and colleagues at the place we call NICOS -- notably K.S. Prasad and Marimar Villagarcia my office mates, and David Methven my dinner companion on the night shift. Dr. Richard Haedrich always provided advice (gardening and otherwise), encouragement, and the necessary computer hardware to get the job done.

Funding for this program was provided by National Centres of Excellence -- Ocean Production Enhancement Network (OPEN), Natural Sciences and Engineering Research Council of Canada (NSERC) through D. Schneider, and an A.G. Hatcher Memorial Scholarship to the author.

Contents

Figures

Tables

Chapter 1. Background and Approach

1.1 Introduction

Heterogeneity in spatial distributions of organisms is a long-recognized attribute of both terrestrial (Watt 1925, 1947) and aquatic (Hensen 1911; Hardy 1935, 1936) ecosystems. Quantifying spatial heterogeneity as a function of scale has been used to judge the applicability of small scale experiments to larger scale natural settings (Mercer and Hall 1911), to identify domains of equivalent spatial variability (Fairfield Smith 1938), to identify scales of maximum heterogeneity (Greig-Smith 1952; Kershaw 1957), and to provide clues to biological or physical processes that generate observed spatial variance patterns (Greig-Smith 1983; Denman and Powell 1984; Legendre and Demers 1984; Mackas et al. 1985).

In aquatic ecosystems, well established theory states that spatial variance of passive particles is determined by the surrounding flow field. Energy that creates spatial variance patterns originates at large scales (e.g. eddies, gyres) and is transferred by turbulent advection to successively smaller scales until viscous dissipation becomes important (Kolmogorov 1941; Okubo 1980). This cascade of energy is characterized by a power function where the spatial variance of a passive particle is proportional to the inverse of scale (wavenumber or frequency) raised to a negative exponent. When the logarithm of variance is plotted as a function of logarithm of frequency, the slope of the line is equal to the exponent. A decrease in spatial variance with scale is commonly observed among passive particles and organisms in marine and freshwater environments including surface water temperature (Saunders 1972; Fasham and Pugh 1976; Estrada

and Wagensburg 1977; Richerson et al. 1978; Star and Mullin 1979; Weber et al. 1986), sea level (Wunsch 1972), and phytoplankton (Platt et al. 1970; Platt 1972; Powell et al. 1975; Fasham and Pugh 1976; Denman 1976; Estrada and Wagensburg 1977; Horwood 1978; Weber et al. 1986).

The spatial variance pattern of at least one mobile aquatic organism was found to differ from that of passive tracers. The rate of change in spatial variance of Antarctic krill (*Euphausia superba*) with change in spatial scale was on average lower than that of surface temperature or phytoplankton over resolution scales of 2 km to 100 km (Fig. 6, Weber et al. 1986). The magnitude of average spatial variance in krill was less at large scales and greater at small scales than surface temperature or phytoplankton. Weber et al. (1986) attributed the increased spatial variability of krill at smaller scales to an unspecified behavioural mechanism. In a subsequent study, Levin et al. (1989) extended the sampling resolution to 200 m and observed a shallow negative slope in krill spatial variance down to scales of 1 km. The slight negative slope of krill spatial variance plots was observed in both studies but processes influencing spatial variance patterns and the generality of these patterns have not been systematically investigated for mobile aquatic organisms.

Early studies that quantified variability in organism distribution focused on spatial and temporal distributions of phyto- and zooplankton (e.g. Gran and Braarud 1935; Riley and Bumpus 1946; Bainbridge 1957; Cassie 1960). Plankton were treated as passive particles with short turnover times. Statistical indices and descriptive models used to quantify variance in plankton distributions are not directly applicable to long-lived organisms that can move independently of the surrounding fluid. Spatial

variance models of terrestrial systems are also not directly transferable to aquatic environments as they are limited to two dimensions and often assume homogeneous environments (e.g. Wiens 1976; Hassell and Anderson 1988). As a result, there is a limited number of models that quantify spatial variance of mobile organisms in aquatic environments.

Spatial variance studies of mobile, predator-prey systems in fluid environments are also rare. Spatial and temporal variability in the density of prey may ultimately determine foraging success of a predator. In the northwest Atlantic, predator-prey spatial variance studies are limited to seabirds-pelagic fish (Schneider and Piatt 1986; Schneider 1989) and demersal-pelagic fish (Rose and Leggett 1989, 1990). These and other similar studies demonstrate that observed spatial variance in the distribution of mobile aquatic organisms is dependent on the spatial and temporal scale of measurement (Schneider and Duffy 1985; Schneider 1989; Piatt 1990; Rose and Leggett 1990). Therefore, to examine the spatial dynamics of mobile predator-prey interactions it is imperative to quantify spatial associations of predator with prey over a wide range of scales and to explicitly report spatial and temporal scales of measurement.

These observations were used to formulate an approach to evaluate scale-dependent spatial variance in the distribution of mobile, interacting organisms:

1) Use previous knowledge to evaluate the relative importance of biological and physical processes that potentially generate spatial variance as a function of scale.

2) Conduct preliminary sampling to verify survey design, sampling scale, and analytic techniques.

3) Quantify spatial variance in the quantity of interest as a function of scale.

4) Confirm hypothesized variance generating processes.

5) Generalize results from specific cases and identify the next analytic steps.

This thesis is divided into eight chapters. The remainder of this chapter reviews efforts to characterize spatial variance in distributions of aquatic organisms and in interactions of predators with their prey. Background is provided on Atlantic cod (*Gadus morhua*) and capelin (*Mallotus villosus*) which are used as an example of a mobile predator-prey pair. The second chapter uses dimensionless ratios of rates to quantify the relative importance of processes that potentially generate spatial and temporal variance in any biological quantity of interest. This method is then used to identify dominant biological processes influencing spatial variance patterns of cod and capelin at logistically feasible sampling scales. Chapters 3 and 4 quantify variance in the distribution of capelin and cod from relative density data collected using hydroacoustics in Conception Bay, Newfoundland. Spatial variance patterns observed in the distribution of cod and capelin are compared to those of drifting particles and other mobile species. Chapter 5 focuses on scales of spatial association between cod as predator and capelin as prey. Observed patterns of spatial association between the two species are interpreted using bioenergetic calculations. A particle simulator is used in Chapter 6 to confirm the influence of hypothesized biological processes from Chapters 3 and 4 on spatial variance patterns of mobile aquatic organisms. Chapter 7 reviews

the treatment of spatial variance in ecology and speculates where progress in the prediction and analysis of spatial variance will continue. The final chapter summarizes contributions of this thesis.

1.2 Characterizing spatial variance in organism distribution

Early efforts to verbally describe distributional patterns of organisms were indirect methods of examining spatial variance at one or more scales. Numeric techniques attempted a more exact detection and description of spatial variance by comparing empirical indices of aggregation to an expected value under the assumption of randomness. These indices assess variance at a single scale for each calculation. To quantify spatial variance as a function of scale, quadrat size can be sequentially increased from the sample resolution to one half of the sample range (Greig-Smith 1952). A chronologic detailing of the development of statistics measuring departure from randomness and determining scale will be reviewed in the penultimate chapter.

The ability to detect concentrations of spatial variance has largely been determined by available sampling technology. Early surveys based on net samples found that spatial variance in plankton distributions peaked at the scale of tens of kilometers (Bainbridge 1957; Cushing and Tungate 1963; Steele 1974). The development of *in vivo* fluorometry (Lorenzen 1966), the Longurst-Hardy plankton recorder (Longhurst et al. 1966), and application of the Coulter counter (Sheldon and Parsons 1967) to plankton sampling dramatically increased the resolution of horizontal sampling in aquatic environments (cf. Fig. 1, Denman and Mackas 1978). Subsequent analysis resulted in a reduction in estimates of phytoplankton patch sizes (cf. Table 1, Legendre

and Demers 1984). The application of spectral analysis to phytoplankton data (Platt 1972; Platt and Denman 1975) facilitated the analysis of spatial variance over a continuous range of spatial scales. Spectral analyses of phytoplankton counts and other passive particle data confirmed that spatial variance peaked at low frequencies (large scales) and monotonically decreased to high frequencies (small scales) (e.g. Denman and Platt 1975; Fasham 1978).

Efforts to explain biological spatial variance commonly match characteristic scales of biological pattern to dominant physical processes at the same scale. The hypothesized coupling of biological patterns to physical processes is most common in pelagic communities comprised of phytoplankton (e.g. Denman and Powell 1984), zooplankton (e.g. Legendre and Demers 1984), and larval fish (e.g. Sheperd et al. 1984; Sissenwine 1984). One of the first studies directly coupling physical to biological processes was Gran and Braarud (1935) who explained the low abundance of phytoplankton in the Bay of Fundy by the lack of vertical stability in the water column. This observation and other physical-biological coupled studies (Bigelow et al. 1940; Riley 1942) were used in the development of the critical depth concept (Sverdrup 1953). The importance of physical-biological coupling in marine ecosystems has been reviewed by Walsh (1981), Denman and Powell (1984), and Mackas et al. (1985).

An implicit assumption in this matching approach is that biological pattern is directly coupled to physical processes at the same scale. This has been demonstrated in descriptions of plant communities with reference to environmental gradients (e.g. Greig-Smith 1952; Kershaw 1958), and the coupling of spatial variance patterns in passive tracers to flow structures in fluid environments (e.g. Denman and Powell 1984;

Mackas et al. 1985). This may not be true in all cases. There is both theoretical (e.g. May 1976) and experimental (e.g. Dwyer and Perez 1983) evidence to suggest that non-linear relationships occur between ecosystem components. An aquatic example is growth of phytoplankton altering the transmission of light in the water column due to self shading (Shigesada and Okubo 1981). The assumption of direct coupling at a single scale also excludes multiple processes influencing pattern at a single scale, and the propagation of effects across spatial or temporal scales (e.g. adult cohort size established at an early life history stage).

A second assumption of this matching approach is that the coupling of biological spatial variance to any variance generating process occurs at a characteristic scale. Single plots of variance as a function of scale show concentrations of spatial variance among terrestrial (Greig-Smith 1952; Kershaw 1957) and marine (Grassle et al. 1975; Schneider 1989; Rose and Leggett 1990) organisms. But in all studies, scales of maximum spatial variance differ among transects. In the few studies that increase the temporal scale by averaging multiple plots (Weber et al. 1986; Schneider 1994a), these scale-dependent concentrations of spatial variance often do not occur. It remains unclear whether variance in the spatial distribution of mobile aquatic organisms occurs at characteristic scales.

A third assumption in this matching approach is that the creation of biological spatial variance is generated exclusively by physical processes. Biological processes can also influence spatial variance over a range of scales. Phytoplankton critical patch size is a classic example. One theory is that the size of a phytoplankton patch is determined by the opposing forces of horizontal diffusion and phytoplankton

reproductive rates (Skellam 1951; Kierstead and Slobodkin 1953). The critical patch size theory was later expanded to include herbivore grazing (O'Brien and Wroblewski 1973a; Wroblewski et al. 1975). The assumption that spatial variance of passive tracers is generated exclusively by physical processes is also contradicted by the idea that the dominating process determining phytoplankton spatial variance switches between physical and biological processes over time (Demers and Legendre 1979, 1981). Reliance on matching biological pattern to physical processes was due, in part, to a lack of analytic tools that quantify the relative importance of variance generating processes. The relative influence of biological and physical processes on spatial variance of mobile aquatic organisms has not been extensively studied.

Initial attempts to describe spatial variance of mobile aquatic organisms also looked for characteristic scales of maximum spatial variance. The first diagrammatic portrayal of scale-dependent biological variance was Haury et al.'s (1978) conceptual model of macrozooplankton biomass distribution. Dominant features in the zooplankton diagram (cf. Fig. 1, Haury et al. 1978) matched dominant physical features in the original Stommel diagram of sea level (cf. Fig. 1, Stommel 1963). Magnitudes of zooplankton biomass variance or sea level variance were not quantified in either diagram. One of Stommel's (1963) major points was that this task was virtually impossible given the number of required measurements. Haury et al. (1978) included a relative 'measure of biological importance' when estimating magnitudes of zooplankton variance. The units of 'importance' were not quantified. More recently, Marquet et al. (1993) advocate the use of Stommel diagrams to characterize spatial and temporal variance of biological and physical quantities. They recommend the use of spectral

analysis to quantify scale-dependent spatial and temporal variance despite restrictive assumptions of the technique and difficulties collecting synoptic data at large scales.

Evidence from spectral analyses shows that spatial variance patterns of mobile organisms do not match those of passive tracers in the surrounding fluid. Weber et al. (1986) examined spatial variance of Antarctic krill (*Euphausia superba*) in relation to surface temperature and chlorophyll fluorescence as a measure of phytoplankton abundance. This study was the first comparison of spatial variance patterns of mobile organisms to passive tracers in an aquatic environment. It was also the first examination of scale-dependent spatial variance at more than one temporal scale. The rate of change in krill spatial variance with change in spatial scale was lower than that of either surface temperature or phytoplankton over resolution scales of 2 km to 100 km. The magnitude of average spatial variance in krill was smaller at low frequencies (large scales) and greater at high frequencies (small scales) than surface temperature or fluorescence. Weber et al. (1986) attributed increased spatial variance of krill abundance at smaller scales to an unspecified behavioural mechanism. In a subsequent study, Levin et al. (1989) extended sample resolution to 200 m and observed a shallow negative slope in krill spatial variance down to scales of 1 km. Spatial variance dropped rapidly at scales smaller than 1 km (cf. Fig. 4, Levin et al. 1989). The abrupt change in spectral density slope implies that different processes may be influencing spatial variance over different ranges of scales. Potential variance generating mechanisms include physical as well as biological processes. These two studies clearly demonstrate the scale dependence of spatial variance and the necessity of multi-scale observations in distributional studies of aquatic organisms.

Studies of the spatial variance of mobile aquatic organisms have largely been limited to single taxonomic groups. Weber et al. (1986) and Levin et al. (1989) quantified spatial variance of krill biomass over a wide range of scales. A series of studies examined scale-dependent spatial variance of marine birds and the association with pelagic schooling fish and physical flow structures (Schneider and Piatt 1986; Schneider 1989; Piatt 1990). This approach was used to examine predator-prey associations of Atlantic cod with capelin as a function of spatial scale (Rose and Leggett 1990). To confirm the generality of patterns observed within groups of mobile organisms, a comparison is required of scale-dependent spatial variance across taxonomic groups at temporal scales greater than that of a single transect.

1.3 Scale-dependent predator-prey interactions

The scale-dependence of spatial variance in the distribution of a single species also applies to predator-prey interactions. Analytic techniques used to quantify interactions of predators with prey have largely been adopted from single species studies. The traditional goal of these studies is to identify scales of maximum association between predator and prey. Having identified a characteristic scale of interaction, dominant physical processes at the same scale are often proposed as mechanisms that concentrate prey. This matching approach has been successful when prey organisms move passively with the surrounding fluid but may not apply when organisms can move independent of fluid motions.

The temporal scale of spatial sampling potentially influences observed spatial variance patterns of predator-prey interactions. Identification of a characteristic scale

of spatial association based on a single or limited number of samples implicitly represents short temporal scales. Among studies that present results from multiple transects (Schneider and Piatt 1986; Weber et al. 1986; Schneider 1989; Rose and Leggett 1990) the scale of maximum spatial association differs among transects. With the exception of the study by Weber et al. (1986), there has not been a combining of association values from a number of transects to examine spatial scales of association between aquatic predators and prey at larger temporal scales.

Temporal and spatial scales used in theoretical predator-prey models frequently differ from those used to test predictions in the laboratory or field (Kareiva 1989, 1990). The temporal resolution of population-interaction models is implicitly set at the generation time of the predator. But the temporal scale of survey transects is typically short relative to the life span of the predator or even the prey. Field and laboratory observations are commonly conducted at temporal scales equivalent to that of a foraging bout. In addition, the range of spatial scales used to formulate predator aggregative-response models have also differed from those tested in the field. Theoretical descriptions of aggregative responses by predators are based on changes in prey density at a single spatial scale (e.g. Holling 1965, 1966; Murdoch and Oaten 1975). Field studies identify the type of response and range of spatial scales over which aggregative responses occur (e.g. Heads and Lawton 1983; Piatt 1990). To ensure compatibility between theoretical models and empirical experiments the spatial and temporal scale of both theory and observation must be explicitly stated when quantifying interactions between predators and prey.

Predator-prey interactions among mobile aquatic organisms potentially occur over

a wide range of spatial and temporal scales. Therefore scales of maximum association between predator and prey can only be confirmed by analyzing variance over a continuous range of spatial and/or temporal scales. Biological processes must not be excluded when determining mechanisms that create observed patterns of spatial variance.

1.4 Cod-Capelin interactions in the northwest Atlantic

Capelin are a pelagic, schooling osmerid species inhabiting sub-Arctic and Arctic waters in the Atlantic and Pacific oceans (Jangaard 1974). In the northwest Atlantic, adult capelin (≥ 3 yr) migrate from offshore to coastal waters to spawn on gravel beaches during late June and July (Templeman 1948; Carscadden 1983). Spawning mortality exceeds 80% (Carscadden and Miller 1980). Eggs hatch within the beach gravel in 9-20 days (Templeman 1948; Frank and Leggett 1981) and larvae are transported offshore (Fortier and Leggett 1982, 1983). Surviving adults and juveniles remain offshore during fall and winter (Bigelow and Schroeder 1963; Bailey et al. 1977). During the spawning season Atlantic cod, a semi-demersal gadoid, complete a post-spawning migration to coastal waters to feed on capelin along the coast of Newfoundland (Templeman 1979; Akenhead et al. 1982; Lilly 1987; Rose 1993). Capelin have formed the basis of a multimillion dollar commercial fishery (Anon. 1980; Carscadden 1983) and are a key forage species for marine mammals, fish and marine birds (Winters and Carscadden 1978; Bailey et al. 1977).

Capelin are a major prey of cod in offshore (Turuk 1968; Campbell and Winters 1973; Stanek 1975; Minet and Perodou 1978; Lilly et al. 1984; Lear et al. 1986; Lilly

1986, 1987, 1991) and coastal (Thompson 1943; Templeman 1965; Aggett et al. 1987; Lilly 1987; Methven and Piatt 1989) waters. But the proportion of capelin reported in cod diet studies differs depending on the geographic area and time of year that samples were obtained. In NAFO Divisions 2J and 3KLNO, Campbell and Winters (1973) estimated that capelin composed 32% by volume of cod diet annually. Minet and Perodou (1978) found that capelin comprised 56% by weight of cod diet from a set of stomachs sampled during winter and summer in NAFO Divisions 2J and 3K. Annual consumption of capelin by cod was then estimated to be 28% by weight under the assumption that capelin are not consumed during spring and fall. This estimate forms a minimum as Lilly (1987) found that capelin comprised 15% by weight of cod stomach contents collected in NAFO Division 3L, and 16% (1982) to 36% (1985) by weight of cod stomachs sampled during autumn in NAFO Divisions 2J and 3K.

There are few published studies on the food of cod from inshore Newfoundland areas (Lilly and Botta 1984). Using a series of stomach samples from cod caught in cod traps, Templeman (1965) found that capelin formed 96% of cod stomach contents by volume during June to August, and 55% from May to November. Capelin represented 99% by weight of cod stomach contents from traps sampled in July 1968 and 1969 (Lilly and Flemming 1981).

There is little doubt that cod feed heavily on capelin but the dependence of cod diet on capelin abundance and availability has not been clearly demonstrated. Concern about the impact of reductions in capelin abundance on cod dynamics appeared as early as 1835 (Akenhead et al. 1982). The limited results that indicate capelin are important to cod growth and survival are correlative and largely focused on changes in

commercial catches or growth rates of cod in response to changes in capelin abundance. Using commercial catch data from 1970 to 1978, Akenhead et al. (1982) found that fluctuations in capelin biomass were not related to catch or growth rates of cod in NAFO Divisions 2J3KL. Indices of capelin abundance explained 35% of the variation in cod inshore catches from 1975 to 1984 (Lear et al. 1986). Aggett et al. (1987) observed a correlation of 0.5 (25% of explained variance) between cod catches in inshore traps and the proportion of capelin found in cod stomachs. Rose and Leggett (1989) found that correlations between hydroacoustic abundance estimates of cod and capelin ranged from 0.3 to 0.6. These values were within the 0.2 to 0.9 range of correlations observed by Lilly (1991) between cod stomach fullness index and annual estimates of capelin biomass from 1978 to 1986. Shelton et al. (1991) found no relationship between cod growth and capelin abundance but found a large probability of Type II error, failure to detect a real response. A common statement at the end of all these correlative studies is a call for quantitative, causal examination of the importance of capelin to the growth and population dynamics of cod.

Spatial associations between Atlantic cod and capelin densities have been examined in the northern Gulf of St. Lawrence. Rose and Leggett (1989) found that positive correlations between predator and prey were a function of high prey densities (> 100 capelin/10^5 m^3 water) and the presence of favourable water temperatures (1-9 °C). Cod and capelin densities were not correlated at temperatures outside of this range. At the temporal scale of a day, spatial coherence between cod and capelin was positive at spatial scales ranging from 4 and 10 km and negative at scales less than

capelin aggregation dimensions (3-5 km) (Rose and Leggett 1990). On a single occasion when cod were actively feeding on capelin, predator and prey were coherent at a scale of 3.5 m (Rose and Leggett 1990).

Chapter 2. Evaluating Spatial Variance

2.1 Introduction

Recent publications (e.g. Wiens 1989; Menge and Olson 1990; Holling 1992; Levin 1992) re-iterate the importance of scale in the description of ecological variability. The scale-dependence of biological and physical measurement is well recognized in both aquatic (Stommel 1963; Smith 1978; Steele 1978a) and terrestrial (Watt 1925, 1947; Greig-Smith 1952; Urban et al. 1987) ecosystems. Many techniques have been developed to quantify scale-dependent ecological pattern (see reviews in Platt and Denman 1975; Ripley 1981; Greig-Smith 1983) and standard data sets are regularly used to compare the consistency of spatial and temporal patterns among techniques (e.g. O'Neill et al. 1991; Cullinan and Thomas 1992; Turner et al. 1992). Despite efforts to quantify and compare scale-dependent spatial variance, there has not been a concomitant development of techniques that evaluate the relative importance of processes that generate spatial variance patterns.

Scale-dependent physical or biological pattern can be summarized in a diagram by plotting variance of a quantity as a function of spatial and temporal scale. The first diagrammatic descriptions of scale-dependent physical variability were estimates of sea level and deep ocean current variance (Stommel 1963). Haury et al. (1978) used this presentation to develop a conceptual model of zooplankton biomass variability. This was the first comparison of biological variance across a wide range of scales and remains the only published Stommel diagram of an ecological variable (Marquet et al. 1993). Variations of Stommel diagrams show concentrations of spatial and temporal

variability as a function of space and time scale for aquatic (e.g. Steele 1978b, 1989; Harris 1986; Dickey 1990) and terrestrial (e.g. Delcourt et al. 1983) ecosystems. These are intuitive diagrams where the boundaries of any feature in a plot indicate the minimum and maximum scales of variability for the quantity of interest. The construction of a true Stommel diagram requires simultaneous variance estimates at all spatial and temporal scales. This is rarely possible at intermediate or large spatial scales as the passage of time during data collection precludes independent calculation of spatial and temporal variance. Stommel diagrams summarize scale-dependent variability in a quantity of interest. They do not indicate the biological or physical processes that generate observed patterns.

As an alternative to inferring process from statistical descriptions of biological variance, I propose the use of dimensionless ratios to evaluate the relative importance of variance generating processes as a function of scale. Comparison of scale-dependent rates in the form of a dimensionless ratio assesses the relative contribution of biological or physical processes in the generation of biological variability. Similar comparisons using a complete set of ratios identify all potential processes that regulate variability in a biological quantity of interest. Dimensionless ratios have been used in ecology to identify sources of plankton variability (O'Brien and Wroblewski 1973b; Denman and Platt 1976; Okubo 1978), examine growth and physiological rates as a function of body size (Günther 1975; Platt and Silvert 1981; Heusner 1987), summarize spatial variability in marine nekton (Schneider 1991, 1994a), and evaluate complex problems in wildlife management (Schneider et al. 1993).

In this chapter I use dimensionless ratios to summarize knowledge of variance

generating processes across spatial and temporal scales. This summary identifies dominant variance generating processes at any scale of interest and can be used to improve the design of field sampling programs. The application of dimensional reasoning to evaluate competing processes complements the quantitative description of scale-dependent biological pattern. It neither replaces statistical techniques, nor is it directly comparable to them.

2.2 Methods

Prior to any field sampling, a crucial task is to identify variables to be measured and appropriate scales of measurement for each variable. A scale of measurement has two components -- a resolution and a range. The resolution or grain is the minimum sample unit (e.g. quadrat size) while the range is the maximum extent of the sample (O'Neill et al. 1986; Wiens 1989). To summarize the relative importance of biological or physical processes that generate scale-dependent biological variability, I propose a 'generic' procedure consisting of 4 steps:

1) State the quantity of interest.
2) Write an equation incorporating all potential sources of variability for this quantity.
3) Calculate dimensionless ratios.
4) Plot and contour ratio values in rate diagrams using existing data.

To illustrate this procedure, I examine the spatial and temporal dynamics of capelin biomass distribution in the northwest Atlantic. From the life history of capelin described in Chapter 1, it is apparent that changes in the distribution of capelin biomass

are a result of demographic (recruitment, mortality), growth, and kinematic (active and passive movements) processes acting within a wide range of spatial and temporal scales.

The quantity of interest in this example is the proportional rate of change of capelin biomass in the northwest Atlantic. The rate of change of biomass has dimensions time^{-1}. The biomass B of a group of organisms i is the product of the number of animals N multiplied by their individual mass M:

$$B = \sum_{i=1}^{n} N_i M_i \tag{2.1}$$

The concentration of biomass is defined as:

$$[B] = \frac{N M}{V} \tag{2.2}$$

where V is the volume occupied. To simplify the notation a dot over a symbol is used to signify the proportional rate of change in the quantity represented by the symbol. Hence, the proportional rate of change in the concentration of biomass $[\dot{B}]$ is:

$$[\dot{B}] = [B]^{-1} \frac{d[B]}{dt} \tag{2.3}$$

The second step is to write an equation containing potential processes that affect the concentration of capelin biomass. Change in the concentration of biomass $[\dot{B}]$ is a function of change in biomass due to recruitment and mortality $\dot{N}$, somatic growth $\dot{M}$, the divergence due to fluid motions $\dot{V}_F$ and the divergence due to individual motions relative to the fluid $\dot{V}_I$ as shown in Appendix 2.1. Five research areas are integrated by the equation that expresses the rate of change in biomass concentration:

$$[\dot{B}] = \dot{N} + \dot{M} - \dot{V}_F - \dot{V}_I \qquad (2.4)$$

biomass distribution | demographics | growth | fluid mechanics | behaviour

The third step combines terms from equation (2.4) to form dimensionless ratios. If variables in an equation are dimensionally heterogeneous, a complete set of ratios is obtained by dimensional analysis (Bridgman 1922). If all terms in an equation have the same units then ratios can be combined from any pair or group of terms. This flexibility enables the formation of ratios relative either to a process of interest (e.g. Schneider 1992) or to the combination of multiple terms into functionally important single terms (Fischer et al. 1979). Three ratios can be formed from equation (2.4) relative to the fluid mechanics term or combine demographic and kinematic terms to form population dynamics and construct a single ratio with somatic growth.

In the capelin biomass example, all terms in equation (2.4) have dimensions of time^{-1} so ratios were formed from the equation. Biological reasoning was used to select groups of terms to compare. For example, I was more interested in comparing the two kinematic terms, $\dot{V}_F$ and $\dot{V}_I$, than comparing one of the kinematic terms to demographics $\dot{N}$ or somatic growth $\dot{M}$. A formal approach illustrating the use of dimensional analysis to form ratios from equation (2.4) is provided in Appendix 2.2. The formal approach ensures that redundant ratios are not included.

The first dimensionless ratio compares somatic growth $\dot{M}$ to the net result of demographics $\dot{N}$ and kinematics $\dot{V}$.

$$\frac{\dot{M}}{\dot{N} - \dot{V}} \qquad (2.5)$$

Biomass concentration increases if animals grow ($\dot{M} > 0$), increase in number ($\dot{N} > 0$), or contract into a smaller volume of water ($\dot{V} < 0$). At small time scales relative to the life span of the organism, changes in population biomass due to somatic growth are limited and the value of the ratio is expected to be much less than 1. Spatial or temporal variability of a sample becomes a function of the change in number of individuals or the volume in which they occur rather than a change in mass of organisms. Over longer temporal scales the value of the ratio is expected to approach 1. Large positive changes in growth $\dot{M}$ and a ratio greatly exceeding 1 are typical for long-lived ($\dot{N}$ small) species that are managed in large geographic areas ($\dot{V}$ small). Small changes in somatic growth $\dot{M}$ coupled with a ratio much less than 1 ($\dot{N}$ large, $\dot{V}$ small) are expected at spatial and temporal scales associated with the capelin spawning season.

The demographic to kinematic ratio relates recruitment and mortality to movements.

$$\frac{\dot{N}}{\dot{V}} \tag{2.6}$$

If the ratio is greater than 1 then demographics prevail over kinematic processes. A ratio less than 1 indicates that kinematics will dominate over demographic processes. Values of the ratio can be expected to be near unity at time scales of a cohort and at space scales comparable to the range of the population. In many populations, kinematic processes dominate at small temporal and spatial scales, while demographic processes

dominate at larger temporal and spatial scales.

The kinematic ratio compares locomotory velocities of the organism to passive velocities due to fluid motions.

$$\frac{\dot{V}_I}{\dot{V}_F} \tag{2.7}$$

If individual motions dominate, the kinematic ratio will exceed 1. The magnitude of $\dot{V}_I$ is a function of the locomotory capacity and life history stage of the organism. An example is the relative mobility of fish larvae compared to adults. As the mobility of an organism decreases, $\dot{V}_I$ approaches 0. When organisms drift passively with the fluid, the value of the ratio is much less than 1. Values of $\dot{V}_F$ are sensitive to study location and spatial scale. Lentic and lotic environments will differ in the potential for passive drift of any organism. Passive drift may also be important to terrestrial organisms, including seeds, small insects, and spiders. At large spatial scales, the range of a study may encompass autonomous circulation features associated with the fluid (e.g. gyres), thereby making $\dot{V}_F$ small and the kinematic ratio large. If the value of the ratio is approximately equal to 1, changes in the distribution of biomass due to movement depend on the interaction between biological and physical processes. High, intermediate, and low values of this ratio correspond to Wiebe and Flierl's (1983) biological, physical-biological, and physical distributional mechanisms.

The demographic ratio measures the importance of recruitment $\dot{N}_r$ relative to mortality $\dot{N}_z$. In capelin, as in other commercially important species, mortality $\dot{N}_z$ is partitioned into natural $\dot{N}_m$ and harvesting $\dot{N}_f$ mortality.

$$\frac{\dot{N}_r}{\dot{N}_m + \dot{N}_f} \tag{2.8}$$

Over short time scales, this ratio is greater than 1 during the breeding season of capelin and less than one during the remainder of the year. At the spatial scale of the population range (100's km) and the temporal scale of a cohort (5 yr), the value of the ratio will approach unity. In unexploited populations, maintenance of biomass levels at equilibrium is indicated by a value of 1. Increased mortality due to predation or the onset of harvesting reduces this value below unity unless a compensatory increase in recruitment occurs at low densities. Commercial fisheries managers attempt to maintain the value of this ratio near unity at time scales of several years by regulating harvest mortality $\dot{N}_f$ through quotas and gear restrictions.

The fourth step in the procedure is the plotting of each dimensionless ratio as a function of spatial (x-axis) and temporal (y-axis) scale using existing data. In many ecological systems precision of calculations may be limited by a paucity of data at large spatial and temporal scales. If data are limited or unavailable, calculations can be made at benchmark spatiotemporal scales. Nominal (<1, 1, >1) contours are then drawn based on these benchmarks. If data are available over a wide range of scales, spatiotemporal scales where transitions between dimensionless ratio values occur are marked. Contour lines are then drawn to connect transition points. Location of dimensionless ratio contours are refined as additional data are obtained from field studies. The inability to calculate dimensionless ratio values at a specific scale indicates a potentially important research area. This method can be used by groups of researchers to make perceptions of the relative importance of competing processes

explicit. Comparisons of rate diagrams from each individual can be used to highlight discrepancies between ratio values and to focus the discussion of large research groups on dominant scale-dependent processes.

Data from capelin assessment documents and published velocities of the Labrador and Newfoundland inshore currents were used to estimate scale-dependent ratios in rate diagrams. Order of magnitude calculations showed whether the absolute value of any dimensionless ratio was less than, equal to, or greater than 1 at a given spatiotemporal scale. Contour lines marked the spatial and temporal scales where dimensionless ratios changed value.

2.3 Results

The major feature in the rate diagram of capelin growth to population dynamics ratio (Fig. 2.1a) reflects the persistence of Newfoundland-Labrador capelin populations at large scales. At spatial scales larger than the continental shelf and temporal scales larger than a year the value of the ratio is greater than 1. This is a result of changes in the concentration of biomass due to somatic growth exceeding changes due to population dynamics. On average capelin growth, as indicated by length, increases a total of 40,900% or 10,225% of initial hatch length per year during the first 4 years of life (Templeman 1948). This rate exceeds that of partial recruitment to the adult stock -- 53% per year (Carscadden and Miller 1981), spawning mortality -- 80% of spawning stock per year (Carscadden and Miller 1980), fishing mortality -- 0.05% of estimated biomass per year (Carscadden et al. 1991), and the net kinematic rate -- 0% because the population remains on the continental shelf. Recruitment, mortality and kinematic rates

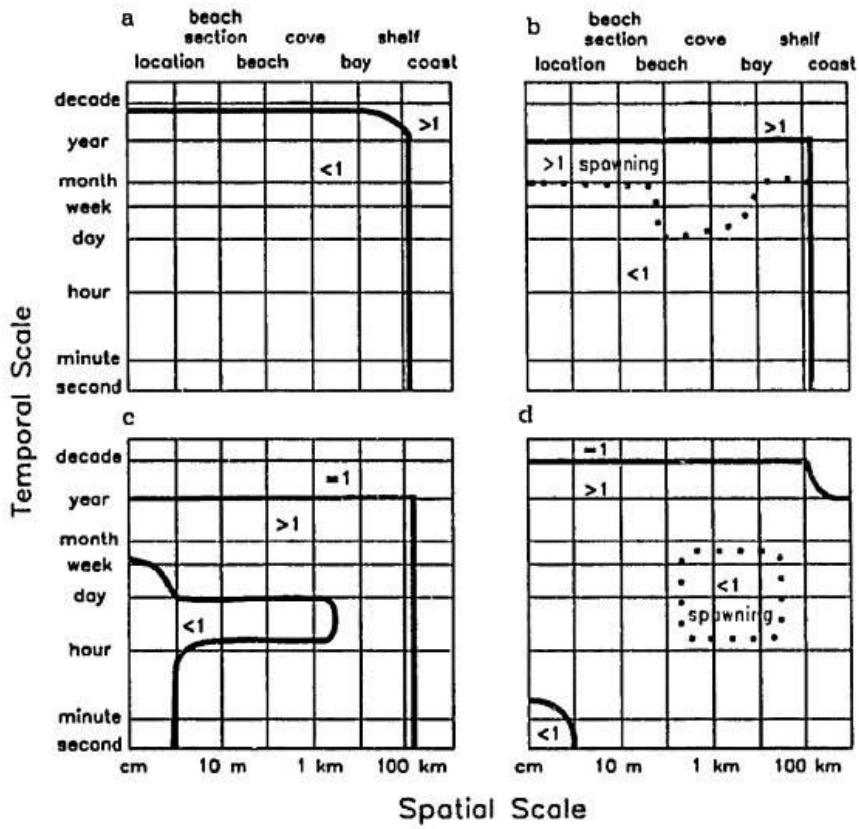

Fig. 2.1 Contoured rate diagrams of dimensionless ratio values for adult capelin biomass distribution in the northwest Atlantic. Ratios are contoured less than 1 (<1), equal to 1 ($=1$), and greater than 1 (>1). a) Growth to population dynamics (demographics - kinematics) ratio, $\frac{\dot{M}}{\dot{N}-\dot{V}}$ b) Demographics (recruitment + mortality) to kinematic (locomotory + passive motions) ratio, $\frac{\dot{N}}{\dot{V}}$. Dotted line indicates shift in contour during spawning season. c) Locomotory to fluid (passive) motion ratio, $\frac{\dot{V}_l}{\dot{V}_f}$ d) Recruitment to natural plus harvesting mortality ratio, $\frac{\dot{N}_r}{\dot{N}_m+\dot{N}_f}$. Dotted line indicates scales of mortality during spawning season.

exceed somatic growth rates at smaller scales and the value of the ratio is less than 1.

Values of the demographic to kinematic ratio (Fig. 2.1b) vary depending on capelin reproductive status. At temporal scales of a year and spatial scales of the continental shelf changes in the concentration of capelin biomass due to demographic processes exceed changes due to kinematics and the value of the ratio is greater than 1. Partial recruitment to the adult population (4 years) is 53% per year (Carscadden and Miller 1981). Natural mortality is typically assumed to be 30% per year in capelin (e.g. Carscadden and Miller 1980). Changes in the volume occupied by capelin populations are negligible at these scales and therefore the value of the kinematic term is near zero. At sub-annual scales passive and active movements of capelin increase the value of the kinematic term and the value of the ratio drops below 1. During the spawning season, the location of the unity contour shifts to the spatial scale of a spawning beach or cove (100-1000 m) on a day to weekly scale. This is a result of increased mortality due to spawning -- approximately 2% of spawning fish per day (Carscadden and Miller 1980) and inshore harvesting -- 0.001% of total estimated biomass per day (Carscadden et al. 1991). Concentrated predation on capelin by fish, seabirds and marine mammals also occurs during this period (cf. Carscadden 1983) but lack of data prevented an estimate of mortality rates due to natural predation.

The unity contour in the diagram of the kinematic ratio (Fig. 2.1c) is also located at the scale of the entire population. On the continental shelf over an annual cycle, passive drift associated with the Labrador Current -- typical surface speed of inshore branch 0.1 m s^{-1} (Helbig et al. 1992), is balanced by the annual migratory cycle of adult fish (cf. Carscadden 1983). At temporal scales less than a year and a spatial scale of

the continental shelf, changes in biomass concentration due to swimming exceed changes due to passive drift and the value of the ratio is greater than 1. At spatial scales of kilometres to metres and temporal scales of weeks to seconds, potential changes in the concentration of biomass due to passive drift with tides, currents and internal waves (Yao 1986, de Young et al. 1993) exceed changes due to active movements. Hence the value of the ratio is less than 1. The dominance of passive movements at these scales disappears during the spawning season when aggregations of adult capelin migrate to coastal waters.

At the largest scales in the rate diagram of the demographic ratio (Fig. 2.1d), persistence of a population requires a balance between recruitment and mortality. The resulting value of the demographic ratio must equal 1. On an annual scale over the spatial range of the population, recruitment generally exceeds natural and harvesting mortality. Large decreases in recruitment combined with increased natural and harvesting mortality may reduce the value of the ratio below unity at these scales in any particular year. For example, capelin recruitment measured as 2-year-olds dropped by a factor of 35 between the 1973 and 1976 year-classes in NAFO Division 2J3K (Carscadden and Miller 1981). During the spawning season, mortality exceeds recruitment to the adult population. This reduces the value of the demographic ratio to less than one at spatial scales of hundreds of metres to tens of kilometres and temporal scales of hours to weeks. At the scale of an individual capelin (less than a metre, a few minutes), changes in biomass due to natural and harvesting mortality are greater than those due to recruitment.

2.4 Discussion

The proposed framework is not a panacea for evaluating pattern generating processes. It is a technique that summarizes and displays existing knowledge of scale-dependent processes in any ecological system. Rate diagrams can be used to evaluate the relative importance of variance generating processes at any scale of interest and to identify sampling scales in process oriented research. This is an iterative procedure where ratio values and contour locations are refined as new data are gathered.

A plot depicting biological variability as a function of space and time combined with a set of rate diagrams synthesizes available knowledge of scale-dependent pattern and process for a biological quantity. Comparison of prominent variance features to dimensionless ratio values at the same scale identifies processes that are likely to generate spatial or temporal variance in the quantity of interest. This presentation avoids the assumption that a single biological or physical process is directly linked to pattern at any scale, and that coupling of biological and physical processes occur at characteristic spatial and temporal scales. To further illustrate the advantages of using dimensionless ratios, I constructed a set of zooplankton rate diagrams to identify potential variance generating processes in the Haury et al. (1978) Stommel diagram of zooplankton biomass variability (Fig. 2.2a). Dimensionless ratio values were estimated and nominal contours (< 1, 1, > 1) were plotted across the same range of scales in a column of rate diagrams (Fig. 2.2b - 2.2e). Zooplankton were assumed to be an unexploited population of mid-latitude zooplanktonic organisms with the limited locomotory capability of copepods.

Fig. 2.2 a) Stommel diagram of zooplankton biomass variability (from Haury et al. 1978). Nominal contoured rate diagrams (<1, $=1$, >1) of b) growth to population dynamics dimensionless ratio, $\frac{M}{N-V}$ c) demographic to kinematic dimensionless ratio, $\frac{N}{V}$ d) locomotory to fluid (passive) motion dimensionless ratio, $\frac{V_I}{V_F}$ and e) recruitment to natural and harvesting mortality dimensionless ratio, $\frac{N_r}{N_m+N_f}$. Shaded regions indicate a ratio value greater than 1.

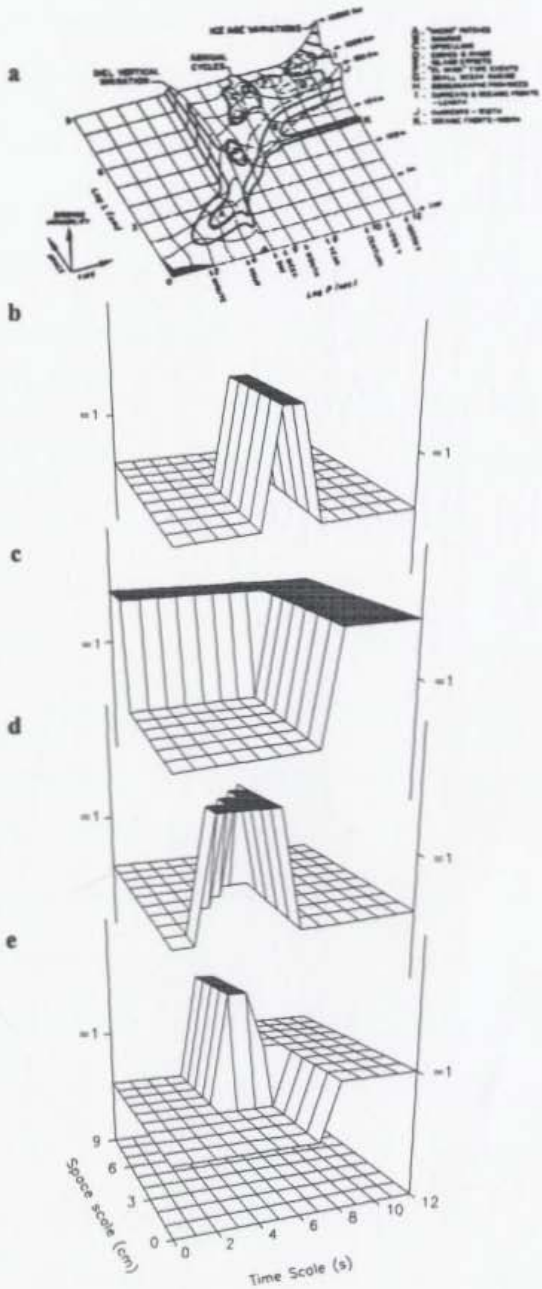
a
b
c
d
e
=1
=1
Space scale (cm)
0
3
6
9
Time Scale (s)
0
2
4
6
8
10
12

The rate diagram of the growth to population dynamics ratio (Fig. 2.2b) shows greater change in the concentration of biomass due to somatic growth than due to demographic and kinematic processes at spatial scales up to a kilometre (10^5 cm) and temporal scales from days to a month (10^4 s - 10^6 s). The value of the ratio is less than 1 at all other scales. In the demographic to kinematic rate diagram (Fig. 2.2c) at the scale of the population, biomass changes due to the succession of generations exceed biomass changes due to movement. At scales shorter than annual cycles and smaller than the continental shelf, biomass changes due to swimming and passive movements dominate over demographic changes and the value of the ratio is less than 1. The rate diagram of the kinematic ratio (Fig. 2.2d) reflects the locomotory capacity of the organism. Changes in biomass due to swimming and diel migration dominate at scales of days and hundreds of metres, resulting in a ratio value greater than 1. At larger scales passive motions associated with flow structures (e.g. currents, gyres, upwelling) determine the distribution of biomass and the value of the ratio is reduced below 1. In the rate diagram of the demographic ratio (Fig. 2.2e), changes in biomass due to recruitment and natural mortality are approximately equal at all spatial scales over annual and larger temporal scales. The value of the ratio is greater than 1 at spatial scales greater than a kilometre and at temporal scales of weeks to months as a result of the turnover in generations. Changes in biomass due to predation and natural mortality dominate at all other scales, thereby reducing the value of the ratio below 1.

Comparison of the rate diagrams with the zooplankton Stommel diagram showed that of the eleven features in the Stommel diagram (designated by letters A-K), six were attributable to dominant processes in rate diagrams at the same spatial and temporal

scales. The remaining five features (C,F,I,J,K) in the Stommel diagram are attributed to fluid motions, while plots of rates indicate that demographic processes should prevail at the space and time scales of these features. Based on the rate diagrams, I hypothesize that variability in zooplankton concentration at the space and time scales of features C,F,I,J,K in the Stommel diagram are due more to demographic than to fluid processes. Biomass distribution, locomotory capacity and passive drift data at large temporal scales are needed to test this speculation.

2.4.1 Identifying Appropriate Sampling Scales

If a research program is focused on a particular process (e.g. somatic growth), rate diagrams can be used to identify relevant sampling scales for a field program. For example the rate diagram of the growth to population dynamics ratio (Fig. 2.1a) indicates that somatic growth exceeds demographic and kinematic rates at a spatial scale of hundreds of kilometres and a temporal scale of several years. This spatiotemporal scale is a logical choice of sampling resolution when quantifying the contribution of somatic growth to changes in capelin biomass concentration. At smaller spatiotemporal scales, changes in capelin biomass concentration are dominated by demographic and kinematic processes (i.e. ratio < 1). Scales where interaction between competing processes may be important are indicated by dimensionless ratio values approximately equal to 1. Interactions between growth and population dynamic processes are likely to occur at annual and continental shelf scales (Fig. 2.1a).

The plotting of dimensionless ratios can also be used to quantify the range of scales over which research conclusions can be generalized. Ecosystem process models

should not be generalized across scales, just as regression models should not be extrapolated beyond limits of sampled data. For example, the capelin biomass rate diagrams indicate that a spatial variance model for the capelin spawning season over spatial scales less than 10 kilometres should include fishing and spawning mortality (Figs. 2.1b, 2.1d). Rate diagrams indicate that expansion of the model to annual cycles over the continental shelf would require the inclusion of recruitment and growth processes (Figs. 2.1a, 2.1b, 2.1d).

2.4.2 Evaluating Variance Generating Processes

Comparison of ratios derived from dimensional analysis provides considerable insight into the relative importance of pattern generating processes. After setting the temporal and spatial scales of interest, a set of rate diagrams and order of magnitude calculations can be used to identify potentially dominant processes prior to field sampling. To illustrate by way of example, what sampling scales should be used and which processes should be measured to quantify the spatial variance of capelin distribution in nearshore waters during the spawning season? From capelin life history it is known that the spawning season lasts approximately six weeks every year and occurs along most of the Newfoundland coast. Onset of spawning may follow a south to north latitudinal trend (Templeman 1948) but suitable spawning habitat is assumed along the entire coast. Therefore the temporal scale at which to evaluate competing processes is approximately six weeks. Logistic sampling constraints set the spatial scale to that of a bay (20-40 km). At this spatiotemporal scale, the rate diagram of the growth to population dynamics ratio (Fig. 2.1a) indicates that demographic and

kinematic processes are more important than growth processes. The ratio of demographic to kinematic rates (Fig. 2.1b) is near 1, indicating that both demographic and kinematic processes may be important to capelin spatial dynamics during the spawning season. Further comparison shows that kinematic processes are dominated by divergence due to swimming motions (Fig. 2.1c) and that mortality exceeds recruitment in the demographic ratio (Fig. 2.1d) at this time of year.

Order of magnitude calculations can be used to compare the relative importance of individual motion $\dot{V}_I$ to mortality $\dot{N}_m + \dot{N}_f$ at this scale. Using the relation between body size and swimming speed (Okubo 1987), a 15 cm capelin has a range of approximately 24 km day^{-1}. Mortality averages approximately 2% day^{-1} due to spawning (Carscadden and Miller 1980) and 0.00125 % of the total biomass day^{-1} in NAFO divisions 2J3KL during 1989 due to harvesting (Carscadden et al. 1991). Using 20 and 40 kilometre sampling ranges, there is a 60%-119% day^{-1} rate of capelin divergence compared to a total mortality of 2% day^{-1}. At the scale of a bay, research effort on the spatial dynamics of capelin during the spawning season should begin by examining kinematics.

Plotting dimensionless ratios within rate diagrams can be used to define time and space scales required to manage renewable resources. The ratio of growth to population dynamics (equation 2.5) assesses the effects of resource management policy. Large positive changes in somatic growth $\dot{M}$ combined with a ratio greatly exceeding 1 indicate a potential for growth overharvesting. Small changes in somatic growth coupled with a ratio much less than 1 indicates recruitment overharvesting. Widely-used fishery models (Ricker 1954; Beverton and Holt 1957) were developed for

situations where $\dot{M}$ was large and the ratio in equation (2.5) greatly exceeded 1. This is typical for long-lived, demersal species that are managed over large areas. In contrast, heavy fishing pressure on pelagic species increases both $\dot{N}$ and $\dot{V}$ as mortality increases and the spatial range is contracted to maintain school densities (Murphy 1966; Winters and Wheeler 1985; Csirke 1988). The size of management areas for demersal and some pelagic fish stocks are typically on the order of hundreds of square kilometres. These are chosen to contain population movements over an annual cycle. This reduces the value of the demographic to kinematic ratio (equation 2.6) below 1 and the kinematic ratio (equation 2.7) becomes large as $\dot{V}_F$ approaches 0. Wide ranging species (e.g. whales, tuna) clearly require much larger management areas to maintain similar values in ratios containing kinematic terms.

The management of exploited populations is summarized, in part, by the demographic ratio (equation 2.8). Resource populations are regulated through the allocation of quotas $\dot{N}_f$. Natural mortality $\dot{N}_m$ is rarely measured for commercial fish stocks. It is traditionally assigned a constant value in stock assessments, typically 0.2 year^{-1} for demersal species. Fisheries research has largely focused on recruitment processes $\dot{N}_r$ in an effort to predict conditions of high recruitment. Fluctuations in annual recruitment of fish species have ranged from a factor of 2 to a factor of 100 (Cushing 1982) but the process is not well understood. The demographic ratio can also be used to calculate harvesting rates needed to maintain or increase resource levels. The onset of harvesting dramatically increases $\dot{N}_f$ relative to $\dot{N}_r$. If the recruitment rate is known, resource managers can prevent recruitment overharvesting by limiting harvesting at levels equal to or below recruitment rates during the long-term

management of the resource.

Contouring dimensionless ratio values as a function of space and time scales provides a comprehensive method to summarize knowledge of pattern generating processes in complex ecological systems. It can be used by individuals conducting research programs or by agencies managing renewable resources. This technique summarizes the spatial and temporal dynamics of any organism, evaluates the relative importance of pattern generating processes at single or multiple scales, identifies potential research areas and appropriate sampling scales for field studies, and quantifies the range over which spatiotemporal models can be generalized. Aquatic examples were used to demonstrate the method but the same procedures should be applicable to organisms in terrestrial or aerial environments.

As a brief terrestrial example I examine factors affecting the rate of change in the concentration of seed producing balsam fir (*Abies balsamea*) trees. The rate of change in the concentration of trees $[\dot{N}]$ is a function of recruitment $\dot{N}_r$, natural $\dot{N}_m$ and harvesting $\dot{N}_h$ mortality, and the lateral divergence of trees due to seed dispersal $\dot{A}_D$.

$$[\dot{N}] = \dot{N}_r + \dot{N}_m + \dot{N}_h - \dot{A}_D \tag{2.9}$$

or simply:

$$[\dot{N}] = \dot{N} - \dot{A} \tag{2.10}$$

A forest manager or conservationist may be interested in changes in the density of spruce trees. Changes in density reflect the relative importance of demographic and kinematic processes, indicated by the change in number of trees relative to the areal spread of a balsam stand or of the species $\frac{N}{A}$. If for example recruitment to the balsam tree population $\dot{N}_r$ is approximately 0.1% year^{-1}, then mortality $\dot{N}_m + \dot{N}_h$ might be expected to exceed recruitment at small spatiotemporal scales. At scales greater than

100 kilometres and the lifespan of a tree (100 years) recruitment is expected to equal mortality. At spatial and temporal scales of a single tree values of the ratio are predicted to equal 1, although soil conditions and stand succession stage will influence local values. At annual scales the ratio will exceed unity due to blowdown, disease, insect damage, and seed movement. At the scale of centuries kinematic changes due to lateral divergence might be expected to exceed those due to demographics and the ratio will be less than 1. This sketch of the relative importance of competing processes in balsam tree distribution could be depicted in a rate diagram such as Fig. 2.1 or Fig. 2.2, based on estimates of rates and the resulting dimensionless ratios plotted as a function of scale.

The use of dimensionless ratios is highly useful to researchers collecting data in diverse ecosystems, such as the Long-Term Ecological Research (LTER) sites (cf. Magnuson et al. 1991). Variance generating processes of several species can be summarized and compared within or among terrestrial and aquatic environments over a wide range of spatial and temporal scales.

Appendix 2.1: Spatial Dynamics of Biomass

Changes in the concentration of biomass $[\dot{B}]$ of an organism in a fluid environment are a function of recruitment $\dot{N}_r$, natural $\dot{N}_m$ and harvesting $\dot{N}_f$ mortality, somatic growth $\dot{M}$, divergence due to motions within the fluid $\dot{V}_F$, and divergence due to individual motions relative to the fluid $\dot{V}_I$:

$$[\dot{B}] = \dot{N}_r - \dot{N}_m - \dot{N}_f + \dot{M} - \dot{V}_F - \dot{V}_I$$

Definition of terms:

$[\dot{B}]$ instantaneous time rate of change in concentration of biomass. Dimensions are time^{-1}.

$$[\dot{B}] = [B]^{-1} d\frac{[B]}{dt} = \left(\frac{NM}{V}\right)^{-1} \frac{d\left(\frac{NM}{V}\right)}{dt}$$

$\dot{N} = \dot{N}_r - \dot{N}_m - \dot{N}_f$ instantaneous time rate of change in biomass due to births (r), natural mortality (m) and harvesting mortality (f). Dimensions are time^{-1}.

$$\dot{N} = (NM)^{-1} M \frac{dN}{dt}$$

$\dot{M}$ instantaneous time rate of change in population biomass due to growth. Dimensions are time^{-1}.

$$\dot{M} = (NM)^{-1} N \frac{dM}{dt}$$

$\dot{V} = \dot{V}_F + \dot{V}_I$ instantaneous time rate of change in volume occupied by a group of organisms due to the velocity of the fluid $\dot{V}_F$ and the velocity of individuals relative to the fluid $\dot{V}_I$. The divergence theorem can be used to describe the kinematics of biomass in a fluid environment (Schneider 1991). This theorem relates the local rate of change in a volume $\frac{dV}{dt}$ occupied by a group of organisms to horizontal $u = \frac{dx}{dt}$, $v = \frac{dy}{dt}$ and vertical $w = \frac{dz}{dt}$ velocities in an x,y,z co-ordinate system. In compact notation, the rate of change in volume occupied $\dot{V}$ is $\dot{V} = (\nabla \cdot \mathbf{u})$ where $\mathbf{u}$ is the vector of velocities (u,v,w), the dot indicates scalar multiplication, and ∇ is the gradient operator (see Dutton 1976, chapter 5). Dimensions are time^{-1}.

$$\dot{V} = V^{-1}\frac{dV}{dt} = \frac{\partial u}{\partial x} + \frac{\partial v}{\partial y} + \frac{\partial w}{\partial z} = \nabla \cdot \mathbf{u}$$

This equation states that rate of change in the volume occupied by a given population is equal to the divergence of the population, where divergence can be positive (diverging) or negative (converging). Movement of the population in a fluid environment is a result of displacement due to motions of the fluid $\mathbf{u}_F$ and movement of individuals relative to the fluid $\mathbf{u}_I$. For many terrestrial organisms $\dot{V}_F = 0$ and divergence is a function of organism locomotion.

Appendix 2.2: Dimensional Analysis

Dimensionless ratios are calculated by constructing a two-way table where the variables of interest are columns and all fundamental dimensions (e.g. mass, length, time, number of organisms) are rows. Exponents of each variable form the elements of a dimensional matrix (e.g. volume has dimensions length^3). Variables are then combined using the linear algebra (Langhaar 1980) or the successive elimination method (Taylor 1974) to make all values of exponents zero. This results in a set of dimensionless products.

In the capelin biomass example, quantities of interest are: demographic $\dot{N}$, growth $\dot{M}$, and kinematic $\dot{V}$ rates. The fundamental quantities are: length L, mass M, time T, and number of organisms $\sharp$. The dimensional matrix is:

		$\dot{N}$	$\dot{M}$	$\dot{V}$
Dimension	L	0	0	0
	M	0	0	0
	T	-1	-1	-1
	$\sharp$	0	0	0

Since all quantities are rates, dimensions other than time can be dropped. Dividing through by $\dot{V}$ the revised matrix becomes:

		$\frac{\dot{N}}{\dot{V}}$	$\frac{\dot{M}}{\dot{V}}$
Dimension	T	0	0

Dimensionally homogeneous terms can be combined to form logical groups (Fischer et al. 1979). Demographics and kinematics are combined to form the quantity population dynamics $\dot{N} - \dot{V}$ with dimensions time^{-1}. Replacing $\dot{N}$ and $\dot{V}$ by $\dot{N} - \dot{V}$ and dividing the original matrix by $\dot{N} - \dot{V}$ the revised matrix becomes:

		$\frac{\dot{M}}{\dot{N} - \dot{V}}$
Dimension	T	0

Analysis results in two ratios:

$\frac{\dot{N}}{\dot{V}}$ Ratio of demographics (recruitment, natural mortality, harvesting mortality) to kinematics (active movement, drift).

$\frac{\dot{M}}{\dot{N} - \dot{V}}$ Ratio of growth to population dynamics (demographics, kinematics).

Two additional ratios result if demographic and kinematic processes are examined individually.

$\frac{\dot{N}_r}{\dot{N}_m + \dot{N}_f}$ Ratio of recruitment to natural and harvesting mortality.

$\frac{\dot{V}_l}{\dot{V}_F}$ Ratio of locomotory to fluid (passive) motions.

Chapter 3. Influence of Flow Gradients

3.1 Introduction

Theory and observation suggest eastern and northeastern Newfoundland coastal waters have an anisotropic horizontal thermal structure -- greater spatial variation across than along the continental shelf. The late spring to autumn pressure gradient caused by the Bermuda high results in episodic upwelling through local southwesterly winds (Frank and Leggett 1982; Taggart and Leggett 1987; Schneider and Methven 1988) and propagating internal waves (Yao 1986; de Young et al. 1993). The anisotropic physical structure of coastal waters is also augmented by the southward flow of the inshore branch of the Labrador Current (Petrie and Anderson 1983). Anisotropic physical gradients have been shown to influence the distribution of phytoplankton (Iverson et al. 1979; Denman and Powell 1984; Mackas et al. 1985), zooplankton (Herman et al. 1981; Mackas 1984; Ibanez and Boucher 1987), and seabirds (Schneider and Duffy 1985; Briggs 1986; Schneider et al. 1988).

Little work has focused on anisotropic concordance of physical gradients with fish distributions (e.g. Olson and Backus 1985). Capelin are a stenothermal species (Templeman 1948; Scott and Scott 1988; Rose and Leggett 1989) and respond to displacements of horizontal (Buzdalin and Burmakin 1976; Schneider and Methven 1988) and vertical (Methven and Piatt 1991) thermal gradients Therefore a horizontal concentrating of capelin is predicted at a warm/cold water front. The resulting capelin distribution is hypothesized to be patchy at the scale of upwelling cross-shore and patchy at the scale of a capelin aggregation longshore. Schneider and Methven (1988)

and Schneider (1989) examined capelin distribution during upwelling and non-upwelling periods in the Avalon Channel. Capelin aggregations were concentrated at the warm/cold water interface at the scale of upwelling, but analyses were restricted to cross shore transects. The potential anisotropic distribution of capelin aggregations has not been examined in coastal Newfoundland waters.

This chapter quantifies spatial variance in capelin distribution as a function of spatial scale. Long and cross shore spatial variability is compared and contrasted to spatial variance patterns of coastal sea surface temperatures. Sea surface temperatures are used as an example of a passive tracer of the surrounding fluid. Spatial variance patterns of capelin aggregations in synoptic long and cross shore transect pairs are then examined for anisotropy.

3.2 Methods

Hydroacoustic survey were conducted along the northwestern shore of Conception Bay, Newfoundland, from Ochre Pit Cove to Bay de Verde (Fig. 3.1). Transects were oriented parallel and perpendicular to shore, the majority forming a large letter "E" (Fig. 3.1). The location of fishing gear in the area dictated the proximity of long and cross shore transects to the coastline. Transect length was set at 10 kilometres, a distance corresponding to approximately twice the first internal radius of deformation (Rossby radius) at this latitude (Schneider and Methven 1988).

Sea surface temperature ($\pm$ 0.1 °C) was recorded at 60 second intervals using a surface towed thermistor. At the start and end of each transect, water temperature ($\pm$ 0.1 °C) was measured at 5 m depth intervals using an EIL MC5 Salinometer

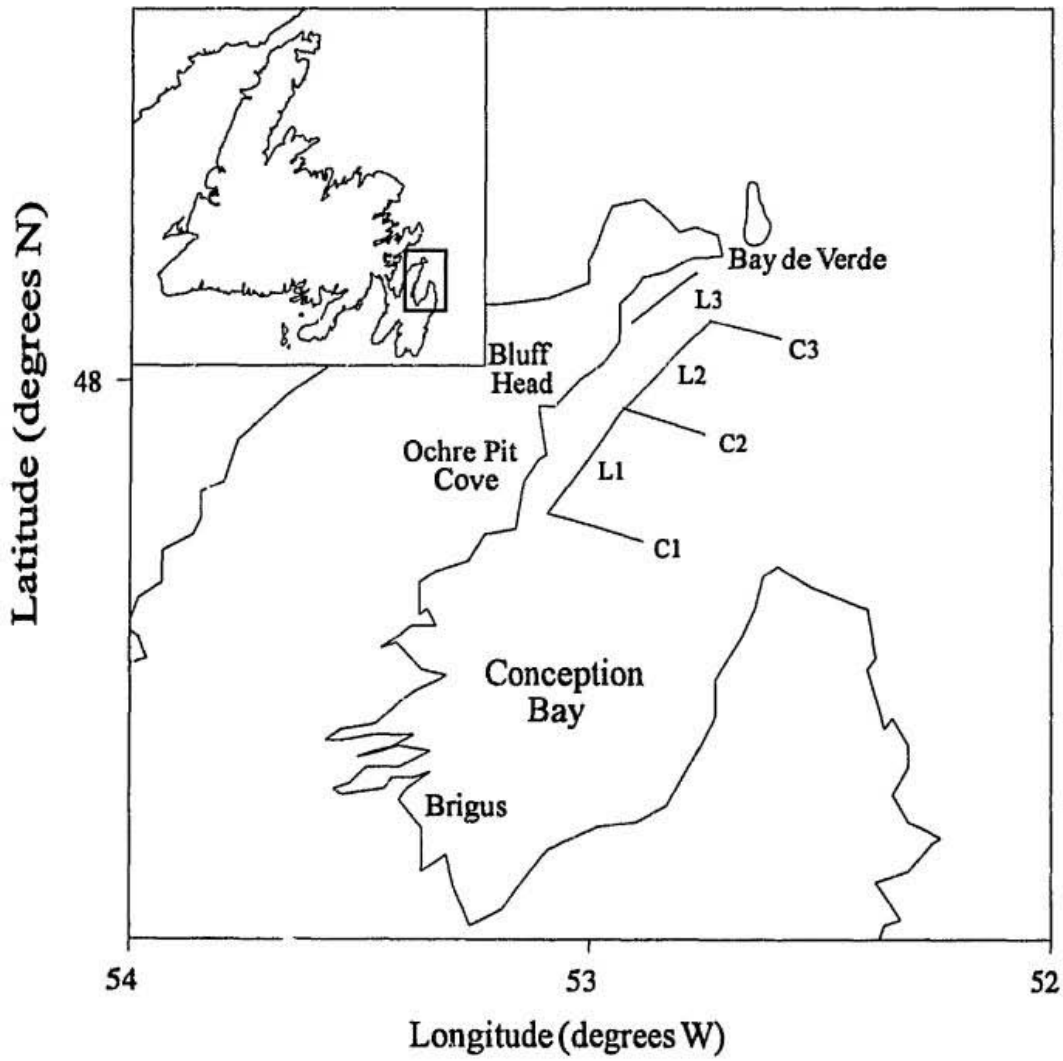

Fig. 3.1 Location of acoustic transects surveyed along the northwestern shore of Conception Bay, Newfoundland. L1, L2, and L3 are longshore transects. C1, C2, and C3 are cross shore transects.

(calibrated to 0 °C). A survey speed of 3.6 m s^{-1} minimized water surface disturbance and disruption of near-surface capelin distribution. Echograms of capelin were obtained using a 50 kHz Furuno 410 paper recording sounder with a beam angle of 19°. Interpretation of traces on echograms as capelin was supported by: simultaneous viewing of near-surface capelin aggregations and traces on echograms, capture of capelin using hook and line while recording traces on echogram, observation and sampling of capelin as the overwhelmingly dominant species in commercial traps in the sampling area, and similarity of echogram traces with those of capelin reported in Newfoundland waters (Atkinson and Carscadden 1979; Whitehead 1981; Piatt 1990). Numbers of discrete capelin aggregations were counted in 100 m horizontal by 5 m vertical blocks from the echogram of each transect. All transect records were scored by one reader and independently verified by another. Wave noise on sounder records was usually distinguishable from fish at the surface but if the two readers disagreed, traces were assumed to be wave noise. The use of a commercial echo-sounder precluded the calculation of absolute capelin abundance because of an uncalibrated time varied gain (TVG). Individual traces were scored equally with contiguous marks on the echogram. The equivalence of single and contiguous echogram traces may result in lowering of mean group abundance and a subsequent underestimate of variance, but this bias is assumed constant across all spatial scales.

Centered spectral analysis was used as an exploratory tool to examine scale-dependent spatial variability in capelin distribution and sea surface temperature data. The spectral density of a continuously recorded variable indicates how the variance of a data series is distributed over a range of frequency bands (Jenkins and

Watts 1968; Koopmans 1974; Chatfield 1980). The range of frequency bands is determined by the length of the series and the sampling resolution. The observational window for any series extends from half the length of the series to twice the sample resolution. Spectral densities were estimated using BMDP1T statistical package (Dixon 1983). A preliminary analysis used three smoothing windows between 0.04 to 0.15 cycles km^{-1}. A smoothing window of 0.10 cycles km^{-1} was chosen as a compromise between accuracy and smoothness and was used in comparative analyses. All spectral density estimates were normalized to permit direct comparison of survey transects (Denman 1975).

3.3 Results

A total of 32 transects, 20 longshore and 12 cross shore, were surveyed between June 26 and July 15, 1990 (Table 3.1). All transects were surveyed between dawn and dusk (05:30 -- 21:30 NDT) over three week periods. Speed over bottom in all transects averaged 3.58 m s^{-1} with a range of 2.58 m s^{-1} to 5.01 m s^{-1}. Spatial resolution of capelin distribution data was set at 100 m horizontal by 5m vertical blocks with a corresponding horizontal temporal resolution of 27.9 seconds. Transects were temporally separated by a minimum of 50 minutes while water column temperature was profiled.

Capelin group distributions were hypothesized to have a Poisson distribution. A G-test with Williams' correction (Sokal and Rohlf 1981) was carried out on the frequency distribution of capelin groups (3664 blocks had 0 capelin present, 683 blocks had 1 group, 81 blocks had 2 groups and 6 blocks had 3 groups; coefficient of

Table 3.1. Start and end locations of acoustic transects sampled in northwestern Conception Bay, 1990. Longshore transects are designated L1, L2, or L3 followed by a transect number. Cross shore transects are designated C1, C2, or C3 followed by a number. Sum is the total number of capelin aggregations observed over the length of the transect. Mean is the average number of capelin aggregations observed per 100 m horizontal block.

Start	End	Transect-Number	Date	Start Time	Sum	Mean
Ochre Pit Cove	Bluff Head	L1-1	26/6	12:35	29	0.305
Bluff Head	Ochre Pit Cove	L1-2	26/6	14:00	35	0.368
Ochre Pit Cove	Bluff Head	L1-5	27/6	7:56	7	0.070
Ochre Pit Cove	Bluff Head	L1-7	4/7	7:04	22	0.214
Ochre Pit Cove	Bluff Head	L1-11	4/7	11:13	9	0.091
Ochre Pit Cove	Bluff Head	L1-15	5/7	9:48	6	0.057
Ochre Pit Cove	Bluff Head	L1-19	12/7	15:32	1	0.010
Bluff Head	Bay de Verde	L2-16	5/7	10:40	26	0.260
Bluff Head	Bay de Verde	L2-20	12/7	16:28	1	0.010
Bay de Verde	Bluff Head	L2-23	13/7	8:51	75	0.528
Bluff Head	Bay de Verde	L2-26	13/7	12:28	52	0.482
Bay de Verde	Bluff Head	L2-31	14/7	5:50	42	0.372
Bluff Head	Bay de Verde	L2-32	14/7	7:03	8	0.059
Bay de Verde	Bluff Head	L2-35	14/7	18:15	59	0.450
Bay de Verde	Capelin Cove	L3-27	13/7	13:37	19	0.275
Capelin Cove	Bay de Verde	L3-28	13/7	15:09	24	0.338

Table 3.1 (cont'd) Start and end locations of acoustic transects sampled in northwestern Conception Bay, 1990. Longshore transects are designated L1, L2, or L3 followed by a transect number. Cross shore transects are designated C1, C2, or C3 followed by a number. Sum is the total number of capelin aggregations observed over the length of the transect. Mean is the average number of capelin aggregations observed per 100 m horizontal block.

Capelin Cove	Bay de Verde	L3-33	14/7	8:13	11	0.149
Bay de Verde	Capelin Cove	L3-34	14/7	9:57	12	0.200
Bay de Verde	Capelin Cove	L3-37	14/7	20:42	21	0.300
Capelin Cove	Bay de Verde	L3-38	14/7	21:32	40	0.571
Ochre Pit Cove	offshore	C1-3	26/6	15:15	8	0.093
offshore	Ochre Pit Cove	C1-4	26/6	16:23	13	0.130
offshore	Ochre Pit Cove	C1-10	4/7	10:12	17	0.167
offshore	Ochre Pit Cove	C1-14	4/7	14:40	3	0.031
Bluff Head	offshore	C2-8	4/7	8:07	70	0.680
Bluff Head	offshore	C2-12	4/7	12:14	20	0.194
Bluff Head	offshore	C2-24	13/7	10:35	11	0.113
offshore	Bluff Head	C2-25	13/7	11:34	16	0.170
Bay de Verde	offshore	C3-21	13/7	6:36	29	0.246
offshore	Bay de Verde	C3-22	13/7	7:43	52	0.416
Bay de Verde	offshore	C3-29	13/7	15:59	5	0.051
offshore	Bay de Verde	C3-30	13/7	16:59	13	0.161

dispersion = 1.035 (A value of 1 indicates a random distribution)). The observed distribution did not deviate significantly from a Poisson distribution ($G=3.978$, $df=2$, $n=4434$, $p=0.1368$) allowing for a 5% Type I error.

Centered, normalized capelin and surface temperature spectral density estimates were calculated for transects having more than 1 capelin aggregation (30 of 32). Pattern detection in spectral density plots was partially dependent on presentation. Plots of spectral densities as a function of frequency (Fig. 3.2a) compressed spatial variability distribution patterns at frequencies less than 1 cycle km^{-1} and obscured patterns at frequencies greater than 1 cycle km^{-1}. Common logarithms of spectral density estimates plotted as a function of frequency only expanded patterns at mid (1 cycle km^{-1}) to high (5 cycles km^{-1}) frequencies (Fig. 3.2b). Transforming spectral density estimates and frequencies to common logarithms (Fig 3.2c) provided a workable compromise. The distribution of spatial variance was discernable at all frequencies and plots were comparable to those of Weber et al. (1986). The slope of the curve is equal to the exponent of a power function across all frequencies but areas under the curve do not represent equal contributions to the sample variance (Denman, 1975).

Spatial variability of capelin distribution in long and cross shore transects was approximately uniform over scales ranging from 10 km to 200 m (Fig. 3.3 a-f). Spectral density estimates were larger and curves were smoother at frequencies less than 1 cycle km^{-1} in all 6 sets of long and cross shore transects. Episodic variation in any single transect was observed at frequencies greater than 1 cycle km^{-1}. Using the colours of the visible spectrum to designate dominant scales of variance, the slight negative slope and non-uniform variation at high frequencies is characterized as being

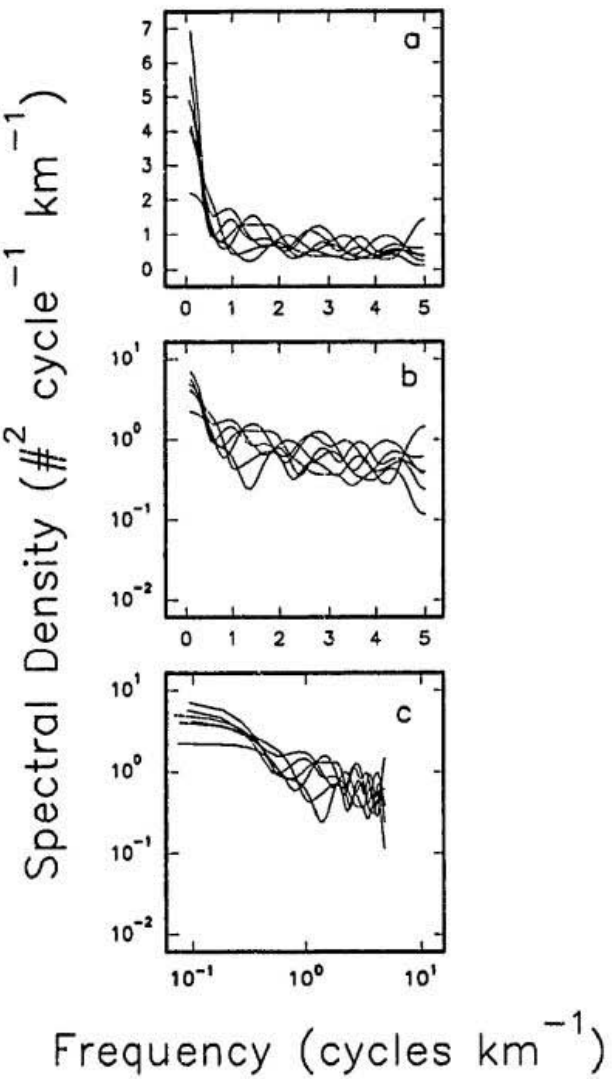

Fig. 3.2 Presentation of capelin aggregation spectral density plots (bandwidth 0.10, centered, normalized). a) Raw spectral densities plotted as a function of frequency. b) Log_{10} spectral densities plotted as a function of frequency. c) Log_{10} spectral densities plotted as a function of log_{10} frequency.

pink with blue ripples. Pink refers to a slight negative slope from large to small scales. Blue ripples refers to the aperiodic peaks of spatial variance observed at small scales. The distribution of spatial variance did not qualitatively differ between long- and cross shore transects.

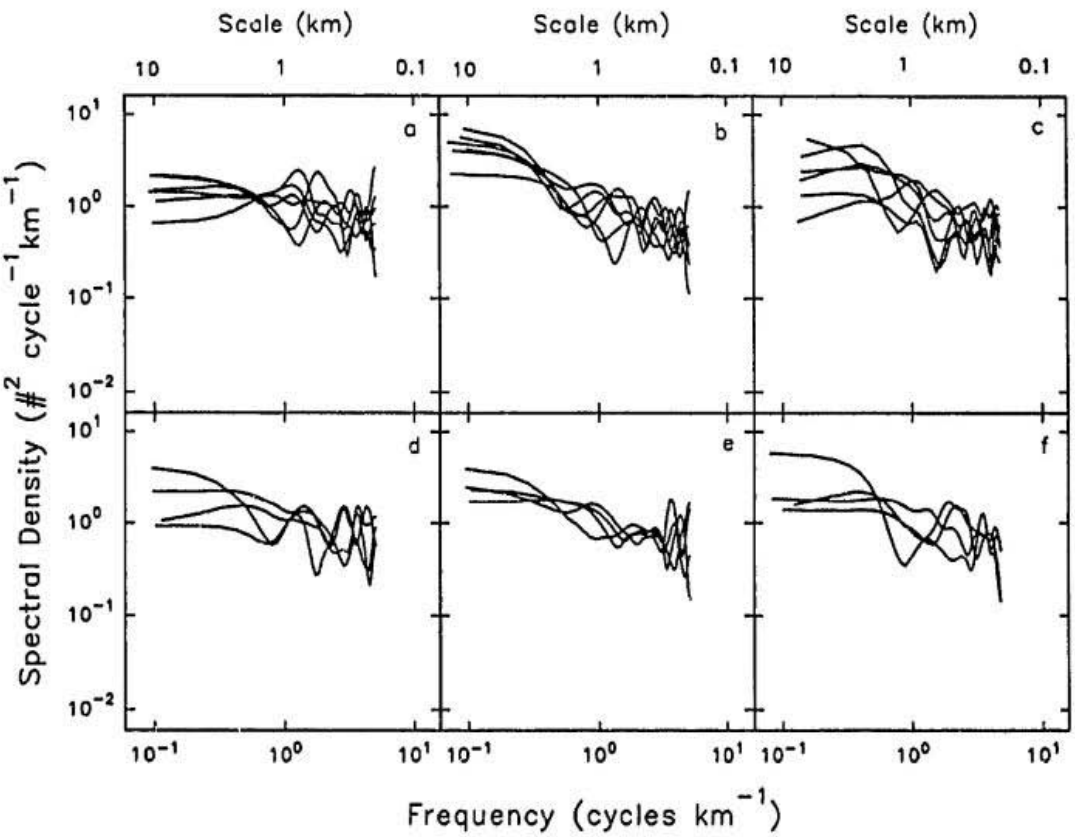

Fig. 3.3 Capelin aggregation spectral density estimates (bandwidth 0.10, centered, normalized) plotted as a function of frequency. Longshore transects a) L1, b) L2, c) L3 are contrasted with cross shore transects d) C1, e) C2, and f) C3. Periods (km) are shown on the upper X axis.

If capelin distribution is tightly coupled to near-surface water temperatures then longshore transects were predicted to have relatively constant variance over a large range of scales while cross shore variance was predicted to peak at the frequency corresponding to the Rossby radius (approximately 0.2 cycles km^{-1} at 47° north latitude). Consistent spectral density patterns were not observed among 7 synoptic pairs of long- and cross shore capelin distribution plots (Fig. 3.4). Cross shore spectra exceeded longshore spectra in only 4 of the 7 pairs at frequencies greater than 0.2 cycles km^{-1}. Long- and cross shore spectra were highly variable at frequencies greater than 1 cycle km^{-1}. Time intervals between long- and cross shore transects did not exceed 75 minutes. Little evidence of anisotropic capelin distribution was observed in long- and cross shore transect pairs.

Long- and cross shore surface temperatures were relatively consistent (range 7 °C - 11 °C) throughout the survey period. Temperature fluctuations on any repeated transect were limited to 2 °C over the three week periods. Strong upwelling events, indicated by large cross shore surface temperature discontinuities, were not observed at the times of sampling. Vertical temperature profiles were also consistent throughout the study. A temperature drop of 7 °C usually occurred in the upper 35 m with a strong thermocline between 15 and 25 m. Transects surveyed during or immediately after wind events had uniform temperatures to 5 m depth, then dropped in a series of 1 °C temperature steps for each 10 meters in depth. Near-bottom temperatures typically ranged between 0 °C and 1 °C. Surface temperatures at inshore transects varied little or not at all within one day. Between days surface cooling or warming was observed,

Fig. 3.4 Synoptic long (solid line) and cross (crossed line) shore capelin aggregation spectral density estimates (bandwidth 0.10, centered, normalized) plotted as a function of frequency. Transect numbers correspond to those listed in Table 1. a) Longshore transect L1-2, cross shore transect C1-3. b) Longshore transect L1-7, cross shore transect C2-8. c) Longshore transect L1-11, cross shore transects C1-10 and C2-12. d) Longshore transect L2-23, cross shore transect C3-22. e) Longshore transect L2-26, cross shore transect C2-25. f) Longshore transect L3-28, cross shore transect C3-29.

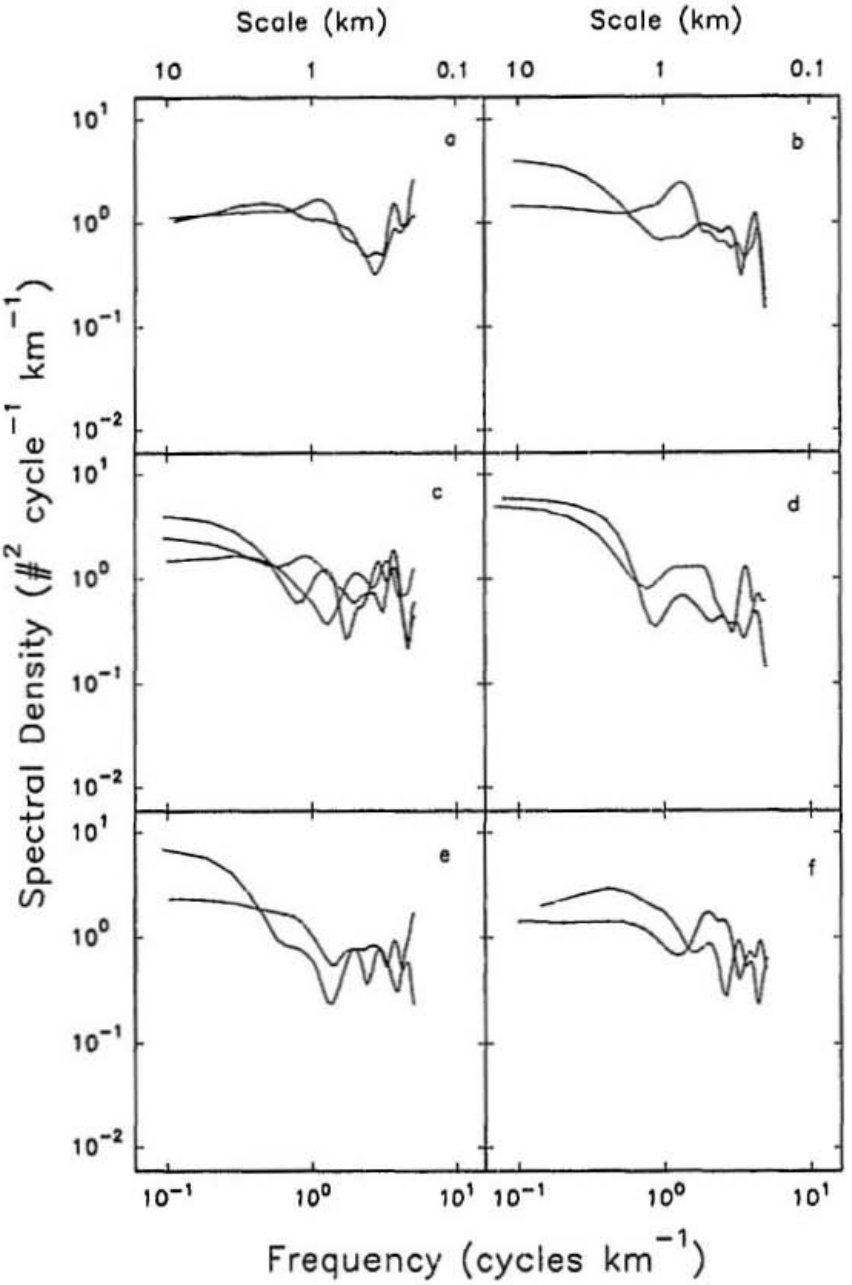
Scale (km)
Scale (km)
10
1
0.1
10
1
0.1
a
b
c
d
e
f
Spectral Density (#^{2} cycle^{-1} km^{-1})
Frequency (cycles km^{-1})

and between weeks surface temperatures fluctuated 2 °C while all other depths warmed 3-4 °C. Temperature sampling was thus considered synoptic over temporal scales of minutes, hours and days.

Surface temperature spectral density estimates among long and cross shore transects were greatest at the largest sampling scales (10 km) and generally decreased monotonically with sampling frequency (Fig. 3.5 a-f). Large portions of the sample variance were found at scales greater than 1 km in all 6 sets of long and cross shore transects. This pattern is a characteristic "red" spectrum where large portions of the sample variance are found at low frequencies and rapidly decrease as frequency increases. Anisotropic surface temperature gradients predict longer dominant scales of spatial variance relative to cross shore scales but distinct peaks in cross shore spectra at the scale of the Rossby radius (0.2 cycles km^{-1}) were not observed. Contrary to prediction, spectral density patterns observed in longshore transects did not qualitatively differ from cross shore transects.

Average long and cross shore surface temperature spectral density plots were steeper than long and cross shore capelin distribution spectral density plots (Fig. 3.6). Surface temperature spectra spanned approximately 2.5 orders of spectral density magnitude with a longshore spectrum slope of -1.38 and a cross shore spectrum slope of -1.31. Average longshore spectral density estimates were not significantly different from average cross shore estimates ($F=0.01$, $p=0.906$, $n=98$). Therefore, long and cross shore average spectral density estimates were used to calculate an overall surface temperature slope of -1.35. Average long and cross shore capelin distribution spectra were much flatter than surface temperature spectra, spanning a single order of

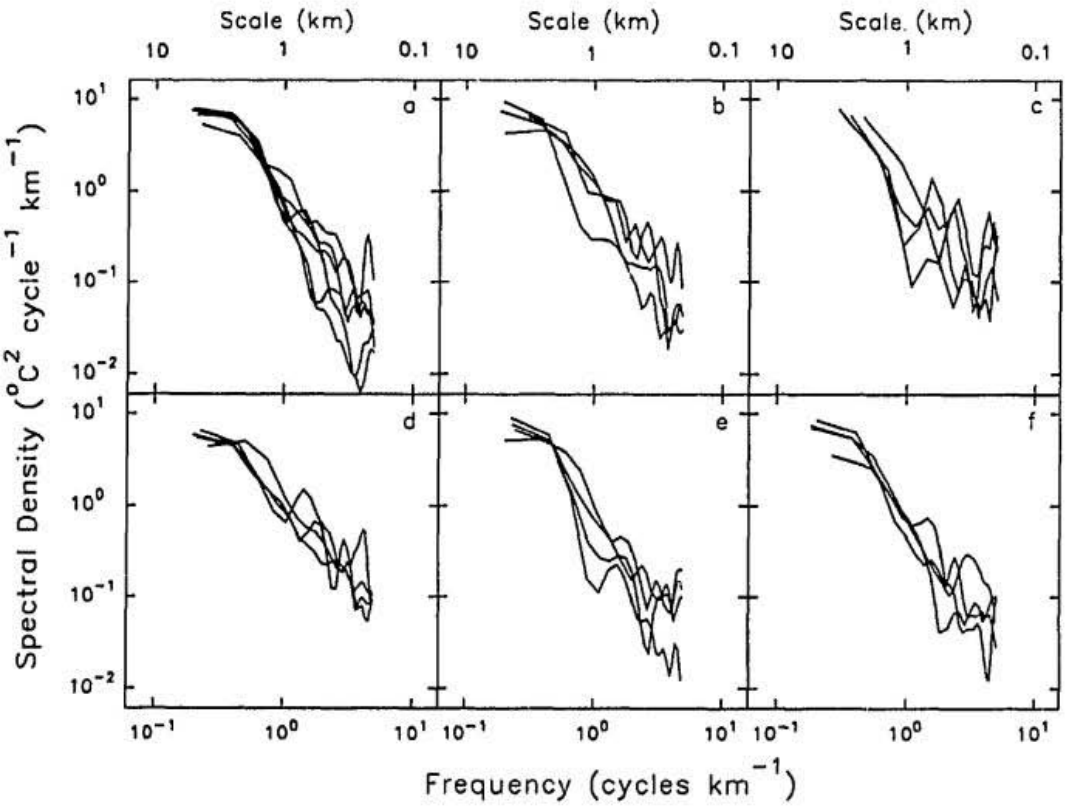

Fig. 3.5 Surface temperature spectral density estimates (bandwidth 0.10, centered, normalized) plotted as a function of frequency. Longshore transects (a-L1, b-L2, c-L3) are contrasted with cross shore transects (d-C1, e-C2, f-C3). Periods (km) are shown on the upper X axis.

magnitude and having average slopes of -0.44 and -0.37. Longshore spectral density estimates did not differ from cross shore estimates ($F=0.34$, $p=0.563$, $n=98$) and were combined to calculate an average slope of -0.40.

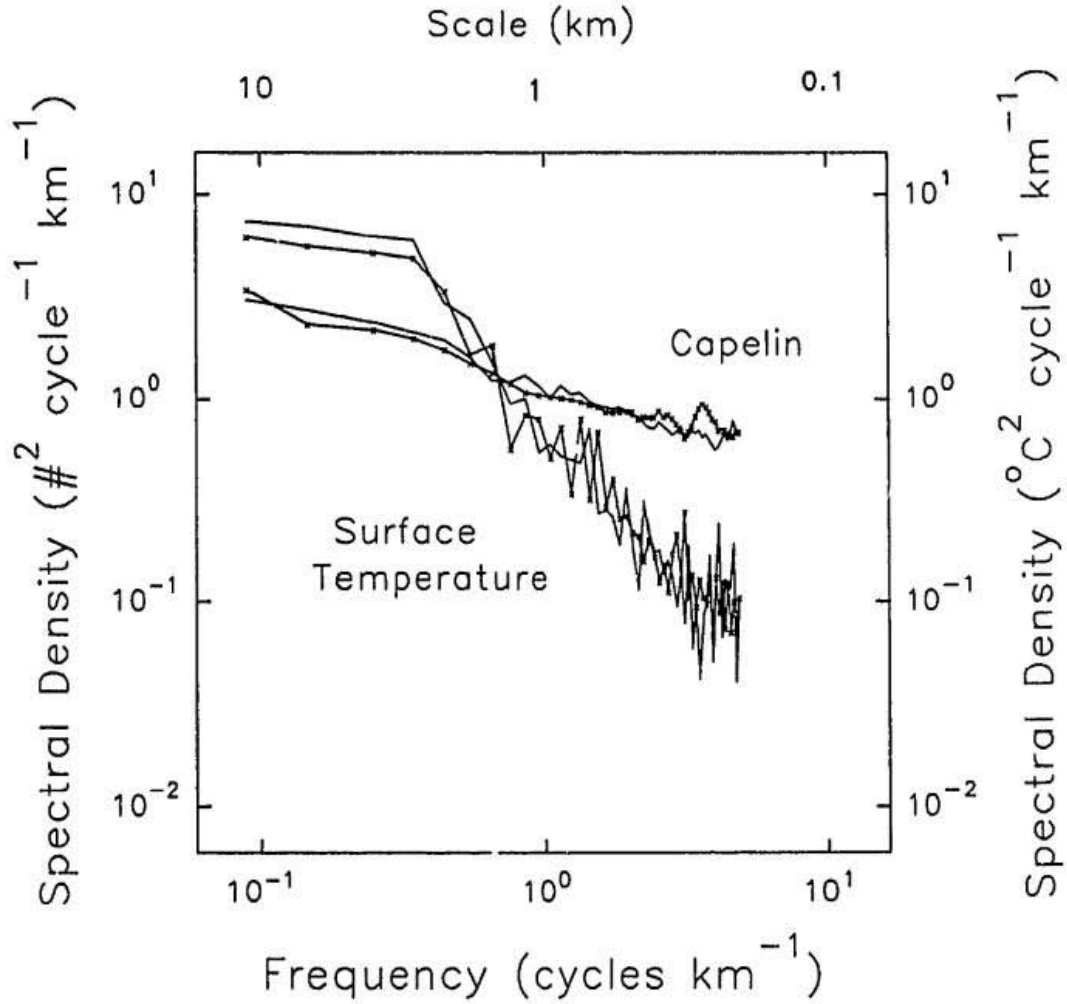

Fig. 3.6 Average capelin aggregation and surface temperature spectral density estimates (bandwidth 0.10, centered, normalized) plotted as a function of frequency. Average longshore estimates (solid line) are plotted with average cross shore (crossed line) estimates.

Observed isotropic capelin aggregation distributions prompted questions about the scales of temporal variance within the 10 km sample length. Plots of capelin aggregation abundance as a function of distance from origin were used to match capelin distributions along repeated transects. Twenty-two repeated transect pairs from the 30 transects had start time intervals ranging from 50 minutes to 17 hours. Based on the average speed of the survey vessel, a kilometer was travelled in 4.7 minutes. Echograms of the two transects were overlaid and the absolute difference in number of capelin aggregations were enumerated in 4.7 minute blocks. Differences in the number of capelin aggregations observed at the same location were predicted to increase as the time interval between two samples increased. The resulting plot showed no consistent divergence with time (Fig. 3.7). Differences at each block were assumed to be independent observations. However, a frequency histogram of the absolute differences in capelin abundances per block was not normally distributed. Association between time interval and absolute differences in capelin aggregations per 4.7 minute block was assessed using Kendall's coefficient of rank correlation (τ). No significant correlations were found between the two variables when all transects were examined as a single group (τ=0.0232, p=0.643, n=205), among longshore transects (τ=0.00043, p=0.995, n=100), or when cross shore transects were grouped together (τ=-0.0024, p=0.973, n=105). Therefore, based on graphical interpretation and rank correlations, there was no observed increased divergence with increased start time interval among repeated transects.

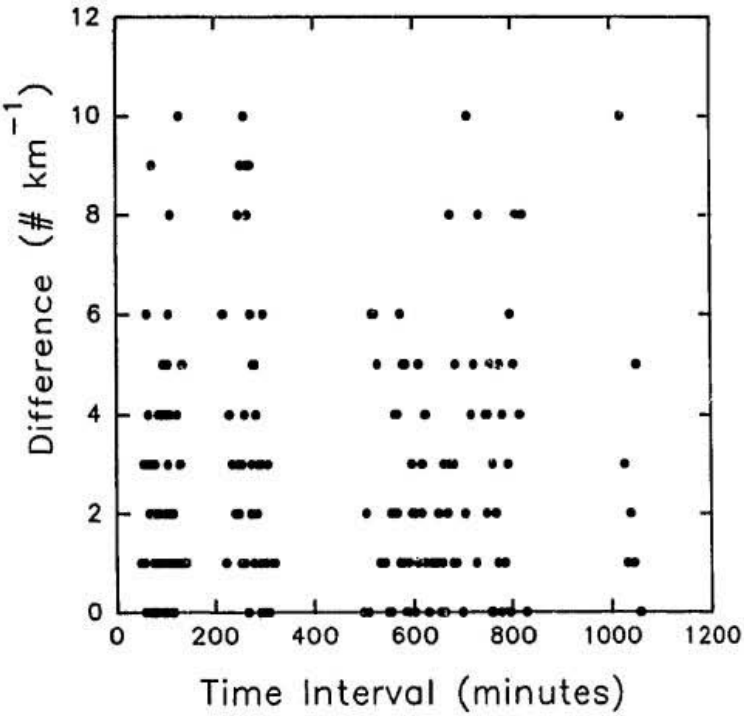

Fig. 3.7 Absolute difference in the number of capelin aggregations per 1 km horizontal block plotted as a function of elapsed time in 22 repeated transect pairs.

3.4 Discussion

Average capelin spatial variance in 20 long and 12 cross shore transects decreased approximately one-half an order of magnitude between 10 km to 200 m scales (Fig. 3.6). Cross shore spectral density estimates were qualitatively similar to longshore estimates, indicating isotropic capelin variability during the sampling period. Large scale surface temperature variation exceeded small scale variation in all surveyed transects. Surface and vertical temperature profiles provided no evidence of upwelling along sampled transects.

Characteristic capelin aggregation sizes or inter-aggregation distances were not observed in long or cross shore composite spectral density plots. Scale-dependent peaks in spatial variance were observed in single transects, but these peaks occurred throughout the 10 km to 200 m scale range. In general, spectral density estimates were greatest at a scale of 10 km and decreased monotonically to a scale of 1 km. At scales less than 1 km, variable amplitude peaks were observed in all 6 sets of spectral density composite plots. This result contrasts with other studies in the northwest Atlantic which identify characteristic capelin patch sizes. Schneider and Piatt (1986) report highly aggregated capelin schools ranging in size from 1.25 to 15 km. Schneider (1989) also observed peaks in capelin spatial variance at 600-1000 m and 2-6 km in the Avalon Channel. The latter patch size matched the scale of wind induced upwelling at the study site. Aggregation dimensions of 3.5 m and 1-4 km were reported for capelin in the northern Gulf of St. Lawrence (Rose and Leggett 1990). Characteristic capelin patch sizes during the present study are outside the range of sampling (larger than 10 km or smaller than 200 m), are temporally very brief (on the order of minutes), or do not exist.

Little evidence was found to support the hypothesized anisotropic capelin distribution in nearshore waters. One possible explanation is the potential for large Type II error (failure to detect a real effect) in non-synoptic long and cross shore paired transect data. A three hour time interval often occurred between the start of the first transect and the end of the second. Paired long and cross shore transects were interrupted at their junction by a hydrography station that profiled water temperature. Given the narrow swath width of the acoustic sampling cone, little lateral movement by

capelin would be required to change distributional patterns over a three hour sampling period. Alternatively, anisotropic distributions of capelin may be a response to horizontal thermal discontinuities caused by upwelling. While previous research has focused on capelin distributions in response to episodic upwelling events (e.g. Templeman 1948; Schneider and Methven 1988; Schneider 1994c), this study shows that predictable gradients in distribution do not occur during non-event periods. Observed surface and upper layer water temperatures along long and cross shore transects were within preferred temperatures (5-10 °C) reported for capelin (Templeman 1948; Rose and Leggett 1989). Isotropic capelin distribution is expected in a homothermal upper water column and the orientation of capelin sampling is therefore not restricted by coastal configuration, unless strong upwelling conditions prevail.

Scale-dependent spatial variability of capelin and sea surface temperature were similar to those observed for krill and sea surface temperature in the Antarctic Ocean (Weber et al. 1986; Levin et al. 1989). Average long and cross shore capelin spectra had slight negative slopes and high frequency variation (pink spectra with blue ripples) while surface temperature spectra peaked at low frequencies and decreased monotonically to high frequencies (red spectra). Capelin spectral average slope (-0.40) was steeper than the average (-0.18) but within the range (0.11 to -0.70) observed for krill. Similarly, northwest Atlantic surface temperature spectral average slope (-1.35) matched the surface temperature spectral average slope (mean -1.66, range -0.74 to -2.48) of the Antarctic. The similarity of capelin and krill spectra and their contrast with surface temperature spectra indicate that biological processes may influence spatial variance patterns of mobile aquatic organisms. This hypothesis is examined in Chapter

4.

As a caveat, capelin and krill average spectral density slopes may not be directly comparable as it is unclear whether krill data had low frequency variation removed (termed pre-whitening in spectral jargon) prior to spectral analysis. Capelin data were not pre-whitened and may be aliased by spatial variance at frequencies below the sampling window. Potential aliasing of low frequency spectral density estimates was checked by combining the data from two consecutive longshore transects. Capelin spectral density estimates of the combined transect exceeded those of composite or average capelin spectral densities at scales larger than 10 km, indicating low frequency trends may still exist in the data.

Observations of pre-spawning capelin over a range of spatial scales has generated hypotheses on potential foraging strategies of capelin predators. At temporal scales of hours to weeks, the slight decrease in capelin spatial variance from large (10 km) to small (200 m) scales indicates that net foraging benefits would be highest at the smallest scale that provides a full ration. Higher energetic demands coupled with small increases in capelin spatial variance would result in lower net foraging benefits if predators increase their average scale of foraging. Episodic concentration of capelin spatial variance at single scales leads to the prediction that predators will shift to larger foraging scales to exploit temporally brief concentrations of capelin. Therefore, capelin-predator coherence is predicted to concentrate at small spatial scales at the temporal scale of a spawning season (approximately 6 weeks every year). However at the scale of a foraging bout (minutes to hours), coherence may be episodically concentrated at any single spatial scale. These hypotheses are examined in Chapter 5.

Chapter 4. Spatial Variance of Mobile Aquatic Organisms

4.1 Introduction

Analyses of krill density distributions (Weber et al. 1986; I evin et al. 1989) indicate that spatial variance of mobile aquatic organisms differs from that of passive tracers (cf. Chapter 1). Mackas and Boyd (1979) were the first to attribute the increase in zooplankton spatial variance, relative to passive tracers, to locomotory behaviour. Examination of biological and physical processes using dimensionless ratios (Chapter 2) confirmed the importance of individual motion independent of the fluid in the generation of capelin spatial variance.

This chapter examines two kinematic processes that potentially influence spatial variance of mobile aquatic organisms at intermediate and small spatial scales: shoaling, and schooling. Shoaling, defined as the convergence of organisms independent of fluid motion, increases small scale spatial variance by altering local densities. Mobility of benthic macrofauna led Jumars (1976) to postulate that distributional variability was locally decoupled from structural features in the environment. By extension, if scale-dependent spatial variance is a function of mobility, then slopes of spatial variance plots should decrease as organism mobility increases (cf. Fig. 8, Fasham 1978). This trend is consistently observed when comparing spatial variance patterns of passive tracers such as surface temperature and phytoplankton to zooplankton (Mackas and Boyd 1979; Star and Mullin 1981; Tsuda et al. 1993). This trend does not extend to spatial variance patterns of larger, more mobile organisms. For example, average slopes of capelin spectral density plots in the southern Labrador Current (Schneider

1994a; Chapter 3) did not differ from those of krill in the Antarctic Ocean (Weber et al. 1986; Levin et al. 1989) over scales of 1 km to 15 km. Patterns in capelin spatial variance could not be attributed to passive motion associated with the surrounding fluid as they did not match spatial variance patterns of surface temperature (Chapter 3). Nor did spatial variance peak at the 5 km scale of coastal upwelling (Schneider 1994a; Chapter 3) predicted from physical theory (Schneider and Methven 1988).

Schooling is a second process that potentially influences spatial variance of mobile organisms at small spatial scales. In contrast to shoaling, schooling is defined as the coordinated movement of a group of aquatic organisms (Pitcher 1986). At scales smaller than the size of an aggregation, even spacing of individuals within groups (Weihs 1973, 1975; Pitcher 1986) should reduce spatial variance of shoaling organisms. This would result in a steeper slope in the spatial variance plot below the scale of an aggregation. Levin et al. (1989) observed a steeper slope at scales less than 1 km than those larger than 1 km in a spectral density plot of krill density. The presence of a change in slope or transition region at the 1 km scale was not emphasized in their study. Their computer simulation using Mangel's (1987) 'patch within patch' model also showed a slight decrease in spatial variance from large to small scales but did not generate a transition at any scale. This result is not unexpected because the spatial range of the simulation did not extend to scales small enough to encompass krill movement into shoals (100 m), Levin et al.'s (1989) proposed factor influencing spatial variance.

Patterns of spatial variance at small scales could also be an artifact of using spectral decomposition techniques to analyze count data. At high sampling resolution,

counts of rare species often contain long stretches of zero counts interrupted by patches of nonzero counts. This contrasts with the continuous presence of physical quantities such as sea surface temperature or salinity. Sampling resolution and organism abundance together determine the mean abundance of any quantity in transect count data. Fasham (1978) found that a decrease in mean abundance caused a reduction in the slope of plankton power spectra when patchy distributions were simulated as doubly stochastic processes. The influence of sampling resolution and the use of a zero bounded variate on spectral density estimates of a continuous data series has not been examined for highly mobile organisms.

Relative density estimates of capelin and Atlantic cod are used to evaluate the influence of shoaling and schooling on scale-dependent spatial variance of mobile marine organisms. Capelin and Atlantic cod were chosen to represent pelagic and semi-demersal mobile aquatic organisms. The contrasting life histories of these two species also permit an investigation of whether the spatial variance of a predator is influenced by that of its prey (Chapter 5).

4.2 Methods

4.2.1 Sampling Procedure

Hydroacoustic surveys were conducted along the western coast of Conception Bay, Newfoundland during the latter half of July and the first week of August, 1991. Linear transects were oriented parallel to the coast within the 100 m depth contour when possible. Stationary fishing gear adjacent to the coast restricted the proximity of

transects to shore. The majority of transects were run during the day but collectively transects span all 24 hours in a day. Transect lengths among the 19 transects used in the analysis varied from 5.5 km to 22.7 km (Table 4.1). Capelin and cod relative density distributions were surveyed using a 120 kHz echosounder (Model 105, Biosonics, Seattle, Washington) with a single-beam 22° transducer mounted in a towed V-fin. Pulse width was 0.8 ms and generated at 2 s^{-1}. Data were heterodyned to 10 kHz using a Biosonics model 171 interface and stored on digital audio tapes for echo integration processing. A calibration tone was recorded at the beginning of each day to standardize playback amplitude levels. The V-fin was towed at a depth of approximately 1.5 m and at a speed of 2.5 m s^{-1}. A pair of 95 Newton expansion springs was used to decouple motions of the boat from that of the V-fin in order to enhance transducer stability. Surface temperature was continuously monitored using a towed thermistor and electronically recorded at 100 m intervals.

4.2.2 Analysis

Acoustic data were integrated using a Biosonics 221 echo integrator which digitally samples voltages at 25 kHz. Relative fish density (RD) estimates were calculated from 20 log R amplified target voltages (V) using an equation from Burczynski (1982):

$$RD_{t,x,z} = \frac{(\sum V_i^2)_{x,z} K_{TVG} K_S}{P_x N_{x,z}} \tag{4.1}$$

Table 4.1. Date, start time, end time, and distance of hydroacoustic transects in Conception Bay, Newfoundland, 1991.

Transect	Date (month/day)	Start time	End time	Distance (m)
9101	7/19	10:47	12:04	11668
9105	7/20	12:47	13:27	5556
9106	7/20	13:43	14:36	7223
9107	7/20	15:05	15:59	8519
9109	7/23	10:17	11:12	8334
9110	7/23	11:39	14:04	19631
9112	7/23	17:22	19:53	23335
9113	7/24	10:36	13:51	20742
9115	7/24	14:04	16:10	19816
9122	7/25	21:03	23:47	22780
9123	7/25	23:59	02:35	20372
9124	7/26	02:44	04:37	14631
9125	8/01	11:26	12:43	10927
9129	8/02	07:43	09:20	10742
9130	8/02	09:34	10:33	8519
9131	8/02	10:44	11:47	6667
3132	8/02	12:32	13:54	9075
9133	8/02	18:00	20:01	9445
9134	8/02	20:08	21:02	8890

where: $RD_{i,x,z}$ is the relative fish density of species i in horizontal bin x (m) at depth interval z (m), $(\sum V_i^2)_{x,z}$ is the squared sample voltages of species i in horizontal bin x (m) at depth interval z (m), K_{TVG} is an empirically determined constant that compensates the $20\log R + 2\alpha R$ amplifier gain for the attenuation of sound α in seawater over R metres, K_S is an empirically determined constant that corrects system parameters to theoretical values, P_x is the number of echo sounder pulses in each horizontal bin, and $N_{x,z}$ is the number of sampled voltages in horizontal bin x at depth interval z.

Data were stratified in 10 m horizontal by 5 m vertical bins to a maximum depth of 112 m. To prevent integration of surface noise or bottom echoes the top 2 m and bottom 1 m of the water column were not included. Each bin was classified as cod or capelin. Cod were distinguished from capelin by: a) classification of targets viewed on an oscilloscope based on signal properties (Rose and Leggett 1988a); b) simultaneous viewing of near-surface capelin aggregations in the water and traces on oscilloscope and echograms; c) capture of capelin and cod using hook and line while recording traces on echograms; d) observation and sampling of capelin and cod as the overwhelmingly dominant species in commercial traps in the sampling area; and e) similarity of echogram traces with those of capelin and cod reported in northwest Atlantic waters (Atkinson and Carscadden 1979; Whitehead 1981; Piatt 1990; Rose 1992). Relative fish densities were integrated vertically to a maximum depth of 112 m and then summed for each 10 m horizontal distance to analyze horizontal variation of capelin relative to cod.

Univariate spectral analysis was used to examine scale-dependent spatial

variability of cod and capelin density distributions. The power spectra of each species was calculated for each transect using the BMDP1T statistical package. Being consistent with Chapter 3, a smoothing window of 0.01 cycles m^{-1} was chosen for comparative analyses as a compromise between accuracy and smoothness. All spectral density estimates were standardized to permit direct comparison of survey transects (Denman 1975). Spectral density estimates of capelin, cod, and surface temperature from each transect were combined and then averaged at a resolution of 0.0001 cycles m^{-1} to produce average spectral density values and plotted as a function of frequency.

The influence of zeros in high resolution count data on patterns of spatial variance was investigated by replacing values of a continuous data series with zeros. The division of a continuous data series into discrete patches is analogous to shoaling by organisms. A 10 km sea surface temperature record with a resolution of 233 m (n=44 data points) was used as the original continuous data series. In each of eight simulations a single temperature value (representing 2.3% of the data) was chosen at random and replaced with a zero. The resulting spectral density estimates were standardized by the variance and plotted as a function of frequency in a common log-log plot. The effects of schooling on patterns of spatial variance were similarly investigated by randomly substituting two consecutive zeros in the original surface temperature data series. Consecutive zero counts result when mobile organisms actively form aggregations and move, creating 'empty' areas along survey transects. The schooling data manipulation was repeated eight times and power spectra were normalized and plotted as a function of frequency.

4.3 Results

4.3.1 Spatial Variance Patterns

At the temporal range of a single transect (ca. 1 h), concentrations of capelin and cod spatial variance occurred throughout the sampled spatial range. Spatial scales of maximum spectral density were not consistent among spatially separated transects, nor within any series of replicated transects. Within the 20 m to 10 km range of analyzed spatial scales, sharp peaks of capelin spatial variance occurred in five of 19 transects. Broader peaks of spatial variance were observed in seven of 19 transects. No concentrations of spatial variance were observed in the remaining seven transects. Among the cod spectral density plots, only two transects contained sharp peaks of spatial variance. An additional seven transects contained peaks in spectral density plots spread over a broader range of frequencies. To provide a representative sample of spatial variance patterns, spectral density estimates of capelin and cod were plotted as a function of frequency for four replicates of a 20 km transect. Spatial variability of capelin in three of four transects (Fig. 4.1a) was similar at all scales ranging from 5000 m to 100 m and then rapidly decreased at smaller scales. Small peaks in spatial variance were observed in spectral density plots of single transects at scales less than 90 m. In contrast, two distinct patterns were present in the plots of cod spectral densities (Fig. 4.1b). Two transects had slight negative slopes down to approximately 80 m and then a sharp decline in spatial variance at smaller scales. Spatial variance of the remaining two transects was approximately uniform across the range of sampled scales. A characteristic pattern of capelin or cod spatial variance was not present among the 19

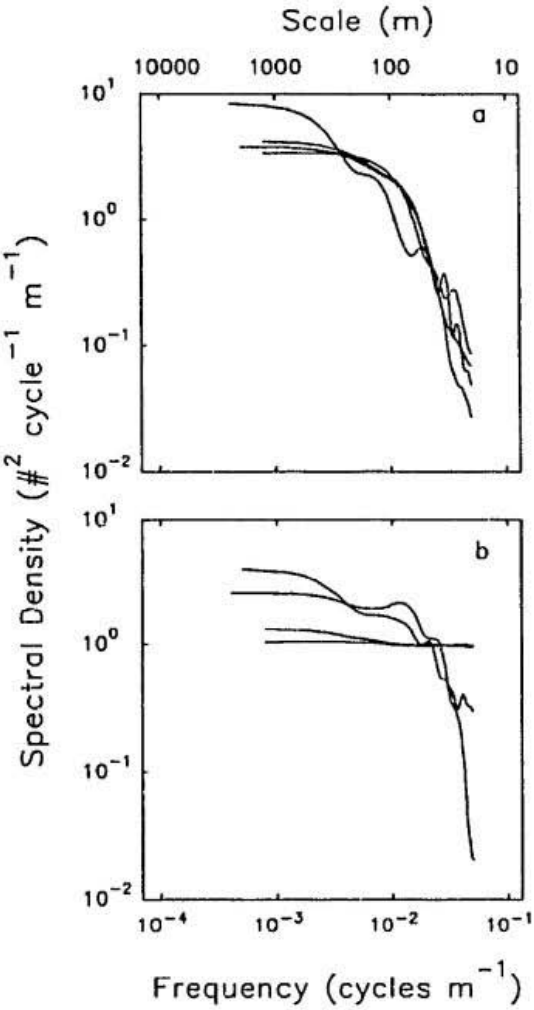

Fig. 4.1 Spectral density estimates of (A) capelin and (B) Atlantic cod (bandwidth 0.01, centered, normalized) plotted as a function of frequency. Periods (m) are shown on the upper X axis. Each graph contains four repetitions of a 20 km transect with a sampling resolution of 10 m located along the western shore of Conception Bay, Newfoundland, Canada.

transects surveyed in Conception Bay.

Spatial variance patterns of capelin and cod over longer temporal scales were examined by averaging spectral density estimates in 0.0001 frequency bins and plotting them as a function of frequency. A characteristic scale of aggregation, indicated by a peak in spatial variance, was not observed in the average power spectra of capelin or cod (Fig. 4.2). Average spatial variance plots of capelin and cod contained two regions of differing slopes separated by a transition region. Slight negative slopes (capelin, -0.21; cod, -0.18) observed at large scales increased to steeper slopes (capelin, -1.05; cod, -1.08) at scales smaller than that of transition regions (capelin $\cong$ 400 m; cod $\cong$ 90 m). An averaged sea surface temperature plot was added to the same graph to compare these spatial variance patterns to those of passive tracers (Fig. 4.2). The steep monotonic slope of the surface temperature power spectrum (-1.06) contrasted to the boomerang-like shape of the capelin and cod power spectra. Average spatial variance of sea surface temperature was concentrated at large scales, a 'red' spectrum in the jargon of spectral analysis. Capelin and cod average spectral density plots had slight negative slopes over a broad range of scales and then decreased rapidly at small scales.

Scales of transition regions in average (n=19) spectral density plots (Fig. 4.2) were compared to tabulations of capelin and cod aggregation sizes. Cumulative frequency distributions of capelin (Fig. 4.3a) and cod (Fig. 4.3b) aggregation sizes (defined as the number of contiguous 10 m blocks with fish present) showed that 98% of capelin aggregations were $\leq$ 400 m (n=2247) and 92.3% of cod aggregations were $\leq$ 100 m (n=642). Distances between aggregations of capelin averaged 46.3 m ($\pm$ 2.0 S.E.)

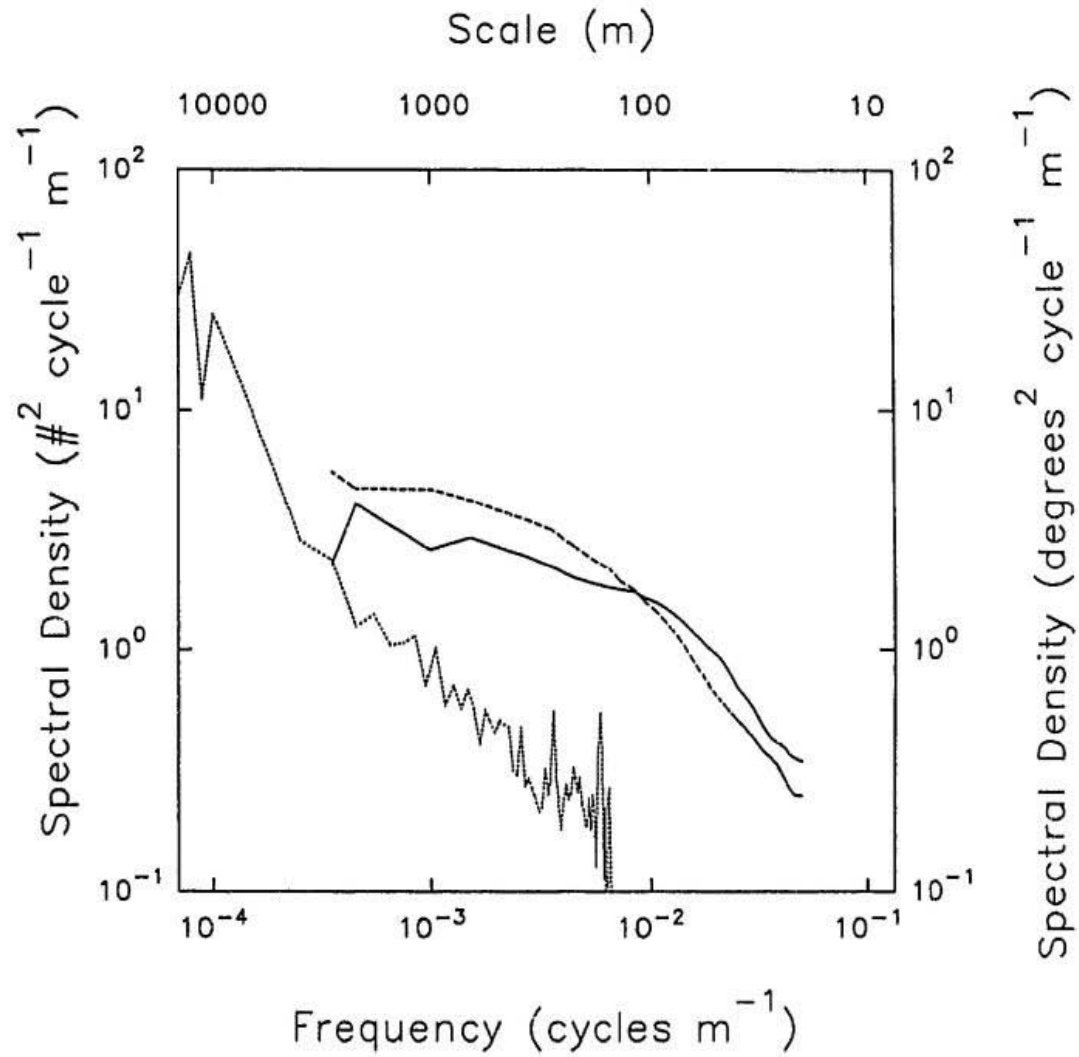

Fig. 4.2 Average (n=19) capelin (broken line), Atlantic cod (solid line), and surface temperature (dotted line) spectral density estimates (bandwidth 0.01, centered, normalized) plotted as a function of frequency. Periods (m) are shown on the upper X axis.

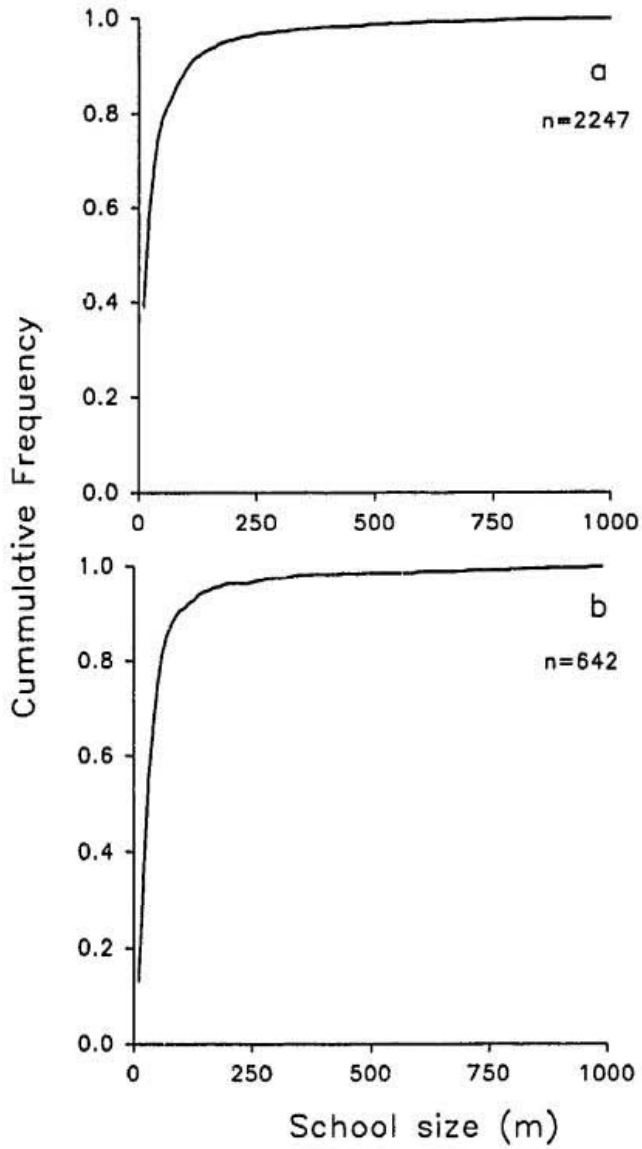

Fig. 4.3 Cumulative frequency histograms of (A) capelin and (B) Atlantic cod shoal sizes. Shoal sizes are tabulated in bins of 10 m. A shoal is defined as the number of contiguous 10 m horizontal blocks with fish present.

compared to 242.5 m (± 24.5 S.E.) for cod. Transition scales in average spectral density plots matched inflection points in cumulative frequency distributions of species aggregation sizes.

4.3.2 Effect of Zeros

The influence of zeros in count data on patterns of spatial variance was examined by randomly replacing values in a surface temperature data series with zeros. Spectral analysis of manipulated surface temperature series showed that substitution of a single zero flattens slopes of power spectra. The slope of the spectral density plot from the original temperature series (Fig. 4.4a) was -2.57 ($n=22$, $r^2=0.962$) compared to an average of -0.36 ($n=176$, $r^2=0.727$) in the manipulated temperature series (Fig. 4.4b). Changes in slope were related to the proportion of zeros substituted in the continuous data series. Similar data manipulations and calculations were made using two other transects 20 km in length with a measurement resolution of 100 m to determine the consistency of this result. Increases in spectral density estimates at small scales occurred in all simulations relative to estimates from the original series.

The substitution of two consecutive zeros in surface temperature series resulted in the formation of a transition region and a decrease in spatial variance at scales below the transition. Slopes from plots of spatial variance as a function of frequency (Fig. 4.4c) decreased slightly at large scales and then dropped sharply below the transition scale of 400 m. The location of the transition frequency was partially influenced by the choice of bandwidth used in spectral analysis. A wider bandwidth smoothed the curve by averaging a larger number of periodogram estimates, often shifting the location of

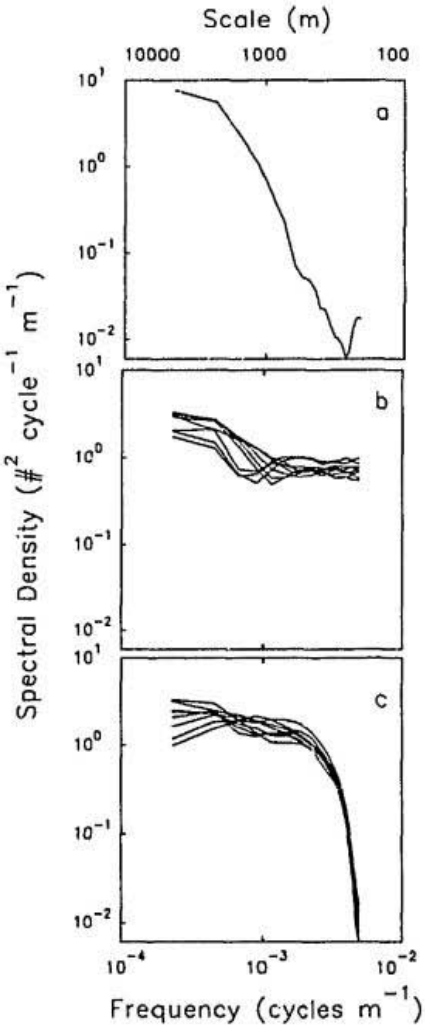

Fig. 4.4 Spectral density estimates of (A) original surface temperature series (length 10 km, resolution 233 m), (B) eight repetitions of surface temperature series with a single zero randomly substituted, and (C) eight repetitions of surface temperature series with two zeros randomly substituted as a block.

the transition to a higher frequency (smaller scale). Similar patterns were consistently observed when data manipulations were repeated using two longer surface temperature data series (20 km) with a higher sampling resolution (100 m). Spectral density plots of manipulated data series resembled patterns observed for capelin and cod.

4.4 Discussion

Spectral analysis of capelin and Atlantic cod relative density data showed that slopes and shapes of spectral density plots were similar to those previously reported for of other mobile marine organisms. At the temporal scale of a single transect spatial variance could be concentrated at any scale. Similar episodic concentrations of spatial variance have been observed in benthic megafauna (Grassle et al. 1975), marine birds (Schneider and Duffy 1985; Schneider 1989), and fish (Schneider 1989; Rose and Leggett 1990). Evaluations of spatial variance at larger temporal scales are less common. When spectral density estimates from individual transects were averaged, capelin and cod spatial variance decreased slightly from large (10 km) to smaller (400-90 m) scales and then dropped rapidly at scales smaller than transition regions. The slight negative slopes of capelin and cod spectra at larger scales contrasted to the more steeply negative slope of the average spectrum of surface temperature, used as an example of a passive tracer of the surrounding fluid. Observed spectral density slopes of capelin and cod were consistent with those of krill in the Antarctic (Weber et al. 1986; Levin et al. 1989). The similarity of slopes in krill and fish spectral density plots contradicts the speculation that the slope of spatial variance becomes flatter as organism mobility increases.

A variety of physical, physical-biological, and biological processes are hypothesized to increase spatial variance at small scales. Based on dye and buoy observations, Langmuir circulation was proposed as a physical process that injects and transfers kinetic energy of passive tracers from small to larger scales (Liebovich 1983; Weller and Price 1988). This transfer is opposite to the 'turbulent energy cascade' commonly assumed for passive tracers in fluids (cf. Fig. 2, Mackas et al. 1985). Rose and Leggett (1988b, 1989) suggested that a combination of biological and physical processes influence the spatial variance and distribution of Atlantic cod. Distribution of cod was attributed to an aggregative response to concentrations of prey, constrained by water column thermal structure. Weber et al. (1986) proposed that swimming behaviour was responsible for the small scale variability in krill biomass distribution that could not be attributed to physical processes. Among biological processes the most commonly proposed mechanism creating spatial variance at small scales is behaviour facilitated by the ability of organisms to move independent of the fluid (Mackas and Boyd 1979; Star and Mullin 1981; Mackas et al. 1985). Scaling arguments (Schneider 1994a; Chapter 2) indicate that among nekton, locomotion relative to the surrounding fluid is the primary source of spatial variance at small scales.

In addition to the proposed kinematic processes, I found that observed patterns of capelin and cod spatial variance could be approximated by randomly substituting zeros in a surface temperature data series. Substitution of a single zero in the surface temperature series is analogous to the divergence of organisms from a point to form two shoals. The resulting reduction in spectral density slope was biologically interpreted as an injection of spatial variance at intermediate scales due to shoaling. In

the second set of simulations, the substitution of two zeros as a block is analogous to the divergence of organisms from a point, forming two shoals and moving as schools. Spatial variance in spectral density plots of these manipulated series decreased at frequencies higher than a transition region. This pattern was similar to the drop in spatial variance in the average spectral density plots of capelin and cod. I attribute the rapid drop in spatial variance at small scales to uniform spacing of fish within schools. Experiments using live fish to test the reduction of spatial variance at small scales due to shoaling or schooling have not been conducted (cf. Pitcher and Parrish 1993).

The presence of zeros in count data potentially introduces an additional source of variance when analyzed with spectral decomposition techniques. Zero counts in transect data can arise from two sources: high resolution sampling, and convergent behaviour of animals. High resolution sampling (small bin sizes) combined with low organism abundance lowers the mean abundance per sample thereby increasing the probability of getting a zero count. Fasham (1978) showed that as the mean count per sample decreased, slopes of spectral density plots also decreased. Zeros in transect counts can also result from biological processes. Sampling patchily distributed organisms such as capelin will result in a higher proportion of zeros compared to the proportion of zeros in counts of more uniformly distributed organisms (e.g. gelatinous zooplankton, cf. Schneider and Bajdik 1992). These effects are amplified when mean abundances are low.

Two methods can be used to separate biological spatial variance from sampling artifacts. The first method subtracts sampling error variance from the total variance in a series. Mackas (1977) proposed that the total variance in zooplankton distribution

data was an additive function of variance due to patches formed by the organism and variance due to random sampling error. Bias due to sampling error is a function of the mean organism count and the number of frequencies analyzed. When bias due to sampling error is large, a Poisson-distributed variance component can be subtracted from spectral density estimates at each frequency (Mackas 1977). Adjusting spectral density estimates by subtracting an error component will have a greater effect at high frequencies. Spectral density estimates generally do not require bias correction except in the vicinity of sharp spectral peaks (Mackas 1977). A second approach to isolating biological spatial variance is to examine the probability of getting a zero count as a function of sample mean. The probability of encountering patchily distributed organisms can be modeled as a Poisson point process. A Poisson distribution is a convenient theoretical distribution used to describe the number of times a zero count potentially occurs in rare and randomly distributed organisms. If the accepted probability of randomly obtaining a zero count in a Poisson process is arbitrarily set to 0.05, then spatial variance can be assessed at sampling resolutions with mean counts equal to or greater than three (cf. Fig. 5.3, Sokal and Rohlf 1981). A plot of mean count as a function of sample size will identify the minimum resolution (measurement frequency) at which the mean count per sample equals three. This scale can then be used to define a minimum scale of biological interpretation. An increase in slope of spectral density plots is inevitable below this resolution, due to an increased number of random zero counts. Caution must be exercised if spectral density estimates are biologically interpreted at scales smaller than the minimum interpretation scale.

Spectral density and coherence estimates of capelin and cod were not adjusted for

random sampling error in this study. Capelin and cod power spectra did not contain strong peaks similar to those seen in plots of passive tracers. In addition, plotting mean density as a function of bin size was not possible due to a lack of absolute fish densities. Species specific target strengths are needed to convert relative to absolute densities. Target strengths were not measured in this study. Despite the lack of target strengths, concentrations of capelin and cod were not predicted to drop below 3 fish per bin within aggregations because aggregation sizes of both species were at least nine times larger than the sample resolution. At scales smaller than the scale of transition, interpretation of spectral density plots was restricted to a comparison of slopes in average spectral density plots.

Comparison of results from this study to spatial variance patterns of Antarctic krill (Weber et al. 1986; Levin et al. 1989) revealed similar features in spectral density plots. At the temporal scale of a single transect, episodic concentrations of spatial variance occurred in plots of capelin, cod, and krill. Characteristic patch sizes, indicated by concentrations of spatial variance at a single scale, were not observed. At larger temporal scales, average spectral density plots contained two regions of differing slopes separated by a transition region. Spectral density slopes of these plots were less than those of passive particles at large spatial scales, but the reduction in slope did not increase as organism mobility, based on body size, increased. At scales smaller than the transition region, slopes of spectral density plots were steeper than those at large spatial scales.

To assess whether these patterns occur more generally among mobile aquatic organisms, all available estimates of spatial variance were plotted in a single diagram.

Figure 4.5 contains average spectral density estimates of phytoplankton, Antarctic krill, capelin, Atlantic cod, and two marine birds -- common murres (*Uria aalge*) and Atlantic puffins (*Fratercula arctica*). Murres and puffins nest on rocky areas along the Newfoundland coastline, feeding extensively on capelin while rearing chicks (Brown and Nettleship 1984). Spectral density estimates of murres and puffins (bandwidth 0.1) from 35 transects were standardized and then averaged over 0.01 cycle km^{-1} bins (D. Schneider unpublished data). A conspicuous feature of Fig. 4.5 is the pairing of spectral density plots by taxonomic group. Spectral density plots of murres and puffins overlap, as do the two krill spectra and the two plots of capelin and cod. Magnitudes of marine bird spectral densities were intermediate between those of plankton and fish. This is attributed in part to differences in mean abundances. Data series with small abundances typically have low means and variances. Spectral density estimates rise when divided by a low variance to standardize variances among transects.

As expected, the spectral density slopes of phytoplankton differed from those of mobile organisms at large and intermediate scales. At scales larger than transition regions, the slope of the phytoplankton spectral density plot was always steeper than slopes of mobile organism plots. Spatial variance patterns of mobile aquatic organisms did not follow the 'turbulent energy cascade' proposed for passive tracers of the surrounding fluid. The reduced slope among mobile organisms is consistent with the hypothesized injection of kinetic energy due to the convergence of individuals into shoals at transition scales.

The most interesting feature in Figure 4.5 is the similarity of spatial variance patterns among mobile organisms. Average power spectra of krill, marine birds and

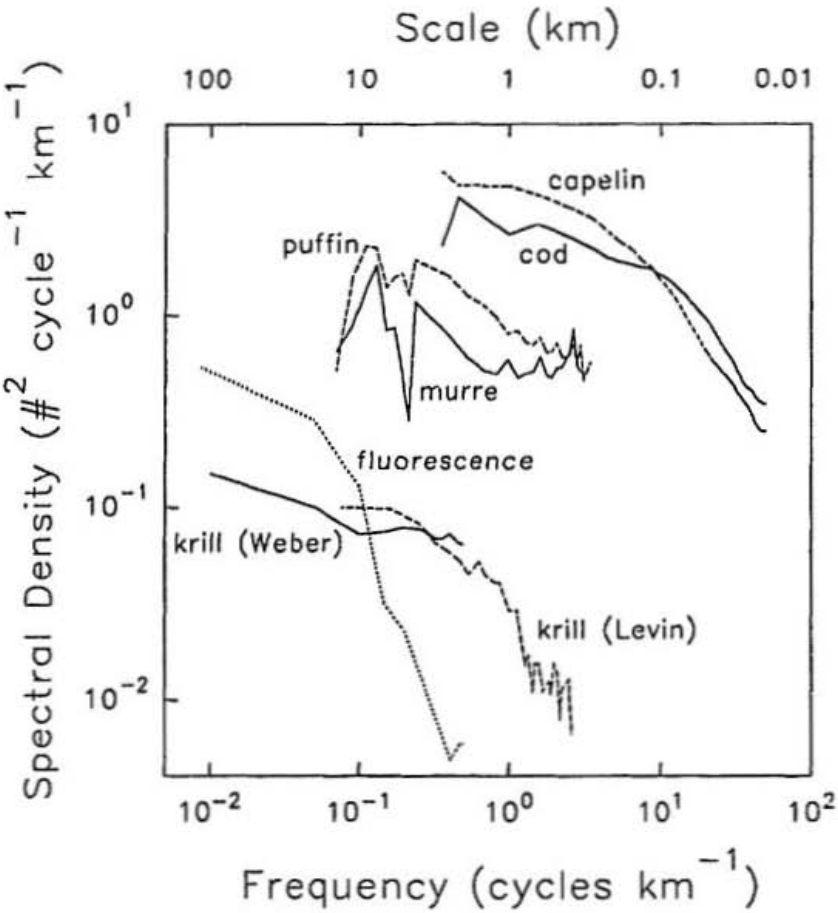

Fig. 4.5 Average spectral density estimates of capelin (broken line), Atlantic cod, Atlantic puffin (broken line), common murre, Antarctic krill (Weber et al. 1986), Antarctic krill (dotted line) (Levin et al. 1989), and fluorescence as an index of phytoplankton (Weber et al. 1986) plotted as a function of frequency. Phytoplankton is plotted as a dotted line to distinguish spectral density plots of mobile organisms from passive tracers of the surrounding fluid. Periods (km) are shown on the upper X axis.

fish all contained two regions of differing slopes separated by a transition region. The steeper slopes of spectral density plots below transition regions were interpreted as reductions in spatial variance due to the regular spacing of organisms within aggregations. The anomalous dip in the power spectra of common murres is attributed to the association of murres with upwelling events at the spatial scale (5 km) of a Rossby radius (Schneider 1989).

Transition regions in spectral density plots of mobile organisms naturally demarcate domains of spatial variance. Ranges of these domains can be formalized using fractal geometry (Mandelbrot 1982). The degree of self-similarity across spatial scales is quantified by converting slopes of spectral density plots to Hausdorf or fractal dimensions (Bradbury et al. 1984; Sugihara and May 1990; Schroeder 1991). A constant value over a range of scales defines a domain that may be generated by a single process (Sugihara and May 1990). Large changes in fractal dimensions indicate scales where there may be a shift in processes that generate spatial variance (Mandelbrot 1982). Among capelin and cod, I found evidence of a shift from shoaling to schooling at scales smaller than transition regions.

Spatial variance domains have two important implications. First, spatial variance domains limit the range of research conclusions (Sugihara and May 1990). Ecosystem process models should not be extrapolated beyond domain boundaries just as regression models should not be generalized beyond limits of sampled data. A second practical application of spatial variance domains is the reduction of field survey costs. By setting sample resolution equal to the smallest spatial scale within a domain, survey costs are minimized and the results can be extrapolated throughout the domain. This indicates

that a wider application of fractal geometry may provide clues to processes that influence spatial distributions of organisms and be used to delineate the range of scales over which they operate.

Spectral analysis was chosen as an analytic tool because it has the advantage over other techniques of simultaneously analyzing variance at several scales. Advantages and disadvantages of statistical techniques used to describe spatial patterns are evaluated in Chapter 7. Despite this advantage, the sensitivity of spectral analysis to the presence of zeros prevents it from being ideally suited to the analysis of patchily distributed, rare organisms. I suggest there is a need for better quantitative tools that assess spatial and temporal variance of count data.

Chapter 5. Spatial Coherence of Mobile Aquatic Organisms

5.1 Introduction

Quantifying interactions between predators and prey continues as a dominant theme in ecology. Theoretical models of this interaction have largely been limited to either the spatial scale of an individual organism or to that of the population (for reviews see Levin 1976; Chesson 1978; Taylor 1988, 1990; Hastings 1990; Reeve 1990; Kareiva 1990; Berryman 1992). At these two spatial scales the dependence of observed patterns on measurement scale has been identified (Waage 1979; Morrison and Strong 1980; Heads and Lawton 1983; Hanski 1991) and the necessity of multiscale quantification of predator-prey theory is regularly expressed in the literature (e.g. Hassell and May 1973; Anderson and May 1985; Holdbrook and Schmitt 1988; Kareiva 1990; Aronson 1992; Schneider 1994a). Quantifying the scale-dependence of predator-prey interactions requires comparison of results over a wide range of spatial scales.

Several recent studies have examined whether mobile, aquatic predators are associated with prey at characteristic spatial scales (Table 5.1). All field surveys cited report spatial scales of maximum association between predators and prey. These conclusions are based on single or a limited number of transects which implicitly represent short temporal scales. Scales of maximum predator-prey association were then matched to dominant physical processes to explain observed patterns of biological variance. This approach assumes that biological pattern is created by physical processes at the same scale. Direct coupling between biological and physical processes

Table 5.1. Spatial scales of maximum covariation among mobile, aquatic predators and their prey.

Predator	Prey	Scale of maximum covariation					Source
		>100 km	100 to 10 km	10 to 1km	1km to 100m	<100m	
Zooplankton	Phytoplankton			1 km			Mackas and Boyd 1979
Zooplankton	Phytoplankton		10 km	1 km	<1 km		Star and Mullin 1981
Krill	Phytoplankton			2.5 km			Weber et al. 1986
Krill	Phytoplankton	500 km					Miller and Monteiro 1988
Birds	Zooplankton		10 to 100 km				Heinemann et al. 1989
Birds	Zooplankton			>5 km			Hunt et al. 1990
Fish	Fish		10 to 20 km	<5 km		3.5 m	Rose and Leggett 1990
Birds	Fish			>1 km			Safina and Burger 1985
Birds	Fish			2 to 6 km	0.25 km		Schneider and Piatt 1986
Birds	Fish			>1 km			Safina and Burger 1988
Birds	Fish			5 km			Schneider 1989
Birds	Fish			>1 km			Erikstad et al. 1990
Birds	Fish			5 km			Piatt 1990

at the same scale is often hypothesized when prey organisms, such as phytoplankton, move passively with the surrounding fluid (e.g. Legendre and Demers 1984; Mackas et al. 1985). The previous chapter demonstrated that spatial variance patterns of organisms that move independent of the fluid do not commonly match those of physical quantities (see also Weber et al. 1986; Levin et al. 1989; Schneider 1994c).

Characteristic scales of interaction between predators and prey may also be influenced by biological processes such as the aggregative response of predators to concentrations of prey (Holling 1965, 1966; Murdoch and Oaten 1975). Concentrations of prey potentially influence the spatial variance patterns of predators and the scale of maximum spatial association between predators and prey. The influence of aggregative responses on the spatial variance of mobile predator-prey interactions have not been examined over a wide range of scales.

Two different scales of maximum spatial association were predicted to occur between Atlantic cod and capelin at the temporal scale of a foraging bout. Spatial association between predator and prey could peak at the scale of maximum prey spatial variance (Fig. 5.1) which maximizes potential contact rate of predator with prey. If the scale of maximum predator-prey spatial association does not match that of maximum prey spatial variance, then I predicted spatial association between predators and prey to peak at an alternate scale that maximizes net energetic benefit to the predator (Fig. 5.1).

Relative density estimates of capelin and Atlantic cod were used to examine scale-dependent spatial associations between a mobile aquatic predator and its prey. Scale-dependent patterns of capelin spatial variance were compared to measures of

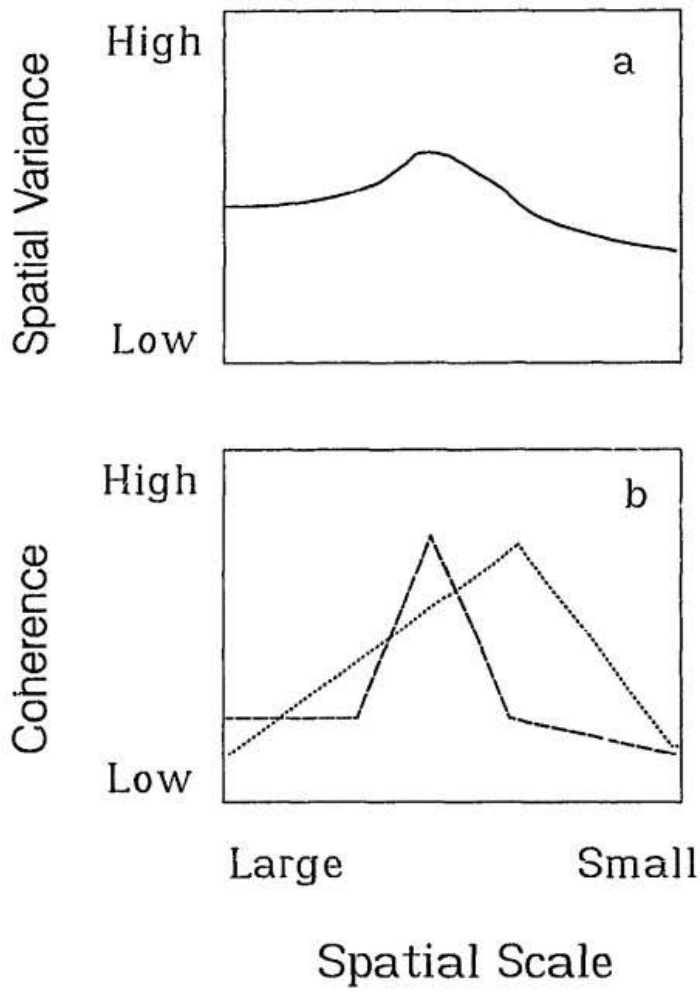

Fig. 5.1 (a) Schematic diagram of prey spatial variance. (b) Coherence between predator and prey as a function of scale Dashed line shows that the peak in coherence between predator and prey matches the scale of maximum prey spatial variance in (a). Dotted line shows that the peak occurs at another scale that potentially maximizes net energetic gain to the predator.

spatial association (coherence) between capelin and Atlantic cod. Low coherence values between predator and prey prompted an examination of cod foraging energetics to see if cod were obligated to track capelin during the spawning season.

5.2 Methods

5.2.1 Spatial Coherence

The data set used in this analysis is identical to that used to examine spatial variance of capelin and cod in the previous chapter. Spatial association between predator and prey was quantified using bivariate spectral analysis. Spatial association between two series is measured using coherence and phase. Coherence measures the strength of association between two variables as a function of frequency and is analogous to a squared correlation, with potential values ranging from 0 to 1. Phase indicates the sign of correlation between two data series. Two series that are less than 90° out of phase are positively correlated and termed in phase. Two series that are greater than 90° out of phase are negatively correlated and termed out of phase. A smoothing window of 0.01 cycles m^{-1} was used in comparative analyses to provide a compromise between accuracy and smoothness. All spectral density estimates were standardized to permit direct comparison of survey transects. The analytic window extends from 20 m to 10 km. Spectral density estimates, coherence, and phase values from all transects were combined and then averaged at a resolution of 0.0001 cycles m^{-1} to produce average spectral density, coherence and phase values. These values were plotted as a function of frequency.

5.2.2 Bioenergetic Calculations

Estimates of daily ration from cod feeding models were compared to surplus energy calculations based on glut foraging on capelin at approximately 4°C. Glut foraging is defined as feeding to repletion. Mean cod length was used to estimate weight of a predator using the weight-length relationship from Bishop et al. (1993):

$$\log W = 3.0879 \log L - 5.2106 \tag{5.1}$$

where $\log W$ is the common logarithm of fish weight (kg) and $\log L$ is the common logarithm of fish length (cm). Estimated daily ration as a function of temperature was calculated using (Jobling 1988):

$$\ln FI = (0.104T - 0.000112T^3 - 1.5) + 0.802 \ln W \tag{5.2}$$

where FI is food intake (kJ day^{-1}), T is temperature (°C), and W is mass of fish (g). This estimate was compared to the average amount of food eaten $\hat{y}_i$ (g day^{-1}) by the i th fish using (Waiwood et al. 1991):

$$\hat{y}_i = \hat{P}_j e^{(-1.66 + 0.6547 x_i)} \tag{5.3}$$

where $\hat{P}_j$ represents the probability of feeding (Table 5, Waiwood et al. 1991) at temperature j and x_i is the natural logarithm of fish mass (g).

Calculated estimates of cod daily ration were compared to estimates of surplus energy Δw (kJ) available to cod from a glut feeding on capelin. Bioenergetic calculations were based on Winberg (1956):

$$\Delta w = pR - T \tag{5.4}$$

where p is a dimensionless coefficient correcting for the unassimilated proportion of ration R (kJ) and T (kJ) is metabolic dissipation. In these calculations p was set at

30% (Brett and Groves 1979). Following Kerr (1971), the metabolic component T was separated into maintenance T_s, digestion T_c, and external activities T_F (i.e. swimming).

$$T = T_s + T_c + T_F \tag{5.5}$$

Maintenance costs $T_s = R_{maint}$ (kcal day^{-1}) were estimated using an equation from Jobling (1982):

$$R_{maint} = 0.017 W^{0.879} \tag{5.6}$$

where W is fish mass (g). Calorific estimates were converted to SI units using 4.184 J cal^{-1}. Digestion costs T_c were set at 11.85% of ingested energy based on laboratory experiments conducted with juvenile cod at 7°C (Soofiani and Hawkins 1982). Gastric emptying of a full cod stomach at 5°C was set at 58 hours or 2.42 days (Tyler 1970). Mean body lengths of capelin and cod were used to estimate swimming speeds using an equation from Okubo (1987):

$$v = 2.69 L^{0.86} \tag{5.7}$$

where v is speed (cm s^{-1}) and L is total length of fish (cm). Maximum potential range of a foraging cod was calculated by multiplying swimming speed by the number of seconds in a day. Swimming costs for cod T_F were estimated using results from respirometer experiments. Amount of oxygen consumed VO_2 (mg O_2 kg^{-1} h^{-1}) at a given temperature was calculated using fish swimming speed U in body lengths per second (Soofiani and Priede 1985):

$$\log_{10} VO_2 = 1.992 + 0.12U \tag{5.8}$$

Oxygen consumed was converted to energy using an oxycalorific coefficient of 3.36 cal kg^{-1} (mg O_2)$^{-1}$ (Brett 1973).

5.3 Results

5.3.1 Spatial Variance Patterns

At the temporal resolution of an individual transect (ca. 1 hour), a characteristic pattern of capelin spatial variance was not present among the 19 transects surveyed in Conception Bay (Chapter 4). Concentrations of spatial variance were observed in individual transects (Fig. 5.2a) but frequencies of maximum spectral density were not consistent among spatially or temporally separated transects. Coherence values between cod and capelin were generally below 0.2 in all transects. Only three of the 19 transects contained recognizable peaks of coherence at any scale (Fig. 5.2b). In all transects, phase spectra of capelin and cod oscillated in and out of phase over the range of analyzed spatial scales (Fig. 5.2c).

To examine patterns of spatial association over longer temporal scales, spectral density estimates of capelin and cod relative densities from all transects were averaged over 0.0001 frequency bins and plotted as a function of frequency. As shown in the previous chapter, average spatial variance plots of capelin and cod (Fig. 5.3a) contained two regions of differing slopes separated by a transition region. A peak in spatial variance indicating a characteristic scale of aggregation was not observed in the average power spectra of either capelin or cod. Coherence between the two species was uniformly near zero (Fig. 5.3b) and in phase (Fig. 5.3c). A characteristic

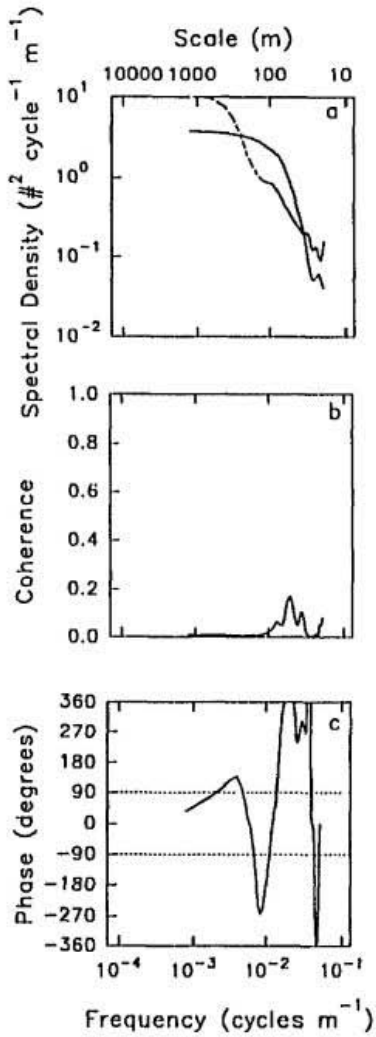

Fig. 5.2 (a) Spectral density estimates of capelin (broken line) and Atlantic cod (solid line) from a 6 km transect plotted as a function of frequency (bandwidth 0.01, centered, normalized). Periods (m) are shown on upper X axis. (b) Coherence of capelin and Atlantic cod plotted as a function of frequency. (c) Phase estimates of capelin and Atlantic cod plotted as a function of frequency.

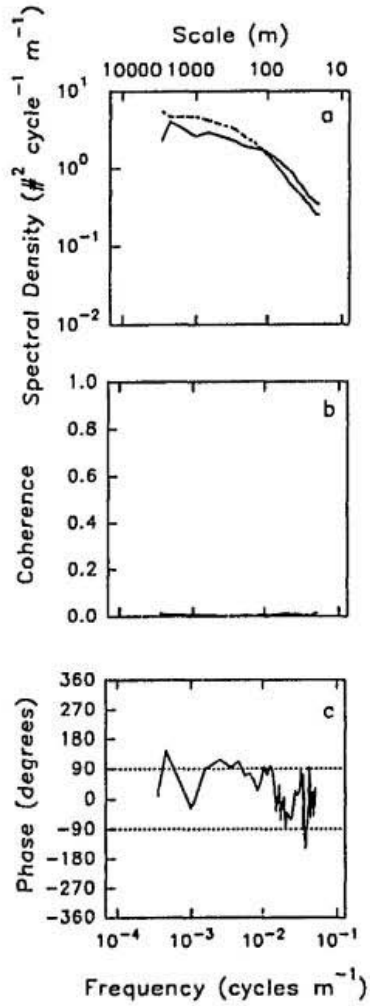

Fig. 5.3 (a) Average spectral density estimates of capelin (broken line) and Atlantic cod (solid line) plotted as a function of frequency (averaged over 0.0001 cycle bins). Periods (m) are shown on upper X axis. (b) Average coherence of capelin and Atlantic cod. (c) Average phase estimates of capelin and Atlantic cod. Area between dotted lines marks region of positive spatial association.

scale of spatial association between capelin and cod was not observed at the temporal scale of an individual transect (approximately 1 hour) or at the scale of averaged transects (approximately 2 weeks).

5.3.2 Bioenergetic Calculations

One potential explanation for the lack of spatial coherence is that cod do not need to track abundant and mobile prey such as capelin. To test this I compared energetic estimates from cod consumption models to empirical back-calculations of cod foraging on capelin.

A sample of 132 capelin caught nearshore had a mean length ($\pm$ S.E.) of 15.36 $\pm$ 0.15 cm. A sample of 140 cod caught in passive fishing traps located in the sampling area had a mean length of 44.4 $\pm$ 0.54 cm. Based on the sample, cod traps catch fish greater than 34 cm in length. Lilly (1987) has shown that cod less than 35 cm in length do not feed on adult capelin. Using the weight-length relationship from Equation 5.1, the mass of a 44.4 cm cod was estimated at 752.2 g. Jobling's (1988) food intake model (equation 5.2) was used to calculate that a 752.2 g fish would ingest 68.07 kJ day^{-1} at 4°C. This is 45% higher than the 11.16 g day^{-1} or 46.87 kJ day^{-1} calculated from Waiwood et al.'s (1991) 'average food eaten' model (equation 5.3). Mass eaten was converted to energy derived from capelin using 1004 calories g^{-1} wet capelin (Jenkins, 1975). If mass eaten was converted to energy using Tyler's (1973) original conversion factor of 4610 calories g^{-1} of dry shrimp *Pandalus montagui* (Leach) and a dry to wet mass ratio of 0.27, the amount of energy required was increased to 58.11 kJ day^{-1}. Consequently, energy requirements for a 752.2 g cod ranged between 58 kJ and

68 kJ per day.

Energy ingested by cod foraging on capelin was calculated by multiplying numbers of fresh capelin observed in cod stomachs by the average energy content of a single capelin. Net energetic gain was calculated by subtracting metabolic costs of egestion, excretion, maintenance, digestion and foraging from total energy ingested. Calculations of energetic costs represent maximum energy demand under hypothetical, and probably extreme, conditions. Based on 50 stomach samples from cod caught in cod traps, a glut ration of capelin typically ranged from eight to 12 fish. Capelin calorimetric yields from fresh capelin samples taken during the spawning season ranged from 3.9 kJ g^{-1} (Montevecchi and Piatt 1984) to 4.2 kJ g^{-1} (Jenkins 1975). Using an average wet capelin weight of 31 g (Jenkins 1975) or a combined male and female average of 34 g (Montevecchi and Piatt 1984), average energy content of capelin was estimated at 131 to 133 kJ $capelin^{-1}$. Setting average caloric content to 132 kJ $capelin^{-1}$ and an average ration of eight to 12 capelin, total energy consumption was calculated to range from 1057 to 1585 kJ per glut feeding. Egestion and excretion of an unassimilated portion of the ration was estimated at 317 (8 capelin ration) to 476 kJ (12 capelin ration). Maintenance costs T_s of a 752.2 g fish incorporating a 58 hour gastric emptying period were estimated at 58 kJ (equation 5.6). Digestion costs T_c ranged from 125 kJ (eight capelin) to 188 kJ (12 capelin). Estimated swimming speeds (equation 5. 7) were 28.19 cm s^{-1} for capelin and 70.23 cm s^{-1} for cod. Swimming speeds of cod may be lower in cold water. For example, He (1991) observed maximum sustained swimming speeds of 0.9 to 1 body lengths per second (B.L. s^{-1}) when temperatures ranged from -0.3 to 1.4°C. Metabolic costs due to swimming T_F

at 1 B.L. s^{-1} were calculated at 129.42 mg O_2 kg^{-1} h^{-1} (equation 5.8) or 1.82 kJ kg^{-1} h^{-1}. Therefore if a 44.4 cm, 752.2 g cod swims continuously at 1 body length s^{-1} during the 58 hours needed to digest the ration, an additional 79.34 kJ of energy would be consumed. During this period a predator could potentially travel a distance of 38.36 km swimming at a speed of one body length per second.

In summary, surplus energy Δw following the consumption of eight to 12 capelin was estimated at 478 to 784 kJ (Table 5.2). These estimates include energetic costs of egestion, excretion, maintenance, digestion, and continuous swimming during ration assimilation. This result shows that cod are not required to continuously track capelin at any spatial scale less than 10 km. Empirical back-calculations of cod glut feeding on capelin were a minimum of 2.9 times higher than those calculated using cod consumption models. Jobling's model (equation 5.2) estimated a consumption of 165 kJ compared to the 140 kJ calculated using Waiwood et al.'s model (equation 5.3). Physiological differences between cod used in consumption model experiments and those sampled for the empirical model may limit comparison between the two classes of models.

Table 5.2. Energetic calculations of cod glut feeding on capelin based on models from Winberg (1956) and Kerr (1971)*.

Model component	8 capelin	12 capelin
Ration (R)	1057 kJ	1585 kJ
Egestion and Excretion (p)	-317 kJ	-476 kJ
Maintenance (T_s)	-58 kJ	-58 kJ
Digestion (T_c)	-125 kJ	-188 kJ
Swimming (T_F)	-79 kJ	-79 kJ
Surplus energy (Δw)	478 kJ	784 kJ

* The predator is assumed to be a 44 cm, 752 g cod with a clearance rate at 5°C of 58 hours (Tyler 1970). Foraging speed is set at 1 body length second^{-1}. Energetic content of the ration was calculated at 132 kJ capelin^{-1}. Egestion and excretion was set at 30% of ration (Brett and Groves 1979). Maintenance of a 752 g cod was calculated at 24 kJ day^{-1} (Jobling 1982). Digestion at 7°C was estimated as 11.85% of ration (Soofiani and Hawkins 1982). Swimming costs at 1 body length s^{-1} were calculated at 1.37 kJ h^{-1} (Soofiani and Priede 1985).

5.4 Discussion

Spatial coherence between capelin and cod was low at all spatial scales among the 19 survey transects. Small concentrations or peaks of coherence occurred in 3 transects but scales of maximum coherence were not consistent among these transects. When transects were averaged, coherence values were near zero across all sampled spatial scales. A characteristic scale of spatial association between capelin and cod was not observed. In the absence of any consistent spatial association, no attempt was made to determine the form of a functional aggregative response.

The lack of a characteristic scale in the statistical description of spatial association between capelin and cod was an unexpected result. Capelin comprise a major component of cod diet (Popova 1962; Lilly 1987, 1991), especially during the capelin spawning season (Thompson 1943; Methven and Piatt 1989). A characteristic scale of association was expected to fall somewhere within the range of a few body lengths to the spatial scale of a small bay. Coherence between adult capelin and Atlantic cod has been observed at the spatiotemporal scale (length < 5 m, duration < 1 hour) of a foraging bout (Rose and Leggett 1990). This was observed only once, during a short (185 m) transect in the day when cod were actively feeding on capelin. I have included samples from all hours of the day (Table 4.1) to ensure sampling occurred when cod were actively feeding on capelin.

One possible explanation for the lack of coherence is Type II error, failure to detect a real effect. Data acquisition and analysis were designed to minimize five sources of Type II error: scale of sampling, choice of bandwidth, vertical integration of data, the presence of zeros in data, and spectral analysis of non-linear interactions.

One potential source of Type II error is taking measurements at the 'wrong' scale. However, this study analyzed mobile predator-prey interactions over four orders of spatial magnitude (20 m to 10 km). A sampling range of this size is rare within a single study. For comparison, the 14 predator-prey interaction studies that report 'characteristic' scales of spatial association (Table 5.1) collectively sample 6 orders of spatial magnitude.

A second procedural step which could contribute to Type II error is the choice of bandwidth used in spectral analyses. Bandwidth influences coherence values by setting the number of adjacent periodograms averaged to estimate spectral density magnitude in each frequency band (Chatfield 1980). In a series of replicated spectral analyses that differed only in bandwidth, I found that coherence values were lower in replicates that used narrow bandwidths. Bandwidths are not commonly reported for spectral analyses of biological data. A narrow bandwidth (0.01) was selected to minimize bias due to smoothing among frequency bands (Diggle 1990).

A third potential source of Type II error is the vertical integration of relative fish abundance data. Abundance data were integrated over the water column to analyze horizontal variation of cod relative to capelin. Two dimensional transects were analyzed as a one dimensional data series. Shoal sizes may be increased due to horizontal overlap between aggregations that are vertically separated in the water column. This is more likely among capelin where aggregations form near the surface and near the thermocline (Methven and Piatt 1991). In spectral analysis the combining of vertically separated shoals to larger aggregations potentially increases the scale of maximum association between the predator and prey. At small scales this may mask

coherence between the two species but strong interactions would remain detectable in spectral density plots. The influence of vertically integrating abundance data on spatial variance patterns of predators and prey could be examined by computing the power spectra and coherence in two dimensions (Ford 1976; Ripley 1981) and comparing results to the one dimensional case. A two dimensional spectral analysis was not conducted because of the requirement of a square data matrix (Ripley 1981). In any transect longer than 112 m, the padding of the vertical dimension with zeros would potentially influence spectral density estimates.

The presence of zeros in a discrete data series is a fourth potential source of Type II error. Coherence values can be lowered by random sampling error of a Poisson process (Mackas 1977). As a compromise between high sample resolution and reducing the probability of getting a zero count, minimum bin size was set at 10 m. The fifth potential source of Type II error is the presence of non-linear interactions between predator and prey. Spectral analysis fits a linear relationship between two variables. Aperiodic, non-linear interactions are underestimated and result in lower coherence estimates (Star and Cullen 1981).

I can neither eliminate nor quantify the amount of Type II error in this analysis. Where possible, data acquisition and analytic procedures were designed to minimize Type II error. A similar approach using spectral analysis has shown that scales of maximum association exist between marine birds and capelin (Schneider 1989). The same potential sources of Type II error exist in the analysis of marine bird data, yet scales of spatial association between predators and concentrations of prey were detected. This result was later confirmed using variance to mean ratios (Piatt 1990).

As an alternative to Type II error, the lack of spatial association between predator and prey in this study could be due the biology of the organisms.

A simple biological explanation for low coherence between capelin and cod is physiological constraints imposed on cod while foraging. If energetic costs of tracking prey over large distances exceed net energy gained by consuming prey, then the spatial coupling of cod to capelin is potentially restricted to scales smaller than those analyzed in this study (20 m). Bioenergetic calculations do not support the hypothesis that foraging cod must track capelin aggregations. Energetic costs of continuously swimming for 58 hours were 10% to 14% of the total energy used to obtain and assimilate the ration. This is a conservative estimate of cod foraging activity. Tracking studies of Atlantic cod show that cod do not swim continuously throughout the day (Hawkins et al. 1985; Keats et al. 1987) or after feeding (Clark and Green 1990). If our assumptions concerning swimming costs are correct, then the energetic cost of digestion was 1.6 to 2.4 times higher than the cost of finding the ration. Our estimate of energetic costs of swimming (1.37 kJ h^{-1}) agreed well with the 1.33 kJ h^{-1} calculated using Tytler's (1969) oxygen consumption model for haddock *Melanogrammus aeglefinus* (L.), another gadoid. The energetic cost of swimming represents a small proportion of the total energy used when cod forage on capelin. I conclude that the lack of coherence between capelin and cod was not due to physiological constraints imposed on foraging predators.

The lack of coherence and bioenergetic calculations are consistent with fishers' observations of cod-capelin interactions. The term 'logy' or 'loggy' is used to describe fish that are resting on bottom (Story et al. 1990). As the end of the capelin spawning

season approaches, cod are described as being 'glutted with capelin'. Cod can not be caught with jigger, baited hook or trawl lines because they have reduced feeding and are not moving large distances (Ches and Gord Jackson, Cavendish, Newfoundland, personal communication).

Differences in energy estimates between food intake models and glut feeding calculations deserves comment. Estimates from food intake models were at least 3 times smaller than those from glut feeding calculations. The food intake models (Jobling 1988; Waiwood et al. 1991) were based on laboratory studies of captive fish which were fed daily. Some of the fish used in the laboratory experiments had been held in captivity for a period of up to 4 years (Waiwood et al. 1991). Energetic gains from glut feeding were calculated by estimating the amount of energy consumed in a capelin ration and then subtracting energy required to maintain the animal, to digest and clear ingested material, and to continuously swim while the ration was cleared from the stomach. Feeding efficiency ($\frac{\Delta w}{R} x\ 100\%$) during this period ranged from 45% to 49% depending on capelin ration size. This is more than double the 20% observed at 7°C for cod feeding on fish pellets (Hawkins et al. 1985). But our calculations encompass a short, intensive feeding period in the wild. Cod sampled for these calculations had probably completed a post-spawning migration from offshore banks (Rose 1993). These fish feed on local concentrations of pre-spawning capelin in coastal waters to replenish depleted somatic and reproductive energy reserves (Turuk 1968). It is also unlikely that activity levels and reproductive cycles of cod used in laboratory experiments would match those of wild-caught fish. Differences in energetic intake and feeding efficiency estimates are attributed to the time of sampling and physiological

differences among animals used in the two types of models.

On average, a characteristic scale of spatial association between capelin and cod was not observed over a measurement window spanning four orders of spatial magnitude. Low coherence between predators and prey across a range of spatial scales has also been observed in zooplankton feeding on phytoplankton (Star and Mullin 1981), birds preying on leaf miners (Heads and Lawton 1983), multiple predators feeding on brittle stars (Aronson 1992), and parasites feeding on chrysomelids (Morrison and Strong 1980, 1981). For cod, an explanation of this lack of association was derived from energetic calculations. These showed that cod do not need to be spatially coupled with prey at scales less than 10 km. Hence cod can function successfully as 'sit and wait' predators. The physiology of the predator, rather than spatial distribution patterns of the prey, explained the absence of a classic form of population interaction at small scales. This chapter illustrates that aggregative responses of predators do not occur at all spatial scales. I speculate that aggregative responses may only occur over a small range of spatial and temporal scales.

Chapter 6. Shoaling and Schooling Simulation

6.1 Introduction

Spatial variance in the distributions of mobile organisms differs from that of passive tracers of the surrounding fluid (Chapters 3, 4). Data manipulations (Chapter 4) demonstrated that shoaling and schooling were two kinematic processes capable of generating slight negative slopes in spatial variance plots of mobile organism distributions. In general, theoretical models of kinematics have not been used to examine the scale or scales at which spatial variance is generated.

Increased spatial variance at intermediate scales among mobile organisms is potentially created in two ways. Spatial variance may be generated at a single small scale and then propagated to larger scales. This hypothesis is opposite to the 'turbulent energy cascade' commonly assumed for spatial variance patterns of passive tracers in fluids (cf. Fig. 2, Mackas et al. 1985). Although one exception is the generation of large scale pattern from the interaction of passive particles with Langmuir circulation (Liebovich 1983; Weller and Price 1988; Schneider and Bajdik 1992). Alternatively, spatial variance may be independently generated at several scales by a variety of kinematic processes. The creation and possible transfer of spatial variance to larger scales has not been quantified for mobile aquatic organisms.

In this chapter a particle interaction model is developed to simulate fish kinematics. The simulator is used to track changes in spatial variance of mobile aquatic organisms due to shoaling and schooling. Slopes of spatial variance plots are predicted to decrease with an increase in shoaling and schooling. Shoaling is defined as the

convergence of organisms independent of fluid motions. Schooling is differentiated from shoaling by the coordinated movement of a group of aquatic organisms (Pitcher 1986; Pitcher and Parrish 1993). Models of the formation and maintenance of fish shoal structure have been based on opposing forces of attraction and repulsion between individuals (Parr 1927; Breder 1954; Jacobson 1990). Magnitudes of forces are a function of distance between individuals, cancelling at an equilibrium distance equal to the mean distance between members of an aggregation. Breder (1954) based the repulsion force on Coulomb's law of magnetism and electrostatics such that the repulsive force between two fish was proportional to the inverse of the distance squared. This maintains a minimum inter-fish distance between all members of a shoal. The schooling component of a simulation model should result in polarized aggregations of fish moving in a coordinated fashion. Jacobson (1990) included a cohesion component in his simulator but imposed a constant fish speed and reflective boundaries within the model domain. The use of closed boundaries disproportionately increased boundary effects and restricted the range of spatial scales examined. To quantify the effects of shoaling and schooling on spatial variance, a shoaling component based on attraction-repulsion forces should be integrated with a schooling component that is unrestricted in spatial range.

6.2 Mobile Particle Interaction Model

6.2.1 Model Development

Consider N fish at positions $\vec{r}_i$, $i = 1, \ldots, N$ in a two dimensional plane (Fig.

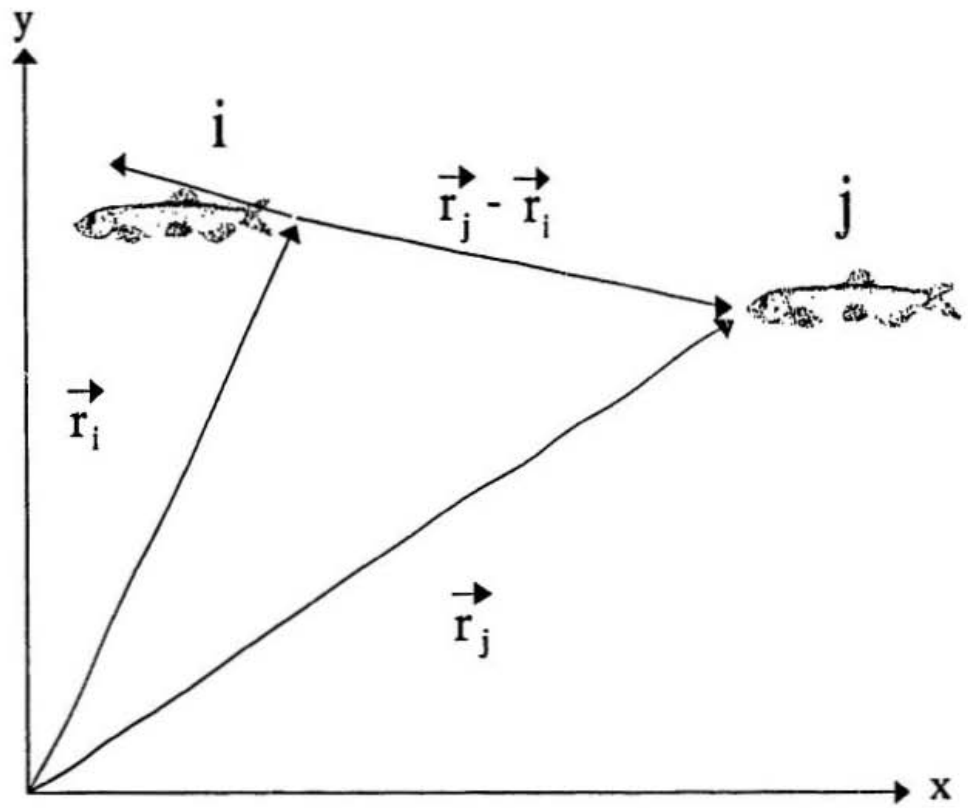

Fig. 6.1 Schematic diagram of attractive and repulsive forces between fish i and fish j.

6.1). All symbols are listed in Appendix 6.1. The force $\vec{F}$ on the ith fish at $\vec{r}_i$ due to attraction A and repulsion R from the jth fish at $\vec{r}_j$, $j = 1, \ldots, N-1$ is defined as

$$\vec{F}_{ij} = \left[\frac{A}{|\vec{r}_i - \vec{r}_j|^m} - \frac{R}{|\vec{r}_i - \vec{r}_j|^n} \right] \frac{\vec{r}_j - \vec{r}_i}{|\vec{r}_j - \vec{r}_i|} \tag{6.1}$$

where m is the exponent of attraction and n is the exponent of repulsion. The force on the ith fish due to the other N fish within an interaction distance is the sum of forces

$$\vec{F}_i = \sum_{\substack{j=1 \\ (\neq i)}}^{N} \vec{F}_{ij} \tag{6.2}$$

The velocity $\vec{V}$ of the ith fish is defined as

$$\vec{V}_i = \frac{d\vec{r}_i}{dt} \tag{6.3}$$

The acceleration $\vec{A}$ of the ith fish is defined as

$$\vec{A}_i = \frac{d^2\vec{r}_i}{dt^2} = \frac{d\vec{V}_i}{dt} \tag{6.4}$$

The acceleration of the ith fish can be decomposed into three parts

$$\vec{A}_i = \vec{F}_i + \vec{f}_i + \vec{\phi}_i(t) \tag{6.5}$$

where $\vec{f}_i$ is a frictional force opposing the motion of fish i and $\vec{\phi}_i$ is a random force acting on the ith fish. The magnitude of the frictional force is calculated using

$$\vec{f}_i = -\frac{1}{2}\rho_f S C_f |\vec{V}_i| \vec{V}_i \tag{6.6}$$

where ρ_f is the density of the fluid, S is the wetted surface area, and C_f is the drag coefficient. By combining parameters into a single friction parameter C this equation simplifies to

$$\vec{f}_i = -C|\vec{V}_i|\vec{V}_i \tag{6.7}$$

The random force has magnitude α so that

$$\vec{\phi}_i(t) = \alpha\vec{\xi}_i(t) \tag{6.8}$$

where $\vec{\xi}_i$ is a random vector with unit variance expressed as

$$<\vec{\xi}_i(t) \quad \vec{\xi}_i(t)> = 1 \tag{6.9}$$

The random force acting on the ith fish is uncorrelated with the force acting on any other fish j

$$<\vec{\xi}_i(t)\,\vec{\xi}_j(t)> = 0 \qquad \text{if} \quad i \neq j \tag{6.10}$$

It is assumed that there is a characteristic period τ, termed a relaxation time constant, when fish respond to a change in the distribution of conspecifics. During this period the random force is correlated to previous time steps and after which it becomes uncorrelated.

$$<\vec{\xi}_i(t)\,\vec{\xi}_i(t')> = 1 \qquad \text{if} \quad |t'| < \tau \tag{6.11}$$

$$<\vec{\xi}_i(t)\,\vec{\xi}_i(t')> = 0 \qquad \text{if} \quad |t'| > \tau \tag{6.12}$$

There are six parameters in our problem: A, R, m, n, α, and C. But only four of these parameters are independent, given the dynamical relationship among variables (equation 6.5). The problem can be nondimensionalized to express it in terms of the four independent parameters. First, consider a dimensionally equivalent equation to (6.5):

$$\frac{d^2 r_i}{dt^2} = \frac{A}{r_i^m} - \frac{R}{r_i^n} + \alpha\xi - C\left(\frac{dr_i}{dt}\right)^2 \tag{6.13}$$

Let $r = qr^*$ and $t = pt^*$, then

$$\frac{q}{p^2}\frac{d^2 r_i^*}{dt^{*2}} = \frac{A}{q^m r_i^{*m}} - \frac{R}{q^n r_i^{*n}} + \alpha\xi - C\frac{q^2}{p^2}\left(\frac{dr_i^*}{dt^*}\right)^2 \tag{6.14}$$

$$\frac{d^2 r_i^*}{dt^{*2}} = \frac{p^2 A}{q^{m+1} r_i^{*m}} - \frac{p^2 R}{q^{n+1} r_i^{*n}} + \frac{p^2\alpha}{q}\xi - Cq\left(\frac{dr_i^*}{dt^*}\right)^2 \tag{6.15}$$

choose p and q so that

$$\frac{p^2 A}{q^{m+1}} = 1 \qquad p^2 A = q^{m+1} \tag{6.16}$$

to remove the coefficient from the attractive force, and

$$\frac{p^2\alpha}{q} = 1 \qquad p^2\alpha = q \tag{6.17}$$

to remove the coefficient from the random force. Solve Equations (6.16) and (6.17) for q

$$\frac{A}{\alpha} = q^m \Rightarrow q = \left(\frac{A}{\alpha}\right)^{\frac{1}{m}} \tag{6.18}$$

and p

$$p = \sqrt{\frac{q}{\alpha}} \tag{6.19}$$

Providing $m \neq 0, n \neq 0$, then

$$\frac{d^2 r_i^*}{dt^{*2}} = \frac{1}{r_i^{*m}} - \frac{p^2 R}{q^{n+1} r_i^{*n}} + \xi - Cq\left(\frac{dr_i^*}{dt^*}\right)^2 \tag{6.20}$$

$$\frac{d^2 r_i^*}{dt^{*2}} = \frac{1}{r_i^{*m}} - \frac{R}{\alpha}\left(\frac{A}{\alpha}\right)^{-\frac{n}{m}}\frac{1}{r_i^{*n}} + \xi - C\left(\frac{A}{\alpha}\right)^{\frac{1}{m}}\left(\frac{dr_i^*}{dt^*}\right)^2 \tag{6.21}$$

Assign

$$\Gamma = \frac{R}{\alpha}\left(\frac{A}{\alpha}\right)^{-\frac{n}{m}} \tag{6.22}$$

and

$$\gamma = C\left(\frac{A}{\alpha}\right)^{\frac{1}{m}} \tag{6.23}$$

Which simplifies Equation (6.21) to

$$\frac{d^2 r_i^*}{dt^{*2}} = \frac{1}{r_i^{*m}} - \frac{\Gamma}{r_i^{*n}} + \xi - \gamma\left(\frac{dr_i^*}{dt^*}\right)^2 \tag{6.24}$$

The nondimensional velocity of the ith fish is

$$\frac{d\vec{r_i^*}}{dt^*} = \vec{V_i^*} \tag{6.25}$$

In nondimensional variables the equations of motion now become:

$$\frac{d\vec{V_i^*}}{dt^*} = \vec{F_i^*} + \vec{f_i^*} + \vec{\xi_i} \tag{6.26}$$

where

$$\vec{F_i^*} = \left[\frac{1}{\left|\vec{r_i^*} - \vec{r_j^*}\right|^m} - \frac{\Gamma}{\left|\vec{r_i^*} - \vec{r_j^*}\right|^n}\right]\frac{\vec{r_j^*} - \vec{r_i^*}}{\left|\vec{r_j^*} - \vec{r_i^*}\right|} \tag{6.27}$$

$$\vec{f_i^*} = -\gamma\left|\vec{V_i^*}\right|\vec{V_i^*} \tag{6.28}$$

and $\vec{\xi_i}$ is a random number with variance 1 as expressed in Equations (6.9), (6.10), (6.11), and (6.12).

6.2.2 Model domain

Acoustic survey data from continental shelf waters are modeled as a unidimensional cut through a large, horizontal 2-dimensional plane. It is not necessary to model all fish on a continental shelf because fish visually detect conspecifics over small distances relative to the breadth of the ocean. The detection distance used in the model can be altered to represent other sensory mechanisms in fish.

The x dimension in the model is set to approximate the length of a typical acoustic transect with boundaries imposed at $x=0$ and $x=L$. Channel length L was set at 1000 m to span three orders of magnitude for spatial variance analysis. This also ensures that L will be a minimum of two orders of magnitude greater than the distance over which two fish can interact. The y boundaries are imposed at $y=0$ and $y=Y$ where Y is the width of the model domain. Channel width is set to ensure a large separation between boundaries relative to the maximum interaction distance between any two fish. Channel width used in the simulations was 40 m, a minimum of 5 times the maximum fish interaction distance of 8 m (see below).

Periodic boundary conditions were used to minimize perimeter effects in a two dimensional, horizontal plane. A periodic boundary condition assumes identical channels to all sides of the model channel. The model domain was set to simulate a hydroacoustic survey transect in open water while maintaining fish density. Simulating a nearshore environment or a vertical profile (i.e. x-z plane) would require reflective boundary conditions at one (i.e. coastline) or more (i.e. surface and bottom) boundaries. Reflective boundary conditions increase edge following behaviour (e.g. Jacobson 1990). Edge following behaviour will enhance the development of fish

schools. The magnitude of this effect is dependent on the perimeter to surface area ratio. In a two dimensional plane of width L and length nL, the perimeter scales by a factor of $2+2n$ as the surface area scales by a factor of length nL. Under periodic boundary conditions, if a fish crosses an upper or lower boundary it retains its x-coordinate and the new y coordinate is the original y coordinate $\pm$ the width of the channel. This positions the fish at an identical distance inside the channel from the opposite boundary. Analogous conditions are set at the ends of the channel at y=0 and y=Y.

6.2.3 Model parameters

The biological premise for the simulator is that fish are attracted to conspecifics but maintain a minimum distance between individuals. Forces of attraction and repulsion are inversely proportional to distance, with the force of attraction dominating at large distances and the force of repulsion dominating at small distances. The net force is zero at the mean inter-fish distance within fish schools (Fig. 6.2).

Values of parameters are based on experiments or empirical observations of pelagic, schooling fish. All parameter values were set to approximate capelin morphology and behaviour (Table 6.1). Inter-fish spacing, also termed nearest-neighbor distances, have been reported for enclosed (e.g. Pitcher and Partridge 1979; Partridge 1980) and free swimming (e.g. Sætre and Gjøsæter 1975; Misund 1993) fish schools. For a variety of species, values approximate one body length between individuals when measured in two or in three dimensions. Attractive and repulsive forces were balanced so that inter-fish spacing within schools equaled one

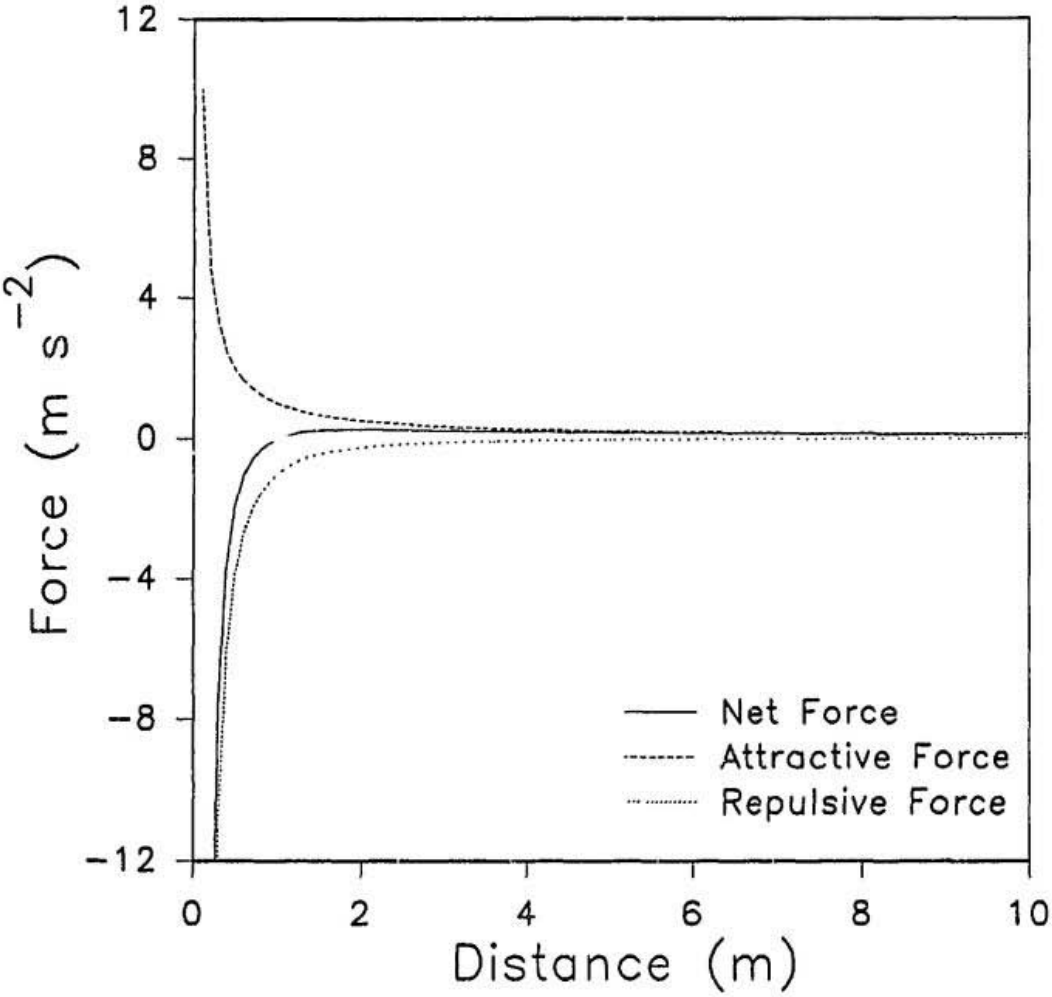

Fig. 6.2 Attractive, repulsive, and net force as a function of distance from Equation (1). The attractive force is inversely proportional to the distance between two fish (i.e. A=1, m=1). The repulsive force is inversely proportional to the square of the distance between two fish (i.e. R=1, n=2).

Table 6.1. Model parameters and values used in the mobile aquatic organism simulator.

Name	Symbol	Equation	Value	Reference
attractive force	A	6.1	1	Breder 1954
repulsive force	R	6.1	1	Breder 1954
attractive exponent	m	6.1	1	Breder 1954
repulsive exponent	n	6.1	2	Breder 1954
density of fluid	ρ_f	6.6	1000 kg m^{-3}	
surface area of fish	S	6.6	0.01 m^2	Webb 1975
drag coefficient	C_f	6.6	0.015	Denil 1936-1938
friction parameter	C	6.7	0.075 kg m^{-1}	
relaxation time constant	τ	6.11, 6.12	0.2 s	Aoki 1984

body length (16 cm). The relative magnitudes of attraction and repulsion forces between fish have not been quantified and were arbitrarily set to 1. To make the attractive force act over a greater distance than the repulsive force, attraction between fish was set inversely proportional to the separation distance (i.e. m=1) and repulsion was set inversely proportional to the separation distance squared (i.e. n=2). A maximum interaction distance was set at 8 m to approximate the visual detection range of fish (Anthony 1981). Swimming speeds for clupeoid fishes, a similar body form to capelin, have been reported to range from under 1 to over 7 body lengths $second^{-1}$ (Beamish 1978). A speed of 3 to 4 body lengths $second^{-1}$ is a valid estimate of sustained school swimming speed among clupeoid fishes (Blaxter 1967). Particle

speeds in the simulator were limited to a maximum of 6.25 body lengths or 1 metre second^{-1}. The friction parameter C was set at 0.075. This is a conservative value based on a fish length of 16 cm, a sea water density of 1000 kg m^{-3}, a wetted surface area of 0.01 m^2 (0.4 x (0.16 m)^2) (Webb 1975), and a drag coefficient of 0.015. The drag coefficient was based on dead drag measurements of 10 cm pelagic fish models towed at a speed of 10 body lengths second^{-1} with a Reynolds number 1.0 x 10^5 (Denil 1936-1938). The relaxation time constant τ was set at two time increments. Aoki (1984) found that values of τ were approximately 2 seconds for 8 member fish schools of juvenile mullet (*Mugil cephalus*) and tamoroko (*Gnathopogon elongatus elongatus*).

6.2.4 Simulations

A total of 800 particles representing capelin were randomly placed throughout the model domain representing a density of 1 fish per 50 m^2 water. This density in two dimensions approximates the mean lower density of capelin (200 fish/10^5 m^3 water or 1 fish/63 m^2) measured in the northern Gulf of St. Lawrence by Rose and Leggett (1990). Simulations were run for 600 seconds at 0.1 second increments. Particle velocities and frictional forces were checked to ensure that random forces did not artificially inflate values. If the x or y component of particle velocity exceeded a maximum velocity (Vmax = 1 m s^{-1}), velocity was reset to Vmax and multiplied by a random component. Friction was recalculated based on the new velocity. In the standard simulation run, positions of each particle were recorded at time iterations 0, 1000, 2000, and 6000 for comparison of spatial variance patterns over time. For each set of reported positions, particles were counted at a resolution of 1 metre along a 20 m swath centered at the

middle of the domain. This width corresponds to the swath of a 22° transducer sounding at a depth of approximately 50 m. Studies in the Gulf of St. Lawrence and off Newfoundland have observed most capelin at depths less than 50 m (Bailey et al. 1977; Atkinson and Carscadden 1979; Methven and Piatt 1991).

Spectral analysis (Jenkins and Watts 1968; Koopmans 1974; Chatfield 1980) was used to examine spatial variance of fish distributions as a function of time. This technique estimates scale-dependent variance of a continuously recorded variable over a range of frequency bands. The range of frequency bands extends from half the length of the series to twice the sample resolution. A smoothing window of 0.01 cycles m^{-1} was used in comparative analyses to provide a compromise between accuracy and smoothness. All spectral density estimates were standardized to permit direct comparison of sample transects (Denman 1975).

6.3 Results

Velocities and frictional forces of particles in the simulation model mimicked those reported in the literature for small-bodied, pelagic fish. The u and v velocity components of eight particles over 250 time steps (Fig. 6.3) oscillated between 0 and 1 m s^{-1}, the maximum velocity permitted in the simulation. Magnitudes and signs of the equivalent frictional forces (Fig. 6.4) fluctuated in synchrony with velocity components.

Groups of particles, representing shoals of fish, formed rapidly once a simulation was started. Using the results of a single simulation run as an example, initial particle

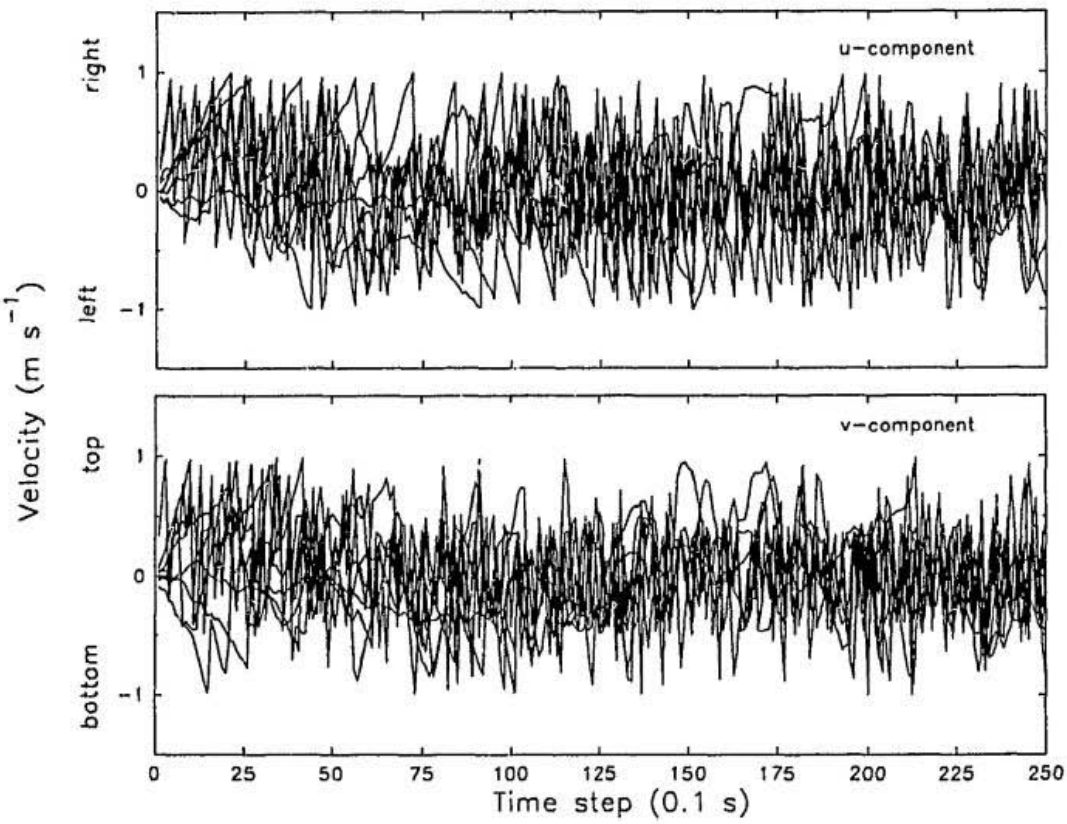

Fig. 6.3 Velocities of eight particles, u component and v component, from the first 250 time steps.

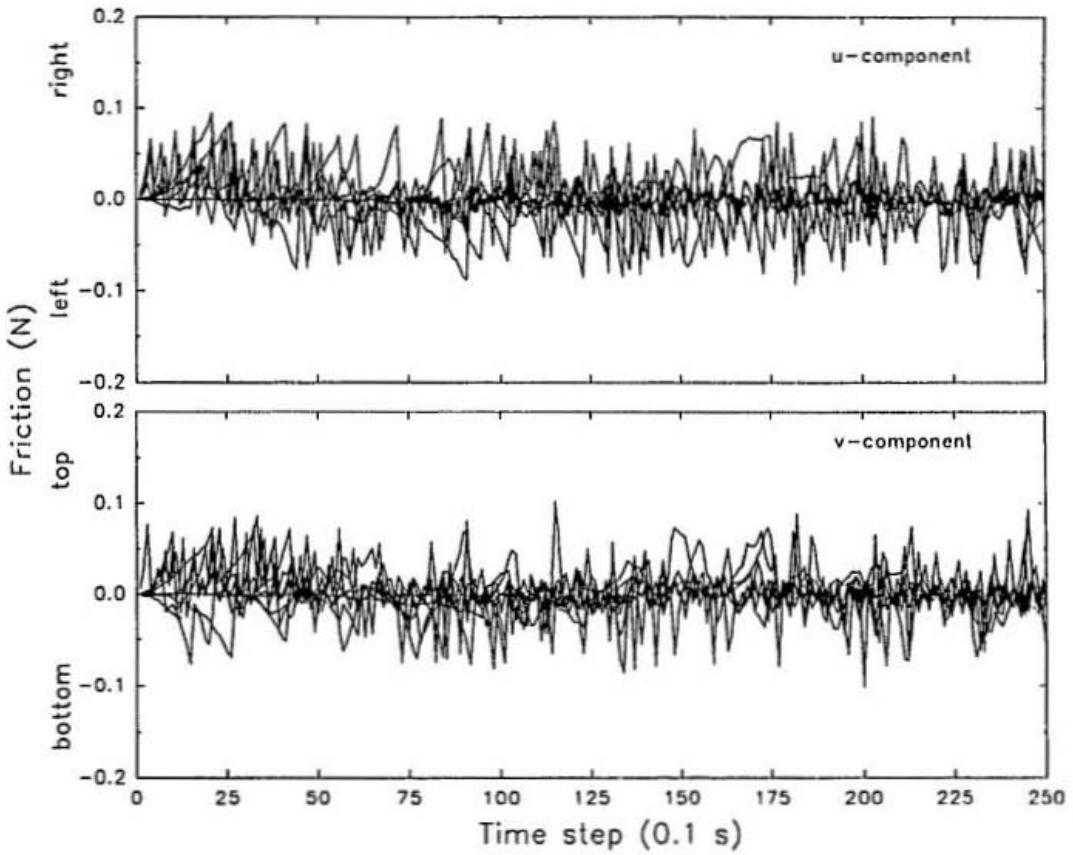

Fig. 6.4 Friction of eight particles, u component and v component, from the first 250 time steps.

positions were assigned randomly (Fig. 6.5a). Separate shoals of fish began to form after approximately the 50th time iteration (Fig. 6.5b) and were clearly separated by the 100th time iteration (Fig. 6.5c). This basic structure was maintained through the remainder of each simulation (Fig. 6.6). As time elapsed, single individuals would join larger shoals and the spacing among individuals became more uniform within shoals.

Once formed, shoals of fish moved in the x and y directions as polarized schools but did not travel large distances. In Figures 6.5 and 6.6 it appears that there was more movement in the y than in the x direction. Given the size of the channel (1000 m long, 40 m wide), particles were more likely to cross boundaries at the 'top' (y=40) and 'bottom' (y=0) of the channel than at the ends (x=0, x=1000) of the channel. The apparent increased movement in the y direction is also attributed to the dimensions of the graphic presentations (16 cm by 4 cm) relative to the actual channel proportions.

Spatial variance patterns in the distributions of particles changed over time. The power spectra of the initial distribution of particles was flat across all scales in the simulations (e.g. Fig. 6.7a). This pattern, called a white spectrum, is commonly found in a randomly distributed series (Schroeder 1991). Early in the simulations, spatial variance decreased and then increased at large scales, increased to a plateau over a broad range of intermediate scales, and decreased at scales smaller than 10 m. The drop in spatial variance at scales smaller than 10 m occurred after the 50th time iteration (Fig. 6.7b). As the simulation progressed (Fig. 6.8), slopes of spectral density plots became steeper at scales smaller than 10 m until time = 6000 (-0.66, n=51, r^2=0.62) and decreased slightly until the completion of the run at time = 12000 (-0.72, n=51, r^2=0.65).

To examine the sensitivity of spectral density estimates to sample resolution, the width of the sample swath was reduced from 20 m to 10 m and spatial variances of particle distributions were recalculated. Slight variations in the magnitude and shifts to smaller scales were observed in peaks and troughs of spectral density plots sampled

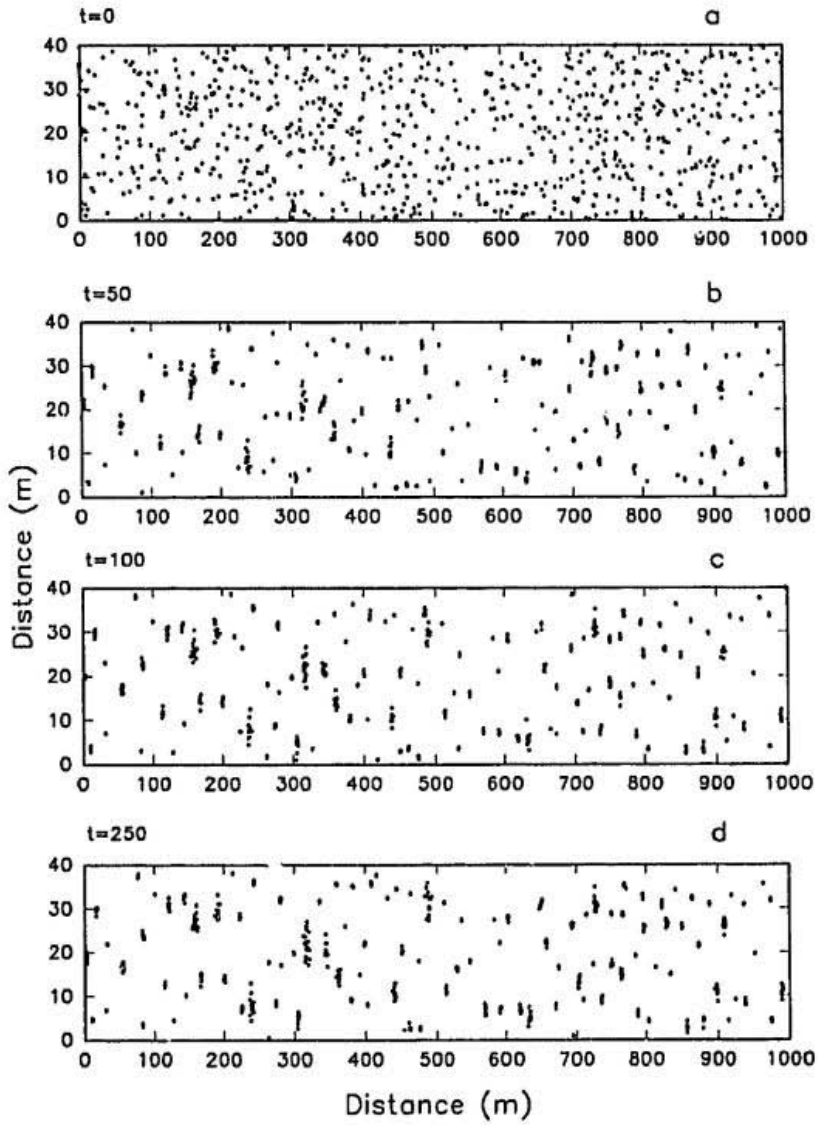

Fig. 6.5 Positions of 800 particles representing capelin at time steps a) 0, b) 50, c) 100, and d) 250.

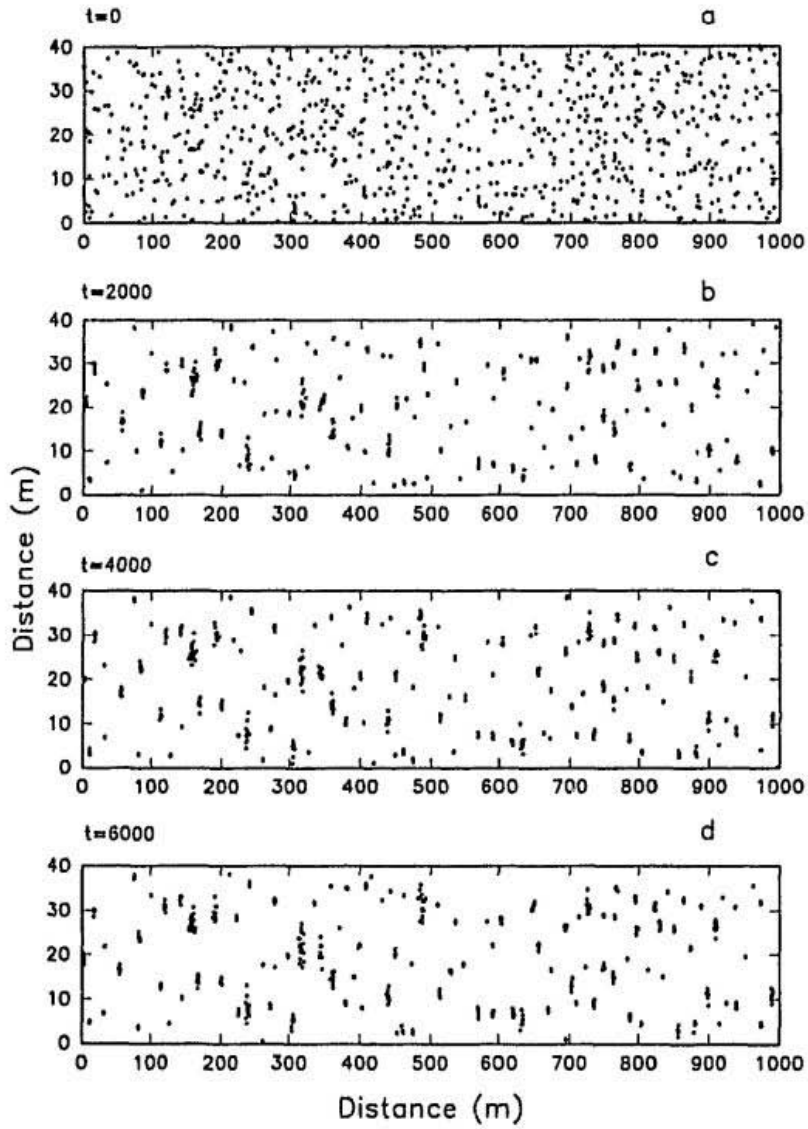

Fig. 6.6 Positions of 800 particles representing capelin at time steps a) 0, b) 2000, c) 4000, and d) 6000.

using the reduced swath width (Fig. 6.9). Spectral density estimates did not significantly differ between plots based on the 20 m (Fig. 6.8) or 10 m swath (Fig. 6.9) width ($F=0.058$, $p=0.81$, $df=493$).

6.4 Discussion

The particle simulator used in this study was developed to provide a tool to examine the effects of shoaling and schooling on spatial variance patterns in mobile aquatic organisms. The form of the model was derived using biological reasoning and parameterized using experimental values from pelagic fish studies. The formation of the model was not an attempt to import and directly apply a physical law to a biological system. Parr (1927) was the first to propose that spacing of fish within schools was a balance between attractive and repulsive forces. This was used by Breder (1954) who applied Coulomb's law of electrostatics to construct and parameterize a schooling model. Breder's model formalized perceptions of biological processes that influence schooling of fish. In contrast to Breder's application of theoretical physical models to fish schooling behaviour, Aoki (1984) formulated two theoretical models (linear differential equations) based on spectral analyses of empirical fish schooling data. Aoki's models describe inter-fish spacing as a function of spatial scale. The approach of this study was to combine a theoretical kinematic model with an analysis of spatial variance as a function of scale.

Modeling studies of schooling have traditionally focused on processes that contribute to the formation and maintenance of uniform spacing among individuals within schools (e.g. Breder 1954; Gerritsen and Strickler 1977; DeAngelis 1978; Aoki

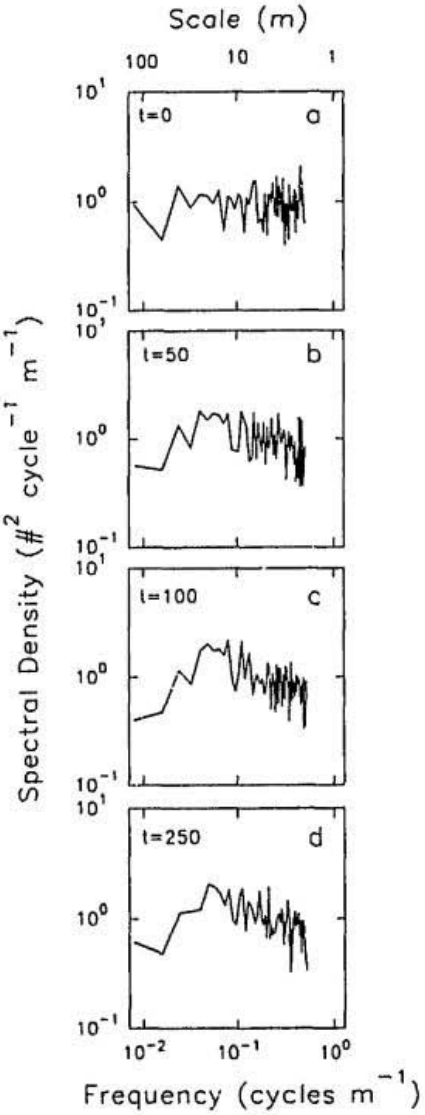

Fig. 6.7 Spectral density estimates of particles representing capelin, plotted as a function of frequency (bandwidth 0.01, centred, normalized). Graphs are particles positions at time steps a) 0, b) 50, c) 100, and d) 250. Periods (m) are shown on upper X axis.

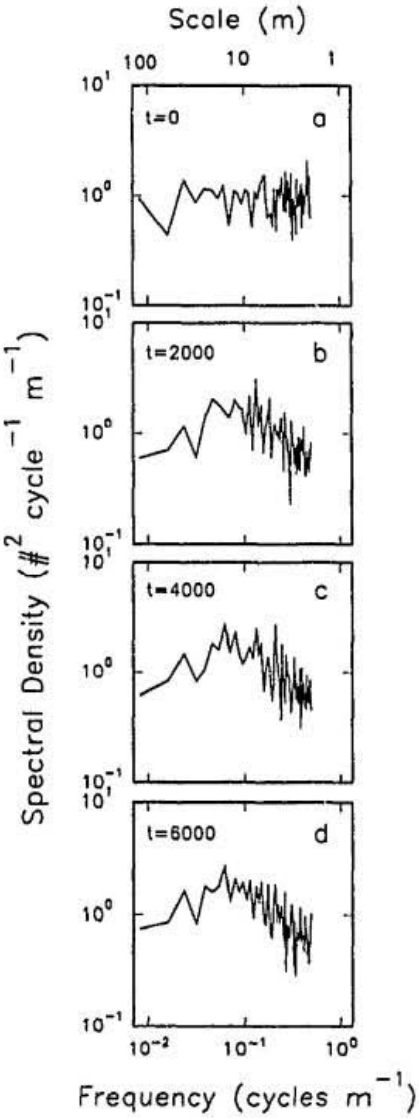

Fig. 6.8 Spectral density estimates of particles representing capelin, plotted as a function of frequency (bandwidth 0.01, centred, normalized). Graphs are particles positions at time steps a) 0, b) 2000, c) 4000, and d) 6000. Swath width was set at 20 m. Periods (m) are shown on upper X axis.

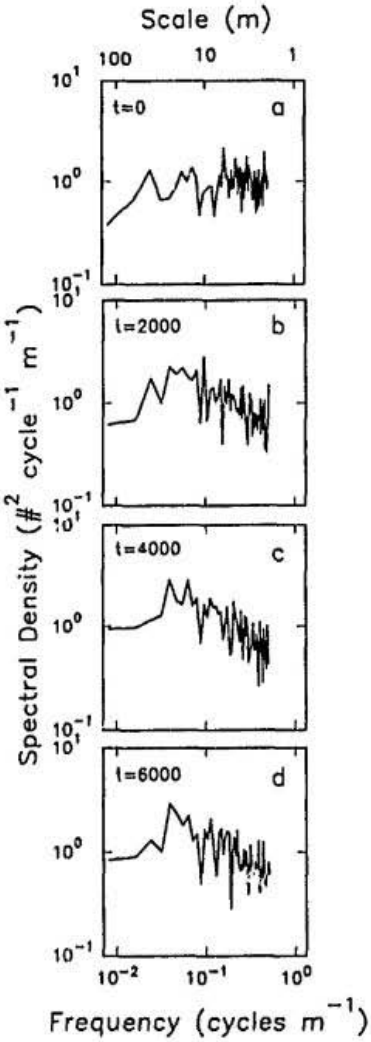

Fig. 6.9 Spectral density estimates of particles representing capelin, plotted as a function of frequency (bandwidth 0.01, centred, normalized). Graphs are particles positions at time steps a) 0, b) 2000, c) 4000, and d) 6000. Swath width was reduced to 10 m. Periods (m) are shown on upper X axis.

1982, 1986; Jacobson 1990). These models can be classified as analytic or simulation models. Analytic models are continuous in time or space but are restricted in the number of possible interactions between model components. Okubo (1986) reviews analytic models of animal grouping, including schooling by fish. Simulation models permit a wide array of interactions between model components but use discrete time and space increments. Sample resolution in simulation models is determined by the temporal or spatial dimensions of cells in the model. Simulation models are frequently used when manipulative experiments are not logistically feasible (e.g. Thompson et al. 1974). Simulated results are compared to empirical observations to evaluate understanding of processes that create patterns (e.g. Levin et al. 1989; Rose and Leggett 1990). Mismatch of simulated and observed results indicates potential research areas. Simulation models are also used to evaluate accuracy and precision of sampling gear and survey designs (e.g. Wiebe 1971; Fiedler 1978).

In this study, spatial variance patterns of simulated capelin distributions were not sensitive to a 50% reduction in sample transect width. Application of this result to acoustic survey design means that abundance estimates and the resulting spatial variance descriptions of aggregated organisms are not overly sensitive to transducer beam angle. But comparison of a reduced swath width in a single transect does not indicate how precision of an abundance estimate may be affected by the number of transects surveyed (e.g. Smith 1978) or the design of the survey (e.g. Fiedler 1978). Abundance estimates based on the sampling of naturally distributed populations are subject to errors that may reduce accuracy or precision of estimates. Precision is potentially affected by organism spatial distribution and variability in the sampling technique (Taylor 1953; Wiebe 1971;

Cram and Hampton 1976). Fiedler (1978) found that patchy distributions of anchovy (*Engraulis mordax*) and survey sample design can be major sources of error in population estimates.

Simulation model results demonstrate that shoaling and schooling increase spatial variance of mobile organisms at intermediate scales and decrease spatial variance at small scales relative to spatial variance patterns of randomly distributed particles. Slopes of spectral density plots were less than those of passive particles at intermediate scales and similar at small scales (cf. Denman and Powell 1984; Mackas et al. 1985). Slight negative slopes over a broad range of scales and a rapid decrease at smaller scales is consistent with average spatial variance patterns in other mobile aquatic organisms: Antarctic krill (Weber et al. 1986; Levin et al. 1989), fish (Chapter 3, 4; Schneider 1994a), and marine birds (Chapter 4). Reduced slopes at intermediate scales is consistent with the hypothesized injection of kinetic energy due to the convergence of individuals into shoals and coordinated movement of schools.

Three lines of evidence support the hypothesis that spatial variance in mobile aquatic organisms can be generated by kinematic processes at local scales and transferred to larger scales. One line of evidence used scaling arguments to show that for organisms greater than several centimeters in length, kinetic energy due to locomotion exceeds that due to flow of the surrounding fluid (Schneider 1994a). This creates spatial variance at the spatial scale of animal movement. Another line of evidence is the results of computer simulations that demonstrate that large scale spatial structure in populations can result from movement and interactions of organisms at small scales (Satoh 1989, 1990; Hassell et al. 1991). This generates spatial variance at

the scale of an aggregation. A third line of evidence is local interaction by organisms with large scale fluid structures (water or air) resulting in movement and convergence of organisms at large spatial scales. The use of timed or directed motion to interact with fluid structures has been observed in zooplankton (Cronin and Forward 1979; Frank and Leggett 1983), fish (Harden-Jones et al. 1978; Arnold and Cook 1984; Boehlert and Mundy 1988), and marine birds (Richardson 1978; Blomqvist and Peterz 1984). Therefore, spatial variance of mobile aquatic organisms can be generated by several kinematic processes at different spatial scales: formation of shoals independent of fluid motions, polarized movements of schools, and migration resulting in large scale population convergences. Spatial variance generated by shoaling, schooling, and migration at small scales potentially generates large scale spatial variance in mobile aquatic organisms.

Application of this particle simulator is not limited to examining scale-dependent spatial variance of mobile, aquatic organisms. Tailoring model parameters to any species of interest facilitates theoretical prediction of shoal sizes, shoal distribution, and inter-shoal distances (cf. Nero and Magnuson 1992). Addition of a second set of particles and rules of interaction enables the simulation of predator-prey interactions and the calculation of potential encounter rates of predators with prey (cf. Schneider et al. 1987). Adding two dimensional equations of motion (cf. Dutton 1976) would enable the calculation of passive organism spatial variance (e.g. phytoplankton, fish eggs) and predator-prey interactions in known flow regimes. The influence of fluid motions on the spatial variance of organism density is expected to increase as organism mobility decreases (cf. Chapter 2).

Appendix 6.1 List of symbols

N	number of fish.
i	fish index number. Values range from 1 to N.
j	fish index number. Values range from 1 to $N-1$
$\vec{r_i}$	position of fish i. Dimensions are length.
$\vec{F_{ij}}$	mass specific net force on fish i due to all other fish j. Dimensions are LT^{-2}.
A	mass specific attractive force at unit distance. Dimensions are LT^{-2}.
R	mass specific repulsive force at unit distance. Dimensions are LT^{-2}.
m	exponent of attraction.
n	exponent of repulsion.
$\vec{V_i} = \frac{d\vec{r_i}}{dt}$	velocity of the ith fish. Dimensions are LT^{-1}.
$\frac{d^2\vec{r_i}}{dt^2}$	acceleration of the ith fish. Dimensions are LT^{-2}.
$\vec{f_i}$	quadratic frictional force opposing the motion of fish i. Dimensions are MLT^{-2}.
$\vec{\phi_i}(t)$	mass specific random force acting on the ith fish at time t. Dimensions are LT^{-2}.
ρ_f	density of fluid. Dimensions are ML^{-3}.

A	surface area of fish. Assumed to be 40% of length squared. Dimensions are L^2.
C_f	drag coefficient. Dimensionless number.
C	friction parameter. Dimensions are ML^{-1}.
α	magnitude of random force $\vec{\phi}_i$.
τ	relaxation time constant determining the period of the random force $\vec{\phi}_i$. Dimensions are T.
$\vec{\xi}_i(t)$	random vector $\vec{\phi}_i$.
r^*	nondimensional unit distance.
t^*	nondimensional time increment.
p	time increment constant. Dimensions are T.
q	distance increment constant. Dimensions are L.
Γ	nondimensional constant of repulsive force.
γ	nondimensional constant of frictional force.

Chapter 7. Spatial Variance in Ecology

7.1 Introduction

The investigation of spatial variance is nearly a century old. During this time the concept has evolved from being treated as a statistical nuisance (Cassie 1963; Steele 1976) to being recognized as a biologically important quantity (Huffaker 1958; Lasker 1975; Platt and Harrison 1985). Concomitant with this change was the realization that observed patterns of spatial variance are dependent on the scale of measurement. Recent advances in computing hardware (speed and memory), the introduction of spatially explicit software (e.g. Geographic Information Systems), and a large increase in scale-sensitive studies (e.g. Wiens 1989; Menge and Olson 1990; Holling 1992; Levin 1992) should accelerate the understanding of spatial variance patterns in biological quantities such as density, mortality, and recruitment.

The dependence of spatial patterns on measurement scale was first investigated in agricultural experiments. To improve statistical control in agricultural uniformity trials, a variety of plot sizes were used to isolate the 'best' scale (Mercer and Hall 1911). Results of these experiments were then used to develop an empirical relation between plot size and variability among plots (Fairfield Smith 1938). Characterizing spatial variance as a function of plot size was later applied to naturally distributed plants using nested (Greig-Smith 1952) and contiguous (Kershaw 1957) quadrats.

Development in the analysis of scale-dependent variance occurred in the following twenty years but four contributions in 1978 consolidated the concept of scale in ecology. First, Smith (1978) explicitly recognized the scale-dependence of

measurement and stressed the importance of choosing an appropriate measuring framework relative to the organism of interest. The second contribution was a proposal by Shugart (1978) that the spatial and temporal range of biological quantities are dependent on its level of organization. This introduced Simon's (1962) concept of hierarchy to ecology. Haury et al. (1978) adapted a schematic diagram by Stommel (1963) to show how the variance of a biological quantity is linked to the spatial and temporal scales of physical processes. Steele (1978b) extended the linkage of spatial and temporal scale to include the mass of an organism.

This chapter reviews the quantification of spatial variance at a single scale and then as a function of scale. I summarize progress in the analysis of spatial variance and conclude by speculating where current analytical trends are headed.

7.2 Spatial variance at single scales

Certainly the most common use of a variance is to measure the precision of a mean. Variance s^2 of a quantity x is a measure of dispersion and is defined as the average sum of squared deviances from a sample mean $\overline{x}$:

$$s^2 = \frac{1}{n-1}\sum_{i=1}^{n}(x_i - \overline{x})^2 \qquad (7.1)$$

The variance of a quantity is used to estimate confidence intervals of sample means for ecological variables. What is not usually considered when making these calculations is that the magnitude of a variance is dependent on the spatial and temporal scale of sampling.

Another common use of variance in ecology has been to quantify the degree to

which organisms are aggregated. The most common technique was to compare an observed index of aggregation to an expected value under the assumption of randomness. These indices were largely based on variance to mean ratios (Fisher et al. 1922; Clapham 1936; Blackman 1942). Expected values were typically calculated from a Poisson distribution (i.e. events are rare and random occurrences). The expected value of the variance is equal to the mean, and hence the ratio of the variance to the mean is expected to be unity. Attributes of a "perfect coefficient" (i.e. index) were compiled by Taylor (1984) who supplemented those listed by Green (1966) and Lefkovitch (1966). Curtis and McIntosh (1950) demonstrated the dependence of several indices on measurement scale. Patil and Stiteler (1974) speculated that variance to mean ratios were a function of measurement scale, but developed the idea no further. A chronologic detailing of the development of variance to mean indices of aggregation and their equivalences can be found in Pielou (1969), Ripley (1981), and Greig-Smith (1983).

Morisita (1954, 1959a) developed an index I_δ based on Simpson's (1949) measure of diversity λ.

$$I_\delta = q \frac{\sum_{i=1}^{q} n_i(n_i - 1)}{N(N-1)} \tag{7.2}$$

where n_i ($i = 1, 2, 3, \ldots, q$) is the number of individuals in q quadrats and N is the total number of individuals observed. Morisita (1959b) recognized the dependence of variance to mean indices on measurement scale and specifically designed I_δ to be independent of sample resolution. Morisita's index compares density variances of

organisms among patches. Values of the index are independent of sample size as long as quadrat sizes are smaller than patches. Index values are less than 1 in regular distributions, approach 1 in random distributions, and exceed 1 in contagious distributions. Patil and Stiteler (1974) caution that this index assumes sample quadrats occur within large patches and that the distribution of organisms is random or regular within patches.

In an attempt to relate spatial distribution to density-dependent behaviour, Lloyd (1967) developed an index of aggregation that measures mean crowding $\dot{m}$ relative to a focal organism:

$$\dot{m} = \frac{s^2}{\bar{x}} + \bar{x} - 1 \qquad (7.3)$$

An index of patchiness was formed by the ratio of mean crowding $\dot{m}$ to average abundance $\bar{x}$. Lloyd (1967) used the equivalence of $\dot{m}$ to I_δ to claim that the mean crowding index $\dot{m}$ was also independent of sample size, and therefore quadrat size could be set at a spatial scale equivalent to the study organism's 'ambit'. Iwao (1968, 1970) linearly regressed $\dot{m}$ on $\bar{x}$ and used the intercept α as an indicator of aggregation size. Confusion over assumptions of the method have resulted in inappropriate conclusions when applied to field data (e.g. Byerly et al. 1978; Gutierrez et al. 1980).

As an alternative to developing an index from a variance to mean ratio, Taylor (1961) described the variance of a quantity as a function of the mean. Taylor's Power Law states that variance in the local density of many species x is proportional to the

mean density $\overline{x}$, raised to an empirically determined exponent β:

$$Var(x) \cong \overline{x}^{\beta} \tag{7.4}$$

The exponent β is used to quantify the degree of aggregation in a population. A β value near 0 indicates a regular distribution, a value equal to 1 indicates a random distribution, and a value greater than 1 indicates an aggregated distribution. The fit of this relation has been checked in a diverse set of populations (e.g. Taylor 1961; Taylor et al. 1978) and shown to require special treatment at low mean abundances (Taylor and Woiwod 1982; Routledge and Swartz 1991). Taylor and Taylor (1977) postulated that this relation results from the balance of attractive and repulsive behaviours among individuals that are attempting to maximize resource consumption. This hypothesis was questioned by Anderson et al. (1982) who showed that the relationship between the variance and mean density can arise from stochastic demographics, rather than complex behaviours.

The detection of a general relation between the variance and the mean of a population retains its appeal. Routledge and Swartz (1991) advocate the use of Bartlett's (1936) quadratic relationship (see below) over Taylor's Power Law to model the variance as a function of the mean. In response, Perry and Woiwod (1992) compare the fit of quadratic, power, split domain (Woiwod and Perry 1989), and generalized linear models (McCullagh and Nelder 1983). Using a ratio of deviances, they found that Taylor's power relationship and the generalized linear model were the best fitting models. The generalized linear model has the added advantage of not requiring stationary variance.

A sixth method to quantify spatial variance in abundance at a single scale is the

use of the parameter k from the negative binomial distribution (Waters 1959). The application of k as an index of dispersion was adopted from Bartlett's (1947) general expression of variance:

$$s^2 = c\bar{x} + \frac{\bar{x}^2}{k} \tag{7.5}$$

where c is a regression constant. Low values of k indicate an aggregated distribution while high values are indicative of a more random distribution. The maximum likelihood estimate of k is found by iteration or numerical maximization (Ripley 1981). Results from an aphid density study (Anscombe 1948) instigated an unsuccessful search by many ecologists for a constant k value among populations. If found, a robust index of aggregation such as k could be used to compare population distributions at different locations or times. Kuno (1968) and Hill (1973) proposed that random removal of individuals does not change observed patterns or the value of $\frac{1}{k}$. Pielou (1969) provided a proof to show that this is true only when the original population has a negative binomial distribution. Even this result does not apply to count data (Ripley 1981) because counts of organisms can not be less than zero. A random thinning of individuals lowers the mean, creates zero counts, eliminates patches of organisms, and changes the variance. Without an increase in sample resolution to compensate for the increased number of zeros due to thinning, spatial variance will increase at small scales (Chapter 4).

At the same time as these empirical measures were being proposed, there were continuing attempts to use theoretical frequency distributions to describe spatial variance. This line of research has been reviewed by Rogers (1974), Douglas (1979),

and Greig-Smith (1983). Motivations for fitting theoretical distributions to empirical observations include population description with a limited number of parameters and interpretation of parameter values for clues to processes that determine spatial structure. The negative binomial distribution was one of the first theoretical distributions used in ecology (Student 1907; Greenwood and Yule 1920). It is commonly used to describe the degree of aggregation in aquatic organisms (e.g. Taylor 1953; Houser and Dunn 1967), despite criticisms of its biological basis (Williams 1964). The Pólya-Aeppli (Pólya 1931), Neyman A, B, C (Neyman 1939), and Thomas double-Poisson (Thomas 1949) frequency distributions all assume a Poisson process of clustered organisms but differ in assumptions concerning the distribution of organisms within clusters. Comparisons of negative binomial distributions to other distributions based on Poisson processes have concluded that the negative binomial distribution is usually the most applicable theoretical frequency distribution, but no single frequency distribution is applicable to all data (Bliss 1941; McGuire et al. 1957; Brown and Cameron 1982).

The dependence of spatial variance on scale of measurement has restricted the application of theoretical frequency distributions to organism density data. Sample resolution was found to influence the fit of any theoretical frequency distribution (Numata and Suzuki 1953; Iwata 1954; Pielou 1957) and to affect the subsequent interpretation of spatial variance patterns. Altering sample resolution may alter the fit of a theoretical frequency distribution to the data, or increase the number of distributions that fit the data equally well. Ambiguous identification of appropriate theoretical frequency distribution models limits their use as descriptive summaries, or as clues to identifying potential variance generating processes.

The criticism that measures of aggregation are dependent on scale of measure applies to all methods of quantifying spatial variance of organism distribution at a single scale. Therefore, comparisons of aggregation indices among populations are only valid if made at the same spatial scale. The next logical step was to examine spatial variance in population dispersion as a function of scale.

7.3 Spatial variance at several scales

Pattern analysis (Greig-Smith 1952) was the first formal method to evaluate spatial variance as a function of scale. Organisms are counted in a grid of contiguous quadrats, with the resolution of the grid decreasing by a factor of two at each count iteration. The mean square from an analysis of variance is then plotted against sample resolution (ie. inverse of quadrat size). If the distribution of organisms is random over the entire grid then the mean squared deviation is independent of resolution and the variance will equal the mean. A patchy distribution will produce a peak of the mean square at the quadrat size of a patch. Kershaw (1957) extended this method by using linear transects of rectangular, contiguous quadrats rather than a grid of square, nested quadrats. This alteration of quadrat shape and layout enabled sampling of larger scales with less effort and facilitated analysis along obvious environmental gradients. Kershaw's transect approach was used to examine spatial variance in numerous plant communities (for examples see Greig-Smith 1983) and adapted to other measures of spatial variability (e.g. Morisita 1959a; Iwao 1972). Pattern analysis has the advantage over earlier methods of explicitly including spatial scale in the analysis. The method was used to identify the scale of maximum variability in any quantity of interest. It can

be used to set the sampling scale for manipulative experiments, and to provide clues to variance generating processes by matching dominant scales of biological variance to physical processes at the same spatial scale.

Plotting mean squares as a function of quadrat size does have limitations. Pielou (1969) cites five drawbacks of Greig-Smith's method: 1. calculated mean squares are not independent thereby preventing variance-ratio tests, 2. entire sites must be sampled within a grid (but this does not apply to transects), 3. observed peaks in plots are influenced by shape of sample quadrat (rectangular or square), 4. intermediate quadrat sizes between quadrat size doublings are not assessed, and 5. distributional patterns of the presence or absence of organisms are indistinguishable in mean square plots. An important drawback omitted by Pielou was the sensitivity of mean and variance estimates to size of the original quadrat and the location of sample grid (Skellam 1952). Usher (1969) and Hill (1973) proposed two different techniques to compensate for the dependence on sample start location but these have not been widely used. Ripley (1981) and Greig-Smith (1983) provide additional examples and detail studies that examine other caveats on pattern analysis.

One method that simultaneously examines a wide range of spatial scales and is not sensitive to sample start location is spectral analysis. The variance of a continuously recorded variable (e.g. organism density), is represented by a set of sine and cosine waves summed over a range of measurement frequencies. The resulting spectral density estimates are plotted as a function of frequency, the inverse of spatial or temporal scale. Peaks in spectral density plots are interpreted as dominant scales of pattern. This technique has been widely used by oceanographers and limnologists to

examine scale-dependent spatial variance of passive tracers of the fluid (e.g. surface water temperature -- Fasham and Pugh 1976; Richerson et al. 1978) or organisms in fluid environments (e.g. phytoplankton -- Platt et al. 1970; Powell et al. 1975). The equivalence of spectral analysis to other indices of aggregation is shown in Ripley (1981) and Schneider (1994b).

Spectral decomposition techniques are not ideally suited to the analysis of patchily distributed, rare organisms. Continuous processes are well described by sine and cosine functions but the non-Gaussian character of point processes, such as mobile organism counts, limit the use of spectral models (Bartlett 1975). Biological density data rarely provide long temporal or spatial series and often violate other assumptions of regular sampling intervals and stationarity of means. The partitioning of variance among frequencies by spectral analysis is sensitive to low means (Fasham 1978) and to the presence of zeros in count data (Chapter 4). Coherence can be lowered by random sampling error in a Poisson process (Mackas 1977), and does not adequately reflect non-linear relationships between two variables (Star and Cullen 1981). Despite these limitations, spectral analysis is at least as reliable as other methods (Ripely 1981) and may be used to demarcate domains of spatial variance (Chapter 4).

Recently there have been several attempts to predict change in spatial variance at a single scale and across scales. Predictions of change in spatial variance are formulated using biological or physical processes that are capable of generating or reducing spatial variance in the quantity of interest. The ability to predict change in scale-dependent spatial variance is important in several ecological contexts including: effects of predators on the stability of prey populations (Pacala et al. 1990; Hassell et al. 1991),

effects of habitat fragmentation on population stability (Kareiva 1990); density-dependent effects of crowding on reproduction and growth (Stephen 1929; Connell 1961), and the effects of predator searching (Salt 1974) and encountering resources (Possingham 1989). Schneider (1992) found that changes in spatial density variance of bamboo worms *Clymenella torquata* could be predicted from the foraging dispersion of an avian predator, the short-billed dowitcher *Limnodromus griseus*, at the spatial scale of intertidal flats (0.2-3 km^2) but not at the scale of plots (1 ha) within flats. Similarly, Schneider and Bajdik (1992) attempted to predict changes in spatial variance in counts of gelatinous zooplankton based on wind-induced Langmuir circulation cells. They found that variance in counts was proportional to spatial scale during a wind event, but the magnitude of change was not easily predicted. These two examples illustrate that predicting changes in spatial variance is difficult, and that methods to predict changes in spatial variance across scales require development.

7.4 The analysis of spatial variance

Progress in assessing spatial variance of ecological quantities has been marked by transitions from verbal acknowledgement to graphical models, and from graphic to formal models of pattern and process. Transitions from verbal to graphical and formal models have not been synchronous in all areas of ecology. However awareness of spatial variance is rapidly spreading. A computer scan of *Current Contents* using keywords 'spatial' and 'variance' in June 1994 resulted in 371 titles from 225 different journals published since September 1992.

A major advance in the analysis of spatial variance was the recognition that

measures of variance depend on the scale of observation. This represented a change from treating variance as a statistical detail to treating it as a biologically important quantity (Steele 1976). One response to this realization was to re-analyze data at a different scale and compare the second set of results to the original. In aquatic systems, Fairweather and colleagues (Fairweather et al. 1984; Fairweather 1988) and Schmitt (1982, 1985) both found that the sign of association between predator and prey changed from negative to positive when the scale of observation was increased. A second response has been to report the analysis of biological quantities at two or more scales (e.g. Pinel-Alloul and Pont 1991; Ives et al. 1993). This approach increases the number and range of observation scales. It does not indicate if observations were set at scales of maximum spatial variance.

The analysis of spatially indexed data has matured from verbal descriptions at discrete scales to graphic representations of spatial variance as a continuous function. This was initiated by the development of pattern analysis (Greig-Smith 1952) and later expanded to include other measures of spatial variance plotted as a function of scale. The computational burden of this approach has been significantly reduced with the wide availability of statistical software packages. Large, spatially explicit data sets are routinely analyzed using geostatistical techniques (e.g. Rossi et al. 1992) which are often incorporated in geographic information systems (GIS). In oceanography spectral analysis is commonly used to describe scale-dependent biological pattern in the frequency domain (e.g. Mackas and Boyd 1979; Weber et al. 1986). The frequency of maximum spatial variance can then be converted to a length scale for biological or physical interpretation.

The most important recent development in the characterization of spatial variance has been the idea of formally expressing biological pattern and processes that generate variance as a function of scale. Empirical indices of spatial variance (e.g. variance to mean ratios, Lloyd's mean crowding index $\overset{*}{m}$, Morisita's I_δ) that were implicitly calculated at single scales are now explicitly calculated as a function of scale (e.g. Schneider and Piatt 1986). Similarly, the exponent β from Taylor's Power Law and slopes of spectral density plots can be used to quantify changes in spatial variance with changes in scale. I could not find any research report in which parameters of a theoretical frequency distribution were expressed as a function of scale in an equation or as a graph. To provide an example, the parameter k from the negative binomial distribution could be estimated using moment ratios (Ord 1972) and expressed as a function of measurement scale L:

$$k = \alpha L^{\beta} \tag{7.6}$$

Estimating k at different scales is accomplished by grouping contiguous values in increasing quadrat sizes or comparing values over larger separation distances. This relation could be used to calculate an expected variance at one scale based on an observed variance at another scale. Alternatively, the exponent β could also be used as an index of the dependence of k on measurement scale. If β equals 0 then k is independent of spatial scale. As the value of β approaches 1, k becomes directly proportional to the scale of observation L.

7.5 The next steps

The treatment of scale-dependent spatial variance has evolved since its recognition as a biologically important quantity. Increased awareness of the importance of scale in the measurement of spatial or temporal variance will ensure that this progress continues. Further development of quantitative tools will help standardize the analysis of spatial variance. Application of new techniques will improve sample design and subsequent data analysis.

A simple and useful standardization is the explicit treatment of measurement scale in sample design. Explicit treatment eliminates any novelty associated with scale and obligates the reporting of all measurement scales in results. A second development in the standardization of survey design would be the use of scale-dependent spatial variance to determine the resolution and number (or frequency) of samples needed to obtain a pre-determined precision of parameter estimates. If the variance of a quantity is dependent on scale of measurement then precision of parameter estimates also depends on measurement scale. One method to maximize precision of parameter estimates is to confine sampling to established domains of spatial variance (Chapter 4). Spatial variance domains minimize changes in spatial variance across scales which maximizes precision of parameter estimates within domains. If domains of spatial variance are very small then the range of sampling should be set to minimize the rate of change in spatial variance across spatial scales. Minimizing the rate of change in spatial variance, by selecting a narrow sample range, also maximizes precision of parameter estimates and potentially increases the ability to theoretically predict sources of spatial variance.

Overall, the standardization of analytic techniques will enhance comparison of pattern and process among diverse ecosystems. A statistical tool that analyzes continuous or discrete data types across a wide range of spatial and temporal scales would reduce problems associated with low means and zeros in count data (Chapter 4) and simplify comparisons of patterns observed at different locations or scales. Legendre and Fortin (1989) provide a comprehensive summary of techniques used to analyze variance in organism distributions as a function of location or as a function of scale. Despite ambiguity in their use of geographic location and spatial scale, they demonstrate the feasibility of explicitly including spatial variables (location, sample resolution) in the analysis of organism distributions. By including measurement variables, the dependence of observed patterns on measurement scale can be tested directly.

The most challenging task ahead is to develop the theory and quantitative methods needed to predict changes in spatial variance of biological quantities as a function of scale. Successful completion of this goal requires: numerical methods that analyze continuous and discrete density data, additional quantitative descriptions and comparisons of scale-dependent variance patterns, tools to quantify the relative importance of variance generating processes, and further attempts to predict changes in spatial variance. In combination, these elements will solidify the theory of spatial variance in ecology.

Chapter 8. Summary

Capelin and Atlantic cod in coastal waters of Newfoundland were selected as being representative of interacting, mobile aquatic organisms. Relative density data from a series of hydroacoustic transects were analyzed to examine spatial variance as a function of scale. Theoretical and empirical results of this study have increased knowledge of scale-dependent spatial variance in mobile aquatic organisms and provided insight to the biological processes that generate these patterns.

The application of dimensionless ratios in rate diagrams is one of the first methods to quantify and summarize the relative importance of biological and physical processes that generate scale-dependent spatial and temporal variance. This procedure can be applied to organisms in aerial, aquatic, or terrestrial environments and used to compare variance generating processes among diverse ecosystems. Rate diagrams provide an alternative to inferring variance generating processes from scales of maximum biological variability.

Capelin and cod relative density variance was quantified and compared to that of plankton and marine birds over four orders of spatial magnitude at two different time scales. Data manipulations and computer simulations were successfully used to demonstrate that shoaling and schooling, two biological processes, influence intermediate and small scale spatial variance in all mobile aquatic organisms. Aggregative behaviour and organism locomotion were previously hypothesized to account for differences in spatial variance between passive tracers and mobile organisms, but were not quantitatively examined.

Energetic calculations verified the absence of a maximum scale of spatial

association between cod as predator and capelin as prey. Previous work on cod and capelin attributed poor spatial association to species-specific thermal responses to wind induced upwelling. This did not explain observed results. An alternate explanation is that cod are not constrained by physiological requirements to aggregate relative to their prey. In general, aggregative responses by aquatic predators do not occur at all spatial scales and may only occur over a limited range of scales. Numerous interaction studies have reported characteristic scales of spatial association between mobile predators and their prey. These conclusions are typically based on analyses of single or a limited number of transects, implicitly representing short temporal scales. Comparison of results among these studies is hampered by failure to explicitly report spatial and temporal sampling scales.

A review of spatial variance research revealed that numerous techniques have been used to quantify variance in biologically important quantities. However a limited number of quantitative tools are available to evaluate processes that generate spatial and temporal variance. As an alternative to simply stating that scale is important, essential research goals were identified and a potential research program was proposed.

References

Aggett, D, Gaskill, H.S., Finlayson, D., May, S., Campbell, C. and Bobbitt, J. (Lear, W.H. and Rice, J.C. (eds.)). 1987. A study of factors influencing availability of cod in Conception Bay, Newfoundland, in 1985. Can. Tech. Rep. Fish. Aquat. Sci. **1562.**

Akenhead, S.A., Carscadden, J., Lear, H., Lilly, G.R. and Wells, R. 1982. Cod-capelin interactions off northeast Newfoundland and Labrador, pp. 141-148. In Mercer, M.C. (ed.) *Multispecies approaches to fisheries management advice.* Can. Spec. Publ. Fish. Aquat. Sci. **59.**

Anderson, R.M. and May, R.M. 1985. Helminth infections of humans. Adv. Parasitol. **24**: 1-102.

Anderson, R.M., Gordon, D.M., Crawley, M.J. and Hassell, M.P. 1982. Variability in the abundance of animal and plant species. Nature **296**: 245-248.

Anon. 1980. Northwest Atlantic Fisheries Organization, Scientific Commercial S Doc. **80/II/I.** 31 p.

Anscombe, F.J. 1948. On estimating the population of aphids in a potato field. Ann. Appl. Biol. **35**: 567-571.

Anthony, P.D. 1981. Visual contrast thresholds in the cod *Gadus morhua* L. J. Fish Biol. **19**, 87-103.

Aoki, I. 1982. A simulation study on the schooling mechanism in fish. Bull. Jap. Soc. Sci. Fish. **48**, 1081-1088.

Aoki, I. 1984. Internal dynamics of fish schools in relation to inter-fish distance. Bull. Jap. Soc. Sci. Fish. **50**, 751-758.

Aoki, I. 1986. A simulation experiment on individual differences in schooling behaviour of fish. Bull. Jap. Soc. Sci. Fish. **52**, 1115-1119.

Arnold, G.P. and Cook, P.H. 1984. Fish migration by selective tidal stream transport: first results with a computer simulation model for the European continental shelf, pp. 221-261. In McCleave, J.D., et al. (eds.) *Mechanisms of Migration in Fishes.* Plenum Press, New York.

Aronson, R.B. 1992. Biology of a scale-independent predator-prey interaction. Mar. Ecol. Prog. Ser. **89**: 11-13.

Atkinson, D.B. and J.E. Carscadden. 1979. Biological characteristics of inshore capelin, *Mallotus villosus* (Müller), June-July 1977. Can. Tech. Rep. Fish. Aquat. Sci. **881**.

Bailey, B.J.F., Able, K.W. and Leggett, W.C. 1977. Seasonal and vertical distribution and growth of juvenile and adult capelin (*Mallotus villosus*) in the St. Lawrence estuary and western Gulf of St. Lawrence. J. Fish. Res. Board Can. **34**: 2030-2040.

Bainbridge, R. 1957. The size and shape and density of marine phytoplankton concentrations. Biol. Rev. **32**: 91-115.

Bartlett, M.S. 1936. Some notes on insecticide tests in the laboratory and in the field. Supplement to J. R. Statist. Soc. **3**: 185-194.

Bartlett, M.S. 1947. The use of transformations. Biometrics **3**: 39-52.

Bartlett, M.S. 1975. *The statistical analysis of spatial pattern.* Chapman and Hall, London.

Beamish, F.W.H. 1978. Swimming capacity, pp. 101-187. In Hoar, W.S. and Randall, D.J. (eds.) *Fish Physiology*. Academic Press, New York.

Berryman, A.A. 1992. The origins and evolution of predator-prey theory. Ecology **73**: 1530-1535.

Beverton, R.J.H. and Holt, S.J. 1957. On the dynamics of exploited fish populations. Fish. Invest. London **2**.

Bigelow, H.B. and Schroeder, W.C. 1963. Family Osmeridae. In *Fishes of the Western North Atlantic*. Mem. Sears. Found. Mar. Res. **1**(3): 553-597.

Bigelow, H.B., Lillick, L.C. and Sears, M. 1940. Phytoplankton and planktonic protozoa of the offshore waters of the Gulf of Maine. Part I. Numerical distribution. Trans. Am. Philos. Soc. N.S. **31**: 149-191.

Bishop, C.A., Murphy, E.F., Davis, M.B., Baird, J.W. and Rose, G.A. 1993. An assessment of the cod stock in NAFO Divisions 2J+3KL. Northwest Atlantic Fisheries Organization Scientific Council Report **93/86**.

Blackman, G.E. 1942. Statistical and ecological studies in the distribution of species in plant communities. I. Dispersion as a factor in the study of changes in plant populations. Ann. Bot. **6**: 351-370.

Blaxter, J.H.S. 1967. Swimming speeds of fish. FAO Conference on Fish Behavior in Relation to Fishing Techniques and Tactics Review Papers **3**, 1-32.

Bliss, C.I. 1941. Statistical problems in estimating populations of Japanese beetle larvae. J. Econ. Entomol. **34**: 221-232.

Blomqvist, S. and Peterz, M. 1984. Cyclones and pelagic seabird movements. Mar. Ecol. Prog. Ser. **20**, 85-92.

Boehlert, G.W. and Mundy, B.C. 1988. Roles of behavioral and physical factors in larval and juvenile fish recruitment to estuarine nursery areas. Am. Fish. Soc. Symp. **3**, 51-67.

Bradbury, R.H., Reichelt, R.E. and Green, D.G. 1984. Fractals in ecology: methods and interpretation. Mar. Ecol. Prog. Ser. **14**: 295-296.

Breder Jr., C.M. 1954. Equations descriptive of fish schools and other aggregations. Ecology **35**: 361-370.

Brett, J.R. 1973. Energy expenditure of sockeye salmon, *Oncorhynchus nerka*, during sustained performance. J. Fish. Res. Bd. Can. **30**: 379-387.

Brett, J.R. and Groves, T.D.D. 1979. Physiological Energetics, pp. 279-352. In Hoar, W.S., Randall, D.J. and Brett, J.R. (eds.) *Fish Physiology* vol. VII. Academic Press, New York.

Bridgman, P.W. 1922. *Dimensional Analysis*. Yale University Press, New Haven.

Briggs, K.T. 1986. Scales of patchiness in seabirds off central California. Pac. Seabird Group Bull. **13**: 19-20.

Brown, M.W. and Cameron, E.A. 198? Spatial distribution of adults of *Ooenevrtus kuvanae* (Hymenoptera: Encyrtidae), an egg parasite of *Lymantria dispar* (Lepidoptera: Lymantriidae). Can. Entomol. 114: 1109-1120.

Brown, R.G.B. and D.N. Nettleship 1984. Capelin and seabirds in the Northwest Atlantic, pp. 184-194. In Nettleship, D.N., Sanger, G.A. and Springer, P.F. (eds.) *Marine birds: their feeding ecology and commercial fisheries relationships*. Canadian Wildlife Services Special Publication.

Burczynski, J. 1982. Introduction to the use of sonar systems for estimating fish biomass. FAO Fisheries Technical Paper **191** (Rev. 1): 49-54.

Buzdalin, Y.I. and Burmakin, V.V. 1976. O svyazhi mezhdu temperaturoi poverxhnosti morya i plotnostyu skoplenii moivi v raione Nyufaundlenda. Trudi PINRO **37**: 57-60.

Byerly, K.F., Gutierrez, A.P., Jones, R.E. and Luck, R.F. 1978. A comparison of sampling methods for some arthropod populations in cotton. Hilgardia **46**: 257-282.

Campbell, J.S. and Winters, G.H. 1973. Some biological characteristics of capelin (*Mallotus villosus*) in the Newfoundland area. ICNAF Res. Doc. **73/90**.

Carscadden, J.E. 1983. Population dynamics and factors affecting the abundance of capelin (*Mallotus villosus*) in the northwest Atlantic. FAO Fisheries Report **291**: 789-811.

Carscadden, J.E. and Miller, D.S. 1980. Analytical and acoustic assessment of the capelin stock in Subarea 2 and Div. 3K, 1979. Northwest Atl. Fish. Org. SRC Doc. **80/13**.

Carscadden, J.E. and Miller, D.S. 1981. Analytical assessment of the capelin stock in Subarea 2 + Div. 3K using SCAM. Northwest Atl. Fish. Org. SRC Doc. **81/4**.

Carscadden, J.E., Nakashima, B.S. and Miller, D.S. 1991. Capelin in NAFO division 2JK and division 3L. CAFSAC Res. Doc. **91/68**.

Cassie, R.M. 1960. Factors influencing the distribution pattern of plankton in the mixing zone between oceanic and harbour waters. N.Z. J. Sci. **3**: 26-50.

Cassie, R.M. 1963. Microdistribution of plankton. Oceanogr. Mar. Biol. Annu. Rev. **1**: 223-252.

Chatfield, C. 1980. *The Analysis of Time Series: an introduction*. Second edition. Chapman and Hall, London.

Chesson, P. 1978. Predator-prey theory and variability. Annual Review of Ecology and Systematics **9**: 323-347.

Clapham, A.R. 1936. Over-dispersion in grassland communities and the use of statistical methods in plant ecology. J. Ecol. **24**: 232-251.

Clark, D.S. and Green, J.M. 1990. Activity and movement patterns of juvenile Atlantic cod, *Gadus morhua*, in Conception Bay, Newfoundland, as determined by sonic telemetry. Can J. Zool. **68**: 1434-1442.

Connell, J.H. 1961. Effects of competition, predation by *Thais lapillus*, and other factors on natural populations of the barnacle *Balanus balanoides*. Ecol. Monogr. **31**: 61-104.

Cram, D.L. and Hampton, I. 1976. A proposed aerial/acoustic strategy for pelagic fish stock assessment. J. Cons. int Explor. Mer. **37**, 91-97.

Cronin, T.W. and Forward Jr., R.B. 1979. Tidal vertical migration: an endogenous rhythm in estuarine crab larvae. Science **205**, 1020-1022.

Csirke, J. 1988. Small shoaling pelagic fish stocks, pp. 271-302. In Gulland, J.A. (ed.) *Fish Population Dynamics*. John Wiley and Sons, New York, .

Cullinan, V.I. and Thomas, J.M. 1992. A comparison of quantitative methods for examining landscape pattern and scale. Lands. Ecol. **7**: 211-227.

Curtis, J.T. and McIntosh, R.P. 1950. The interrelation of certain analytic and synthetic phytosociological characters. Ecology **31**: 434-455.

Cushing, D.H. 1982. *Climate and Fisheries*. Academic Press, New York.

Cushing, D.H. and Tungate, D.S. 1963. Studies on *Calanus* patch. I. The identification of a *Calanus* patch. J. Mar. Biol. Ass. UK. **43**: 327-337.

DeAngelis, D.L. 1978. A model for the movement and distribution of fish in a body of water. **ORNL/TM-6310**. Oak ridge National Laboratory, Oak Ridge.

Delcourt, H.R., Delcourt, P.A. and Webb, T. 1983. Dynamical plant ecology: the spectrum of vegetational change in space and time. Quarter. Sci. Rev. **1**: 153-175.

Demers, S. and Legendre, L. 1979. Effets des marées sur la variation circadienne de la capacité photosynthétique du phytoplancton de l'estuaire du Saint-Laurent. J. Exp. Mar. Biol. Ecol. **39**: 87-99.

Demers, S. and Legendre, L. 1981. Mélange vertical et capacité photosynthétique du phytoplancton estuarien (estuaire du Saint-Laurent). Mar. Biol. **64**: 243-250.

Denil, G. 1936-1938. La mécanique du poisson de rivière; qualité nautique du poisson; ses méthodes des locomotrices; ses capacités; ses limites; résistance du fluide; effet de la vitesse, de la pente; résistance du seuil. Bruxelles.

Denman, K.L. 1975. Spectral analysis: A summary of the theory and techniques. Fisheries and Marine Service Research Development Technical Report **539**. Department of Fisheries and Oceans, Ottawa.

Denman, K.L. 1976. Covariability of chlorophyll and temperature in the sea. Deep-Sea Res. **23**: 539-550.

Denman, K.L. and Platt, T. 1975. Coherences in the horizontal distributions of phytoplankton and temperature in the upper ocean. Mém. Soc. R. Sci. Liège **7**: 19-30.

Denman, K.L. and Platt, T. 1976. The variance spectrum of phytoplankton in a turbulent ocean. J. Mar. Res. **34**: 593-601.

Denman, K.L. and Mackas, D.L. 1978. Collection and analysis of underway data and related physical measurements, pp. 85-109. In Steele, J.H. (ed.) *Spatial Pattern in Plankton Communities*. Plenum Press, New York.

Denman, K.L. and Powell, T.M. 1984. Effects of physical processes on planktonic ecosystems in the coastal ocean. Oceanogr. Mar. Biol. Ann. Rev. **22**: 125-168.

de Young, B., Otterson, T. and Greatbatch, R.J. 1993. The local and non-local response of Conception Bay to wind forcing. J. Phys. Oceanogr. **23**: 2636-2649.

Dickey, T.D. 1990. Physical-optical-biological scales relevant to recruitment in large marine ecosystems, pp. 82-98. In Sherman, K., Alexander, L.M. and Gold, B.D. (eds.) *Large Marine Ecosystems: Patterns, Processes, and Yields*. Amer. Assoc. Advanc. Sci. Publ. No. **90-30s**, Washington, D.C.

Diggle, P.J. 1990. *Time Series: a biostatistical introduction*. Clarendon Press, Oxford.

Dixon, W.J. 1983. *BMDP Statistical Software*. University of California Press, Berkeley.

Douglas, J.B. 1979. *Analysis with Standard Contagious Distributions*. International Co-operative Publishing House, Burtonsville.

Dutton, J.A. 1976. *The Ceaseless Wind*. McGraw-Hill, New York.

Dwyer, R.L. and Perez, K.T. 1983. An experimental examination of ecosystem linearization. Am. Nat. **121**: 305-323.

Erikstad, K.E., Moum, T. and Vader, W. 1990. Correlations between pelagic distribution of Common and Brunnich's Guillemots and their prey in the Barents Sea. Polar Res. **8**: 77-87.

Estrada, M. and Wagensburg, M. 1977. Spectral analysis of spatial series of oceanographic variables. J. Exp. Mar. Biol. Ecol. **30**: 147-164.

Fairfield Smith, H. 1938. An empirical law describing heterogeneity in the yields of agricultural crops. J. Agric. Sci. **28**: 1-23.

Fairweather, P.G. 1988. Correlations of predatory whelks with intertidal prey at several scales of space and time. Mar. Ecol. Prog. Ser. **45**: 237-243.

Fairweather, P.G., Underwood, A.J. and Moran, M.J. 1984. Preliminary investigations of predation by the whelk *Morula marginaiba*. Mar. Ecol. Prog. Ser. **17**: 143-156.

Fasham, M.J. 1978. The application of some stochastic processes to the study of plankton patchiness, pp. 131-156. In Steele, J.H. (ed.) *Spatial Pattern in Plankton Communities*. Plenum Press, New York.

Fasham, M.J. and Pugh, P.R. 1976. Observations on the horizontal coherence of chlorophyll *a* and temperature. Deep-Sea Res. **23**: 527-538.

Fiedler, P.C. 1978. The precision of simulated transect surveys of northern anchovy, *Engraulis mordax*, school groups. Fish. Bull. **76**, 679-685.

Fischer, H., List, E.J., Koh, R.C.Y., Imberger, J. and Brooks, N.H. 1979. Dimensional Analysis, pp. 23-29. In *Mixing in Inland and Coastal Waters*. Academic Press, New York.

Fisher, R.A., Thornton, H.G. and Mackenzie, W.A. 1922. The accuracy of the plating method of estimating the density of bacterial populations, with particular reference to the use of Thornton's agar medium with soil samples. Ann. Appl. Biol. **9**: 325-359.

Ford, E.D. 1976. The canopy of a Scots pine forest: description of a surface of complex roughness. Agric. Meteorol. **17**: 9-32.

Fortier, L. and Leggett, W.C. 1982. Fickian transport and the dispersal of fish larvae in estuaries. Can. J. Fish. Aquat. Sci. **39**: 1150-1163.

Fortier, L. and Leggett, W.C. 1983. Vertical migrations and transport of larval fish in a partially mixed estuary. Can. J. Fish. Aquat. Sci. **40**: 1543-1555.

Frank, K.T. and Leggett, W.C. 1981. Wind regulation of emergence times and early larval survival in capelin (*Mallotus villosus*). Can. J. Fish. Aquat. Sci. **38**: 215-223.

Frank, K.T., and Leggett, W.C. 1982. Coastal water mass replacement: its effect on zooplankton dynamics and the predator-prey complex associated with larval capelin (*Mallotus villosus*). Can. J. Fish. Aquat. Sci. **39**: 991-1003.

Frank, K.T. and Leggett, W.C. 1983. Multispecies larval fish associations: accident or adaptation? Can. J. Fish. Aquat. Sci. **40**, 754-762.

Gerritsen, J. and Strickler, J.R. 1977. Encounter probabilities and community structure in zooplankton: a mathematical model. J. Fish. Res. Bd. Can. **34**, 73-82.

Gran, H.H. and Braarud, T. 1935. A quantitative study of the phytoplankton in the Bay of Fundy and the Gulf of Maine (including observations on hydrography, chemistry and turbidity). J. Biol. Bd Can. **1**: 279-467.

Grassle, J.F., Sanders, H.L., Hessler, R.R., Rowe, G.T. and McLellan, T. 1975. Pattern and zonation: a study of the bathyal megafauna using the research submersible Alvin. Deep-Sea Res. **22**: 457-481.

Green, R.H. 1966. Measurement of non-randomness in spatial distributions. Res. Popul. Ecol. **8**: 1-7.

Greenwood, M. and Yule, G.U. 1920. An enquiry into the nature of frequency distributions representative of multiple happenings with particular reference to the occurrence of multiple attacks of disease or of repeated accidents. J. R. Stat. Soc. **83**: 255-279.

Greig-Smith, P. 1952. The use of random and contiguous quadrats in the study of structure of plant communities. Ann. Bot. Soc. London NS **16**: 293-316.

Greig-Smith, P. 1983. *Quantitative Plant Ecology*. Third edition. Blackwell Scientific Publications, Oxford.

Günther, B. 1975. Dimensional analysis and theory of biological similarity. Phys. Rev. **55**: 659-699.

Gutierrez, A.P., Summers, C.G. and Baumgaertner, J. 1980. The phenology and distribution of aphids in California alfalfa as modified by a ladybird beetle predation (Coleoptera: Coccenellidae). Can. Entomol. **112**: 489-495.

Hanski, I. 1991. The functional response of predators: worries about scale. Trends Ecol. Evol. **6**: 141-142.

Harden-Jones, F.R., Walker, M.G. and Arnold, G.P. 1978. Tactics of fish movement in relation to migration strategy and water circulation, pp. 185-207. In Charnock, H. and Deacon, G. (eds.) *Advances in Oceanography*. Plenum Press, New York.

Hardy, A.C. 1935. A further example of the patchiness of plankton distribution. Papers in Marine Biology Oceanography Deep Sea Research 3 (Suppl.): 7-11.

Hardy, A.C. 1936. Observations on the uneven distribution of oceanic plankton. Discovery Rep. **11**: 513-538.

Harris, G.P. 1986. *Phytoplankton Ecology: Structure, Function and Fluctuation.* Chapman and Hill, London.

Hassell, M.P. and May, R. 1973. Stability in host-parasitoid modes. J. Anim. Ecol. **42**: 693-726.

Hassell, M.P. and Anderson, R.M. 1988. Predator-prey and host-pathogen interactions, pp. 147-196 In Cherrett, J.M. (ed.) *Ecological Concepts*. Blackwell Scientific Publications, Oxford.

Hassell, M.P., Comins, H.N. and May, R.M. 1991. Spatial structure and chaos in insect population dynamics. Nature **353**: 255-258.

Hastings, A. 1990. Spatial heterogeneity and ecological models. Ecology **71**: 426-428.

Haury, L.R., McGowan, J.A. and Wiebe, P.H. 1978. Patterns and processes in the time-space scales of plankton distributions, pp. 277-327. In Steele, J.H. (ed.) *Spatial Pattern in Plankton Communities*. Plenum Press, New York.

Hawkins, A.D., Soofiani, N.M. and Smith, G.W. 1985. Growth and feeding of juvenile cod (*Gadus morhua* L.). J. Cons. Int. Explor. Mer **42**: 11-32.

He, P. 1991. Swimming endurance of the Atlantic cod, *Gadus morhua* L., at low temperatures. Fish. Res. 12: 65-73.

Heads, P.A. and Lawton, J.H. 1983. Studies on the natural enemy complex of the effects of scale on the detection of aggregative responses and the implications for biological control. Oikos 40: 267-276.

Heinemann, D., Hunt, G.L. and Everson, I. 1989. The distribution of marine avian predators and their prey *Euphausia superba*, in Bransfield Strait and southern Drake Passage, Antarctica. Mar. Ecol. Prog. Ser. 58: 3-16.

Helbig, J., Mertz, G. and Pepin, P. 1992. Environmental influences on the recruitment of Newfoundland/Labrador Cod. Fish. Oceanog. 1: 39-56.

Hensen, V. 1911. Das leben im ozean nach zahlungen seiner Bewohner. Ubersicht und resultaten der quantitativen untersuchungen. Ergebn. Plankton Expdn. der Humboldt Stiftung V.

Herman, A.W., Sameoto, D.D. and Longhurst, A.R. 1981. Vertical and horizontal distribution patterns of copepods near the shelf break south of Nova Scotia. Can. J. Fish. Aquat. Sci. 38: 1065-1076.

Heusner, A.A. 1987. What does the power function reveal about structure and function in animals of different size. Annu. Rev. Physiol. 49: 121-133.

Hill, M.O. 1973. The intensity of spatial pattern in plant communities. J. Ecol. 61: 225-235.

Holdbrook, S.J. and Schmitt, R.J. 1988. The combined effects of predation risk and food reward on patch selection. Ecology 69: 125-134.

Holling, C.S. 1965. The functional response of predators to prey density and its role in mimicry and population regulation. Mem. Entomol. Soc. Can. **45**: 1-60.

Holling, C.S. 1966. The functional response of invertebrate predators to prey density. Mem. Entomol. Soc. Can. **48**: 1-86.

Holling, C.S. 1992. Cross-scale morphology, geometry, and dynamics of ecosystems. Ecol. Mon. **62**: 447-502.

Horwood, J.W. 1978. Observations on spatial heterogeneity of surface chlorophyll in one and two dimensions. J. Mar. Biol. Assoc. UK **58**: 487-502.

Houser, A. and Dunn, J.E. 1967. Estimating the size of the thread-fin shad population in Bull Shoal reservoir from midwater trawl catches. Trans. Am. Fish. Soc. **96**: 176-184.

Huffaker, C.B. 1958. Experimental studies on predation: dispersion factors and predator-prey oscillations. Hilgardia **27**: 343-383.

Hunt, G.L., Harrison, N.M. and Cooney, T. 1990. Foraging of Least Auklets: The influence of hydrographic structure and prey abundance. Studies in Avian Biology **14**: 7-22.

Huxley, J.S. 1932. *Problems of Relative Growth*. Methuen, London.

Ibanez, F. and Boucher, J. 1987. Anisotropy of zooplankton populations in the Ligurian Sea front. Oceanol. Acta. **10**: 205-216.

Iverson, R.L., Whitledge, T.E. and Goering, J.J. 1979. Fine-structure of chlorophyll and nitrate in the southeastern Bering Sea shelf break front. Nature **281**: 664-666.

Ives, A.R., Kareiva, P. and Perry, R. 1993. Response of a predator to variation in prey density at three hierarchical scales: lady beetles feeding on aphids. Ecology **74**: 1929-1938.

Iwao, S. 1968. A new regression method for analyzing the aggregation pattern of animal populations. Res. Popul. Ecol. **10**: 1-20.

Iwao, S. 1970. Analysis of spatial patterns in animal populations: progress of research in Japan. Jpn. Rev. Plant Prot. Res. **3**: 41-54.

Iwao, S. 1972. Application of the $m^* - m$ method to the analysis of spatial patterns by changing the quadrat size. Res. Popul. Ecol. **17**: 240-242.

Iwata, T. 1954. Progress of studies on the population distribution in the unit-area sampling and its criticism. (in Japanese) Biol. Sci. Tokyo **6**: 110-116.

Jacobson, P.T. 1990. Pattern and process in the distribution of Cisco, *Coregonus artedii*, in Trout Lake, Wisconsin. Ph.D. thesis, University of Wisconsin-Madison, Madison.

Jangaard, P.M. 1974. The capelin (*Mallotus villosus*) biology, distribution, exploitation, utilization and composition. Bull. Fish. Res. Board Can. **186**.

Jenkins, B.W. 1975. A qualitative and quantitative investigation of the behaviour of the longhorn sculpin, *Myoxocephalus octodecemspinosus* (Mitchell) 1815, with special reference to feeding. MSc. thesis. Memorial University of Newfoundland, St. John's.

Jenkins, G.M. and Watts, D.G. 1968. *Spectral analysis and its applications*. Holden-Day, San Francisco.

Jobling, M. 1982. Food and growth relationships of the cod, *Gadus morhua* L., with special reference to Balsfjorden, north Norway. J. Fish Biol. **21**: 357-371.

Jobling, M. 1988. A review of the physiological and nutritional energetics of cod, *Gadus morhua* L., with particular reference to growth under farmed conditions. Aquaculture **70**: 1-19.

Jumars, P.A. 1976. Deep-Sea species diversity: does it have a characteristic scale? J. Mar. Res. **34**: 217-246.

Kareiva, P. 1989. Renewing the dialogue between theory and experiments in population ecology, pp. 68-88. In Roughgarden, J., May, R.M., and Levin, S.A. (eds.) *Perspectives in Ecological Theory*. Princeton University Press, Princeton.

Kareiva, P. 1990. Population dynamics in spatially complex environments: theory and data. Philos. Trans. R. Soc. London B **330**: 175-190.

Keats, D.W., Steele, D.H. and South, G.R. 1987. The role of fleshy macroalgae in the ecology of juvenile cod (*Gadus morhua* L.) in inshore waters off eastern Newfoundland. Can. J. Zool. **65**: 49-53.

Kerr, S.R. 1971. Prediction of fish growth efficiency in nature. J. Fish. Res. Bd Can. **28**: 809-814.

Kershaw, K.A. 1957. The use of cover and frequency in the detection of pattern in plant communities. Ecology **38**: 291-299.

Kershaw, K.A. 1958. An investigation of the structure of a grassland community. I. The pattern of *Agrostis tenuis*. J. Ecol. **46**: 571-592.

Kierstead, H. and Slobodkin, L.B. 1953. The size of water masses containing plankton blooms. J. Mar. Res. **12**: 141-147.

Kolmogorov, A.N. 1941. The local structure of turbulence in an incompressible viscous fluid for very large Reynolds numbers. Akademiia Nauk SSSR Comptes Rendus (Doklady) **30**: 299-303.

Koopmans, L.H. 1974. *The spectral analysis of time series*. Academic Press, New York.

Kuno, E. 1968. Studies on the population dynamics of rice leafhoppers in a paddy field. Bull. Kyushu Agric. Exp. Stn. **14**: 131-246.

Langhaar, H.L. 1980. *Dimensional analysis and the theory of models*. Krieger Publishing, Huntington, New York.

Lasker, R. 1975. Field criteria for the survival of anchovy larvae: the relation between inshore chlorophyll maximum layers and successful first feeding. Fish. Bull. **73**: 453-462.

Lear, W.H., Baird, J.W., Rice, J.C., Carscadden, J.E., Lilly, G.R. and Akenhead, S.A. 1986. An examination of factors affecting catch in the inshore cod fishery of Labrador and eastern Newfoundland. Can. Tech. Rep. Fish. Aquat. Sci. **1469**.

Lefkovitch, L.P. 1966. An index of spatial distribution. Res. Popul. Ecol. **8**: 89-92.

Legendre, L. and Demers, S. 1984. Towards dynamic biological oceanography and limnology. Can. J. Fish. Aquat. Sci. **41**: 2-19.

Legendre, P. and Fortin, M.-J. 1989. Spatial pattern and ecological analysis. Vegetatio **80**: 107-138.

Levin, S. 1976. Population dynamics models in heterogeneous environments. Ann. Rev. Ecol. Syst. **7**: 287-310.

Levin, S.A. 1992. The problem of pattern and scale in ecology. Ecology **73**: 1943-1967.

Levin, S.A., Morin, A. and Powell, T.M. 1989. Patterns and processes in the distribution and dynamics of Antarctic krill. **SC-CAMLR-VII/BG/20**: 281-296.

Liebovich, S. 1983. The form and dynamics of Langmuir circulations. Ann. Rev. Fluid Mech. **15**: 391-427.

Lilly, G.R. 1986. Variability in the quantity of capelin and other prey in stomachs of Atlantic cod off southern Labrador and northeastern Newfoundland (NAFO Division 2J+3K) during the autumns of 1978-85. NAFO SCR Doc. **86/80**.

Lilly, G.R. 1987. Interactions between Atlantic cod (*Gadus morhua*) and capelin (*Mallotus villosus*) off Labrador and eastern Newfoundland: a review. Can. Tech. Rep. Fish. Aquat. Sci. **1567**.

Lilly, G.R. 1991. Interannual variability in predation by cod (*Gadus morhua*) on capelin (*Mallotus villosus*) and other prey off southern Labrador and northeastern Newfoundland. ICES mar. Sci. Symp. **193**: 133-146.

Lilly, G.R. and Flemming, A.M. 1981. Size relationships in predation by Atlantic cod, *Gadus morhua*, on capelin, *Mallotus villosus*, and sand lance, *Ammodytes dubius*, in the Newfoundland area. NAFO Sci. Coun. Studies **1**: 41-45.

Lilly, G.R. and Botta, J.R. 1984. Food of Atlantic cod (*Gadus morhua* L.) near Bonavista, Newfoundland in 1983. NAFO SCR Doc. **84/51**.

Lilly, G.R., Almeida, M.A. and Lear, W.H. 1984. Food of Atlantic cod (*Gadus morhua*) from southern Labrador and eastern Newfoundland (Div. 2J, 3K, and 3L) in winter. NAFO SCR Doc. **84/88**.

Lloyd, M. 1967. Mean crowding. J. Anim. Ecol. **36**: 1-30.

Longhurst, A.R., Reith, A.D., Bower, R.E. and Seibert, D.L.R. 1966. A new system for the collection of multiple serial plankton samples. Deep-Sea Res. **13**: 213-222.

Lorenzen, C.J. 1966. A method for the continuous measurement of *in vivo* chlorophyll concentration. Deep-Sea Res. **13**: 223-227.

Mackas, D.L. 1977. Horizontal spatial variability and covariability of marine phytoplankton and zooplankton. Ph.D. thesis. Dalhousie University, Halifax.

Mackas, D.L. 1984. Spatial autocorrelation of plankton community composition in a continental shelf ecosystem. Limnol. Oceanogr. **29**: 451-471.

Mackas, D.L. and Boyd, C.M. 1979. Spectral analysis of zooplankton spatial heterogeneity. Science **204**: 62-64.

Mackas, D.L., Denman, K.L. and Abbott, M.R. 1985. Plankton patchiness: Biology in the physical vernacular. Bull. Mar. Sci. **37**: 652-674.

Magnuson, J.J., Kratz, T.K., Frost, T.M., Bowser, C.J., Benson, B.J. and Nero, R. 1991. Expanding the temporal and spatial scales of ecological research and comparison of divergent ecosystems: Roles for LTER in the United States, pp. 45-70. In Risser, P.G. (ed.) *Long-term Ecological Research*. John Wiley and Sons, New York.

Mandelbrot, B.B. 1982. *The Fractal Geometry of Nature*. W.H. Freeman, San Francisco.

Mangel, M. 1987. Simulation of southern ocean krill fisheries. Report for Commission for the Conservation of Antarctic Marine Living Resources, 13 October. **SC-CAMLR-VII/BG/22.**

Marquet, P.A., Fortin, F-J., Pineda, J., Wallin, D.O., Clark, J., Wu, Y., Bollens, S., Jacobi, C.M. and Holt, R.D. 1993. Ecological and evolutionary consequences of patchiness: A marine-terrestrial perspective, pp. 277-304. In Levin, S.A., Powell, T.M. and Steele, J.H. (eds.) *Patch Dynamics*. Springer-Verlag, Berlin.

May, R.M. 1976. Simple mathematical models with very complicated dynamics. Nature **261**: 459-467.

McCullagh, P. and Nelder, J.A. 1983. *Generalized linear models*. Chapman and Hall, London.

McGuire, J.U., Brindley, T.A. and Bancroft, T.A. 1957. The distribution of European corn borer larvae *Pyrausta nubilalus* (Hbn.) in field corn. Biometrics **13**: 65-78.

Menge, B.A. and Olson, A.M. 1990. Role of scale and environmental factors in regulation of community structure. Trends Ecol. Evol. **5**: 52-57.

Mercer, W.B. and Hall, A.D. 1911. The experimental error of field trials. J. Agric. Sci. **4**: 107-132.

Methven, D.A. and Piatt, J.F. 1989. Seasonal and annual variation in the diet of Atlantic cod (*Gadus morhua*) in relation to the abundance of capelin (*Mallotus villosus*) off eastern Newfoundland, Canada. J. Cons. int. Explor. Mer **45**: 223-225.

Methven, D.A. and Piatt, J.F. 1991. Seasonal abundance and vertical distribution of capelin (*Mallotus villosus*) in relation to water temperature at a coastal site off eastern Newfoundland. ICES J. mar. Sci., **48**: 187-193.

Miller, D.G.M. and Monteiro, P.M.S. 1988. Variability in the physical and biotic environment of the Antarctic krill (*Euphausia superba* Dana), south of Africa:

Some results and a conceptual appraisal of important interactions, pp. 245-257. In Sahrhage, D. (ed.) *Antarctic Ocean and Resources Variability*. Springer-Verlag, New York.

Minet, J.P. and Perodou, J.B. 1978. Predation of cod (*Gadus morhua*) on capelin (*Mallotus villosus*) off eastern Newfoundland and in the Gulf of St. Lawrence. ICNAF Res. Bull. **13**: 11-20.

Misund, O.A. 1993. Dynamics of moving masses: variability in packing density, shape, and size among herring, sprat, and saithe schools. ICES J. mar. Sci. **50**, 145-160.

Montevecchi, W.A. and Piatt, J.F. 1984. Composition and energy contents of mature inshore spawning capelin (*Mallotus villosus*): implications for seabird predators. Comp. Biochem. Physiol. **78A**: 15-20.

Morisita, M. 1954. Estimation of population density by spacing method. Mem. Fac. Sci. Kyushu Univ. Ser E Biol. **1**: 187-197.

Morisita, M. 1959a. Measuring of the dispersion of individuals and analysis of the distributional patterns. Mem. Fac. Sci. Kyushu Univ. Ser E Biol. **2**: 215-235.

Morisita, M. 1959b. Measuring of interspecific association and similarity between communities. Mem. Fac. Sci. Kyushu Univ. Ser E Biol. **3**: 65-80.

Morrison, G. and Strong Jr., D.R. 1980. Spatial variations in host density and the intensity of parasitism: some empirical examples. Environ. Ent. **9**: 149-152.

Morrison, G., and Strong Jr., D.R. 1981. Spatial variations in egg density and the intensity of parasitism in a neotropical chrysomelid (*Cephaloleia consanguinea*). Ecol. Ent. **6**: 55-61.

Murdoch, W.W. and Oaten, A. 1975. Predation and population stability. Adv. Ecol. Res. **9**: 1-125.

Murphy, G.I. 1966. Population biology of the Pacific sardine (*Sardinops caerulea*). Proc. Cal. Acad. Sci. **34**: 1-84.

Nero, R.W. and Magnuson, J.J. 1992. Effects of changing spatial scale on acoustic observations of patchiness in the Gulf Stream. Lands. Ecol. **6**, 279-292.

Neyman, J. 1939. On a new class of "contagious" distributions, applicable in entomology and bacteriology. Ann. Math. Stat. **10**: 35-57

Numata, M. and Suzuki, K. 1953. Experimental studies on early stages of secondary succession III. (in Japanese) Jap. Jour. Ecol. **8**: 68-75.

O'Brien, J.J. and Wroblewski, J.S. 1973a. A simulation of the mesoscale distribution of the lower marine trophic levels off West Florida. Inv. Pesq. **37**: 193-244.

O'Brien, J.J. and Wroblewski, J.S. 1973b. On advection in phytoplankton models. J. theor. Biol. **38**: 197-202.

O'Neill, R.V., DeAngelis, D.L., Waide, J.B. and Allen, T.F.H. 1986. *A Hierarchical concept of ecosystems*. Princeton University Press, Princeton.

O'Neill, R.V., Turner, S.J., Cullinan, V.I., Coffin, D.P., Cook, T., Conley, W., Brunt, J., Thomas, J.M., Conley, M.R. and Gosz, J. 1991. Multiple landscape scales: An intersite comparison. Lands. Ecol. **5**: 137-144.

Okubo, A. 1978. Horizontal dispersion and critical scales for phytoplankton patches, pp. 21-42. In Steele, J.H. (ed.) *Spatial Pattern in Plankton Communities*. Plenum Press, New York.

Okubo, A. 1980. *Diffusion and ecological problems: mathematical models.* Springer-Verlag, New York.

Okubo, A. 1986. Dynamical aspects of animal groupings: swarms, schools, flocks, and herds. Adv. Biophys. **22**, 1-94.

Okubo, A. 1987. *Lecture notes in biomathematics*. Number 71. Springer-Verlag, New York.

Olson, D.B. and Backus, R.H. 1985. The concentrating of organisms at fronts: a cold-water fish and a warm-core Gulf Stream ring. J. Mar. Res., **43**: 113-137.

Ord, J.K. 1972. *Families of frequency distributions*. Griffin, London.

Pacala, S.W., Hassel, M.P. and May, R.M. 1990. Host-parasitoid associations in patchy environments. Nature **344**: 150-153.

Parr, A.E. 1927. A contribution to the theorectical analysis of the schooling behavior of fishes. Occas. Pap. Bingham Oceanog. Coll. **1**: 1-32.

Partridge, B.L. 1980. The effect of school size on the structure and dynamics of minnow schools. Anim. Behav. **28**, 68-77.

Patil, G.P. and Stiteler, W.M. 1974. Concepts of aggregation and their quantification: a critical review with some new results and applications. Res. Popul. Ecol. **15**: 238-254.

Perry, J.N. and Woiwod, I.P. 1992. Fitting Taylor's power law. Oikos **65**: 538-542.

Petrie, B. and Anderson, C. 1983. Circulation on the Newfoundland continental shelf. Atmos.-Ocean, **21**: 207-226.

Piatt, J.F. 1990. The aggregative response of Common Murres and Atlantic Puffins to schools of capelin. Stud. Avian Biol. **14**: 36-51.

Pielou, E.C. 1957. The effect of quadrat size on the estimation of the parameters of Neyman's and Thomas's distributions. J. Ecol. **45**: 31-47.

Pielou, E.C. 1969. *An introduction to mathematical ecology*. John Wiley and Sons, New York.

Pinel-Alloul, B. and Pont, D. 1991. Spatial distribution patterns in freshwater macrozooplankton: variation with scale. Can. J. Zool. **69**: 1557-1570.

Pitcher, T.J. 1986. Functions of shoaling behaviour in teleosts, pp. 294-337. In Pitcher, T.J. (ed.) *The Behaviour of teleost fishes*. Croom Helm Ltd, London.

Pitcher, T.J. and Partridge, B.L. 1979. Fish school density and volume. Mar. Biol. **54**, 383-394.

Pitcher, T.J. and J.K. Parrish. 1993. Functions of shoaling behaviour in teleosts, pp. 363-439. In Pitcher, T.J. (ed.) *Behaviour of teleost fishes*. Second edition. Chapman and Hall, London

Platt, T. 1972. Local phytoplankton abundance and turbulence. Deep-Sea Res. **19**: 183-187.

Platt, T. and Denman, K.L. 1975. Spectral analysis in ecology. Ann. Rev. Ecol. Syst. **6**: 189-210.

Platt, T. and Harrison, W.G. 1985. Biogenic fluxes of carbon and oxygen in the ocean. Nature **318**: 55-58.

Platt, T. and Silvert, W. 1981. Ecology, physiology, allometry and dimensionality. J. theor. Biol. **93**: 855-860.

Platt, T., Dickie, L.M. and Trites, R.W. 1970. Spatial heterogeneity of phytoplankton in a near-shore environment. J. Fish. Res. Bd. Can. **27**: 1453-1473.

Pólya, G. 1931. Sur quelques points de la théorie des probabilities. Ann. Inst. Poincaré **1**: 117-162.

Popova, O.A. 1962. Some data on the feeding of cod in the Newfoundland area of the Northwest Atlantic, pp. 228-248. In Marti, Y.Y. (ed.) *Soviet Fisheries Investigations in the Northwest Atlantic*. Translated from Russian for US Dep. Int. Nat. Sci. Found., Washington, DC, by Israel Prog. Sci. Transl. 1963.

Possingham, H.P. 1989. The distribution and abundance of resources encountered by a forager. Am. Nat. **133**: 42-70.

Powell, T.M., Richerson, P.J., Dillon, T.M., Agee, B.A., Dozier, B.J., Godden, D.A. and Myrup, L.O. 1975. Spatial scales of current speed and phytoplankton biomass fluctuations in Lake Tahoe. Science **189**: 1088-1090.

Reeve, J.D. 1990. Stability, variability, and persistence in host-parasitoid systems. Ecology **71**: 422-426.

Richardson, W.J. 1978. Timing and amount of bird migration in relation to the weather: A review. Oikos **30**, 224-272.

Richerson, P.J., Powell, T.M., Leigh-Abbott, M.R. and Coil, J.A. 1978. Spatial heterogeneity in closed basins, pp. 239-276. In Steele, J.H. (ed.) *Spatial pattern in plankton communities*. Plenum Press, New York.

Ricker, W.E. 1954. Stock and recruitment. J. Fish. Res. Bd. Can. **11**: 559-623.

Riley, G.A. 1942. The relationship of vertical turbulence and spring diatom flowerings. J. Mar. Res. **5**: 67-87.

Riley, G.A. and Bumpus, D.F. 1946. Phytoplankton-zoolankton relationships on Georges Bank. J. Mar. Res. **6**: 67-87.

Ripley, B.D. 1981. *Spatial statistics*. John Wiley, New York.

Rogers, A. 1974. *Statistical Analysis of Spatial Dispersion. The Quadrat Method*. Pion, London.

Rose, G.A. 1992. A review of problems and new directions in the application of fisheries acoustics on the Canadian East Coast. Fish. Res. **14**: 105-128.

Rose, G.A. 1993. Cod spawning on a migration highway in the north-west Atlantic. Nature **366**: 458-461.

Rose, G.A. and Leggett, W.C. 1988a. Hydroacoustic signal classification of fish schools by species. Can. J. Fish. Aquat. Sci. **45**: 597-604.

Rose, G.A. and Leggett, W.C. 1988b. Atmosphere-ocean coupling and Atlantic cod migrations: effects of wind-forced variations in sea temperatures and currents on nearshore distributions and catch rates of *Gadus morhua*. Can. J. Fish. Aquat. Sci. **45**: 1234-1243.

Rose, G.A. and Leggett, W.C. 1989. Interactive effects of geophysically-forced sea temperatures and prey abundance on mesoscale coastal distributions of a marine predator, Atlantic cod (*Gadus morhua*). Can. J. Fish. Aquat. Sci. **46**: 1904-1913.

Rose, G.A. and Leggett, W.C. 1990. The importance of scale to predator-prey spatial correlations: An example of Atlantic fishes. Ecology **71**: 33-43.

Rossi, R.E., Mulla, D.J., Journel, A.G. and Franz, E.H. 1992. Geostatistical tools for modeling and interpreting ecological spatial dependence. Ecol. Monogr. **62**: 277-314.

Routledge, R.D. and Swartz, T.B. 1991. Taylor's Power Law re-examined. Oikos **60**: 107-112.

Safina, C. and Burger, J. 1985. Common Tern foraging: seasonal trends in prey fish densities and competition with Bluefish. Ecology **66**: 441-461.

Safina, C. and Burger, J. 1988. Ecological dynamics among prey fish, Bluefish, and foraging Common Terns in an Atlantic coastal system, pp. 95-173. In Burger, J. (ed.) *Seabirds and other Marine Vertebrates*. Columbia University Press, New York.

Salt, G.W. 1974. Predator and prey densities as controls of rate of capture by the predator *Didinium nasutum*. Ecology **55**: 434-439.

Satoh, K. 1989. Computer experiment on the complex behavior of a two-dimensional cellular automation as a phenomenological model for an ecosystem. J. Phys. Soc. Jpn. **58**, 3842-3856.

Satoh, K. 1990. Single and multiarmed spiral patterns in a cellular automaton model for an ecosystem. J. Phys. Soc. Jpn. **59**, 4204-4207.

Saunders, P.M. 1972. Space and time variability of temperature in the upper ocean. Deep-Sea Res. **19**: 467-480.

Sætre, R. and Gjøsæter, J. 1975. Ecological investigations on the spawning grounds of the Barrents Sea capelin. Fiskeri-Direktoratets Skrifter Serie Havundersøkelser **16**, 203-227.

Schmitt, R.J. 1982. Consequences of dissimilar defenses against predation in a subtidal marine community. Ecology **63**: 1588-1601.

Schmitt, R.J. 1985. Competitive interactions of two mobile prey species in a patchy environment. Ecology **66**: 950-958.

Schneider, D.C. 1989. Identifying the spatial scale of density-dependent interaction of predators with schooling fish in the southern Labrador Current. J. Fish Biol. **35** (Supplement A): 109-115.

Schneider, D.C. 1991. The role of fluid dynamics in the ecology of marine birds. Oceanogr. Mar. Biol. Annu. Rev. **29**: 487-521.

Schneider, D.C. 1992. Thinning and clearing of prey by predators. Am. Nat. **139**: 148-160.

Schneider, D.C. 1994a. Scale-dependent patterns and species interactions in marine nekton, pp. 441-467. In Giller, P.S., Hildrew, A.G. and Rafaelli, D. (eds.) *Aquatic Ecology: Scale, Pattern and Process*. Blackwell, Oxford.

Schneider, D.C. 1994b. *Quantitative Ecology*. Academic Press, San Diego.

Schneider, D.C. 1994c. Distribution of capelin (*Mallotus villosus*) in relation to coastal upwelling in the Avalon Channel. J. Northw. Atl. Fish. Sci. **17**, in press.

Schneider, D.C. and Duffy, D.C. 1985. Scale-dependent variability in seabird abundance. Mar. Ecol. Prog. Ser. **25**: 211-218.

Schneider, D.C. and Piatt, J.F. 1986. Scale-dependent correlation of seabirds with schooling fish in a coastal ecosystem. Mar. Ecol. Prog. Ser. **32**: 237-246.

Schneider, D.C. and Methven, D.A. 1988. Response of capelin to wind-induced thermal events in the southern Labrador Current. J. Mar. Res. **46**: 105-118.

Schneider, D.C. and Bajdik, C.D. 1992. Decay of zooplankton patchiness generated at the sea surface. J. Plankton Res. **14**: 531-543.

Schneider, D.C., Gagnon, J.-M. and Gilkinson, K.D. 1987. Patchiness of epibenthic megafauna on the outer Grand Banks of Newfoundland. Mar. Ecol. Prog. Ser. **39**, 1-13.

Schneider, D.C., Duffy, D.C. and Hunt, G.L. 1988. Cross-shelf gradients in the abundance of pelagic birds, pp. 976-981. In Ouellet, H (ed.) *Proceedings XIX International Ornithological Congress*. Ottawa University Press, Ottawa.

Schneider, D.C., Duffy, D.C., MacCall, A.D. and Anderson, D.W. 1993. Seabird-fisheries interactions: evaluation with dimensionless ratios, pp. 602-615. In McCullough, D.R. and Barrett, R.H. (eds.) *Wildlife 2000*. Elsevier, London.

Schroeder, M. 1991. *Fractals, Chaos, Power Laws: Minutes from an Infinite Paradise*. W.H. Freeman, New York.

Scott, W.B. and Scott, M.G. 1988. Atlantic Fishes of Canada. Can. Bull. Fish. Aquat. Sci. **219**.

Sheldon, R.W. and Parsons, T.W. 1967. A continuous size spectrum for particulate matter in the sea. J. Fish. Res. Bd. Can. **24**: 909-915.

Shelton, P.A., Fahrig, L. and Millar, R.B. 1991. Uncertainty associated with cod-capelin interactions: how much is too much? NAFO Sci. Coun. Studies **16**: 13-19.

Sheperd, J.G., Pope, J.G. and Cousens, R.D. 1984. Variations in fish stocks and hypotheses concerning their links with climate. Rapp. P.-v. Réun. Cons. Int. Explor. Mer. **185**: 255-267.

Shigesada, N. and Okubo, A. 1981. Analysis of the self-shading effect on algal vertical distribution in natural waters. J. Math. Biol. **12**: 311-326.

Star, J.L. and Mullin, M.M. 1981. Zooplanktonic assemblages in three areas of the North Pacific as revealed by continuous horizontal transects. Deep-Sea Res. **28A**: 1303-1322.

Star, J.L. and Cullen, J.J. 1981. Spectral analysis: a caveat. Deep-Sea Res. **28**: 93-97.

Steele, J.H. 1974. *The Structure of Marine Ecosystems*. Harvard University Press. Harvard.

Steele, J.H. 1976. Patchiness, pp. 98-115. In Cushing, D.H. and Walsh, J.J. (eds.) *Ecology of the sea*. Blackwell, London.

Steele, J.H. (ed.) 1978a. *Spatial Pattern in Plankton Communities*. Plenum Press, New York.

Steele, J.H. 1978b. Some comments on plankton patches, pp. 1-20. In Steele, J.H. (ed.) *Spatial Pattern in Plankton Communities*. Plenum Press, New York.

Steele, J.H. 1989. The ocean 'landscape'. Lands. Ecol. **3**: 185-192.

Stephen, A.C. 1929. Notes on the rate of growth of *Tellina tenuis* da Costa in the Firth of Clyde. J. Mar. Biol. Assoc. U.K. **16**: 117-129.

Stommel, H. 1963. Varieties of oceanographic experience. Science **139**: 572-576.

Story, G.M., Kirwin, W.J. and Widdowson, J.D.A. (eds.) 1990. *Dictionary of Newfoundland English*. Second edition. Breakwater, St. John's.

Student, S. 1907. On the error of counting with a haemacytometer. Biometrika **5**: 351-364.

Sugihara, G. and May, R.M. 1990. Applications of fractals in ecology. Trends Ecol. Evol. **5**: 79-86.

Shugart, H.H. (ed.) 1978. *Time Series and Ecological Processes*. Society for Industrial and Applied Mathematics, Philadelphia.

Simon, H.A. 1962. The architecture of complexity. Proc. Amer. Phil. Soc. **106**: 467-482.

Simpson, E.H. 1949. Measurement of diversity. Nature **163**: 688.

Sissenwine, M.P. 1984. Why do fish populations vary? pp. 59-94. In May, R.N. (ed.) *Exploitation of Marine Communities*. Springer-Verlag. Berlin.

Skellam, J.G. 1951. Random dispersal in theoretical populations. Biometrika **78**: 196-218.

Skellam, J.G. 1952. Studies in statistical ecology. I. Spatial pattern. Biometrika **79**: 346-362.

Smith, P.E. 1978. Biological effects of ocean variability: time and space scales of biological response. Rapp. P.-v. Réun. Cons. Int. Explor. Mer **173**: 117-127.

Sokal, R.R. and Rohlf, F.J. 1981. *Biometry*. Second edition. Freeman and Company, New York.

Soofiani, N.M. and Hawkins, A.D. 1982. Energetic costs at different levels of feeding in juvenile cod, *Gadus morhua* L. J. Fish Biol. **21**: 577-592.

Soofiani, N.M. and Priede, I.G. 1985. Aerobic metabolic scope and swimming performance in juvenile cod, *Gadus morhua* L. J. Fish Biol. **26**: 127-138.

Stanek, E. 1975. The percentage of capelin in the stomach contents of cod in ICNAF Subareas 2 and 3. ICNAF Res. Doc. **75/5**.

Star, J.L. and Mullin, M.M. 1979. Horizontal undependability in the planktonic environment. Mar. Sci. Commun. **5**: 31-46.

Sverdrup, H.U. 1953. On conditions for the vernal blooming of phytoplankton. J. Cons. Perm. Int. Explor. Mer **18**: 287-295.

Taggart, C.T. and Leggett, W.C. 1987. Wind-forced hydrodynamics and their interaction with larval fish and plankton abundance: a time-series analysis of physical-biological data. Can. J. Fish. Aquat. Sci. **44**: 438-451.

Taylor, A. 1988. Large-scale spatial structure and population dynamics in arthropod predator-prey systems. Ann. Zool. Fenn. **25**: 63-74.

Taylor, A. 1990. Metapopulations, dispersal, and predatory-prey dynamics: an overview. Ecology **71**: 429-436.

Taylor, C.C. 1953. Nature of variability in trawl catches. Fish. Bull. **54**: 143-166.

Taylor, E.S. 1974. *Dimensional analysis for engineers*. Clarendon Press, England.

Taylor, L.R. 1961. Aggregation, variance and the mean. Nature **189**: 732-735.

Taylor, L.R. 1984. Assessing and interpreting the spatial distributions of insect populations. Ann. Rev. Entomol. **29**: 321-357.

Taylor, L.R. and Taylor, R.A.J. 1977. Aggregation, migration and population mechanics. Nature **265**: 415-421.

Taylor, L.R. and Woiwod, I.P. 1982. Comparative synoptic dynamics. I. Relationships between inter- and intra-specific spatial and temporal variance/mean population parameters. J. Anim. Ecol. **51**: 879-906.

Taylor, L.R., Woiwod, I.P. and Perry, J.N. 1978. The density-dependence of spatial behaviour and the rarity of randomness. J. Anim. Ecol. **47**: 383-406.

Templeman, W. 1948. The life history of the capelin (*Mallotus villosus* Müller) in Newfoundland waters. Nfld. Gov. Lab. Bull. **17**: 1-151.

Templeman, W. 1965. Some instances of cod and haddock behaviour and concentrations in the Newfoundland and Labrador areas in relation to food. ICNAF Spec. Publ. **6**: 449-461.

Templeman, W. 1979. Migration and intermingling of stocks of Atlantic cod (*Gadus morhua*), of the Newfoundland and adjacent areas from tagging in 1962-66. ICNAF Res. Bull. **14**: 5-50.

Thomas, M. 1949. A generalization of Poisson's binomial limit for use in ecology. Biometrika **36**: 18-25.

Thompson, H. 1943. A biological and economic study of cod (*Gadus morhua* L.) in the Newfoundland area including Labrador. Nfld. Dep. Nat. Resour. Res. Bull. **14**.

Thompson, W.A., Vertinsky, I. and Krebs, J.R. 1974. The survival value of flocking in birds: a simulation model. J. Anim. Ecol. **43**, 785-820.

Tsuda, A., Sugisake, H., Ishimaru, T., Saino, T. and Sato, T. 1993. White-noise-like distribution of the oceanic copepod *Neocalanus cristatus* in the subarctic North Pacific. Mar. Ecol. Prog. Ser. **97**: 39-46.

Turner, S.J., O'Neill, R.V., Conley, W., Conley, M.R. and Humphries, H.C. 1992. Pattern and scale: statistics for landscape ecology, pp. 17-49. In Turner, M.G., and Gardner, R.H. (eds.) *Quantitative Methods in Landscape Ecology*. Springer-Verlag, New York.

Turuk, T.N. 1968. Seasonal changes of cod feeding in the Labrador and Newfoundland areas in 1964-66. Trudy PINRO **23**: 370-382. (Journal of Fisheries Research Board of Canada Translation Series **1937**).

Tyler, A.V. 1970. Rates of gastric emptying in young cod. J. Fish. Res. Bd. Can. **27**: 1177-1189.

Tyler, A.V. 1973 Caloric values of some North Atlantic invertebrates. Mar. Biol. **19**: 258-261.

Tytler, P. 1969. Relationship between oxygen consumption and swimming speed in the haddock, *Melanogrammus aeglefinus*. Nature **221**: 274-275.

Urban, D.L., O'Neill, R.V. and Shugart Jr., H.H. 1987. Landscape ecology. BioScience **37**: 119-127.

Usher, M.B. 1969. The relation between mean square and block size in the analysis of similar patterns. J. Ecol. **57**: 505-514.

Waage, J.K. 1979. Foraging for patchily-distributed hosts by the parasitoid, *Nemeritis canescens*. J. Anim. Ecol. **48**: 353-371.

Waiwood, K.G., Smith, S.J. and Petersen, M.R. 1991. Feeding of Atlantic cod (*Gadus morhua*) at low temperatures. Can. J. Fish. Aquat. Sci. **48**: 824-831.

Walsh, J.J. 1981. Shelf-Sea Ecosystems, pp. 159-196. In Longhurst, A.R. (ed.) *Analysis of Marine Ecosystems*. Academic Press, London.

Waters, W.E. 1959. A quantitative measure of aggregation in insects. J. Econ. Ent. **52**: 1180-1184.

Watt, A.S. 1925. On the ecology of British beechwoods with special reference to their regeneration. J. Ecol. **13**: 27-73.

Watt, A.S. 1947. Pattern and process in the plant community. J. Ecol. **35**: 1-22.

Webb, P.W. 1975. Hydrodynamics and energetics of fish propulsion. Bull. Fish. Res. Roard Can. **190**. Department of Fisheries and Oceans, Ottawa.

Weber, L.H., El-Sayed, S.Z. and Hampton, I. 1986. The variance spectra of phytoplankton, krill and water temperature in the Antarctic Ocean south of Africa. Deep-Sea Res. **33**: 1327-1343.

Weihs, D. 1973. Hydromechanics of fish schooling. Nature **241**: 290-291.

Weihs, D. 1975. Some hydromechanical aspects of fish schooling, pp. 703-718. In Wu, T.Y.-T., Brokaw, C.J. and Brennen, C. (eds.) *Swimming and flying in nature* Vol. 2. Plenum, New York.

Weller, R.A. and Price, J.F. 1988. Langmuir circulation within the oceanic mixed layer. Deep-Sea Res. **35**: 711-747.

Whitehead, H.P. 1981. The behaviour and ecology of the humpback whale in the northwest Atlantic. Ph.D. thesis. University of Cambridge, Cambridge.

Wiebe, P.H. 1971. A computer model study of zooplankton patchiness and its effects on sampling error. Limnol. Oceanog. **16**, 29-38.

Wiebe, P.H. and Flierl, G.R. 1983. Euphausiid invasion/dispersal in Gulf Stream Cold core rings. Aust. J. Mar. Freshw. Res. **34**: 625-652.

Wiens, J.A. 1976. Population responses to patchy environments. Ann. Rev. Ecol. Syst. **7**: 81-120.

Wiens, J.A. 1989. Spatial scaling in ecology. Func. Ecol. **3**: 385-397.

Williams, C.B. 1964. Some experiences of a biologist with R.A. Fisher and statistics. Biometrics **20**: 301-306.

Winberg, G.G. 1956. Rate of metabolism and food requirements of fishes. Nauk Tr. Belloruskovo Gosudarstvennovo Universiteta imeni V.I. Lenina, Minsk. (Translated from Russian by Journal of the Fisheries Research Board of Canada Translation Series **194**).

Winters, G.H. and Carscadden, J.E. 1978. Review of capelin ecology and estimation of surplus yield from predator dynamics. ICNAF Res. Bull. **13**: 21-30.

Winters, G.H. and Wheeler, J.P. 1985. Interaction between stock area, stock abundance, and catchability coefficient. Can. J. Fish. Aquat. Sci. **42**: 989-998.

Woiwod, I.P. and Perry, J.N. 1989. Data reduction and analysis. Boletin de Sanidad Vegetal (Madrid) **17**: 159-174.

Wroblewski, J.S., O'Brien, J.J. and Platt, T. 1975. On the physical and biological scales of phytoplankton patchiness in the ocean. Mém. Soc. R. Sci. Liège **7**: 43-57.

Wunsch, C. 1972. Bermuda sea level in relation to tides, weather, and baroclinic fluctuations. Rev. Geophys. Space Phys. **10**: 1-49.

Yao, T. 1986. The response of currents in Trinity Bay, Newfoundland, to local wind forcing. Atmos.-Ocean **24**: 235-252.